POLITECNICO DI MILANO
DEPARTMENT OF CIVIL & ENVIRONMENTAL ENGINEERING

DOCTORAL SCHOOL IN
STRUCTURAL, EARTHQUAKE AND GEOTECHNICAL ENGINEERING
XXXI Cycle

PHD THESIS

LIMIT ANALYSIS FOR ROBUSTNESS ASSESSMENT OF EXISTING STRUCTURES

Elisa CONTI

SUPERVISOR:
Prof. Pier Giorgio MALERBA
TUTOR:
Prof. Lorenza PETRINI

THE CHAIR OF THE DOCTORAL PROGRAM:
Prof. Roberto PAOLUCCI

MILAN - MARCH 2019

E. Conti
Limit Analysis for Robustness Assessment of Existing Structures
© March 2019
`elisa.conti@polimi.it`

Department of Civil & Environmental Engineering
Politecnico di Milano

Limit Analysis for Robustness Assessment of Existing Structures

A Thesis
Presented to
The Academic Faculty

by

Elisa Conti

In Partial Fullfilment
of the Requirements for the Degree of
Doctor of Philosophy

in
Structural, Seismic and Geotechnical Engineering

march 2019

LIMIT ANALYSIS FOR ROBUSTNESS ASSESSMENT OF EXISTING STRUCTURES

PhD thesis by Elisa Conti
Supervisor: Prof. Pier Giorgio Malerba
© March 2019

DOCTORAL SCHOOL IN STRUCTURAL, SEISMIC AND GEOTECHNICAL ENGINEERING
DEPARTMENT OF CIVIL & ENVIRONMENTAL ENGINEERING
POLITECNICO DI MILANO

XXXI CYCLE - 2015-2019

BOARD COMMITTEE:
Prof. Raffele Ardito
Prof. Patrick Bamonte
Prof. Fabio Biondini
Prof. Gabriella Bolzon
Prof. Matteo Bruggi
Prof. Claudia Comi
Prof. Alberto Corigliano
Prof. Dario Coronelli
Prof. Gabriele Della Vecchia
Prof. Marco Di Prisco
Prof. Claudio Di Prisco
Prof. Roberto Fedele
Prof. Roberto Felicetti
Prof. Liberato Ferrara
Prof. Attilio Frangi
Prof. Aldo Ghisi
Prof. Cristina Jommi
Prof. Maurizio Lualdi
Prof. Pier Giorgio Malerba
Prof. Stefano Mariani
Prof. Luca Martinelli
Prof. Roberto Paolucci
Prof. Umberto Perego
Prof. Lorenza Petrini
Prof. Gianpaolo Rosati

To my Family

Abstract

The majority of Reinforced and Prestressed Concrete bridges with more than 40-60 years of service life exposed to aggressive environments show significant deterioration and structural deficiency over time. In addition, an increase in the acceptable loading level has to be accounted for. For these reasons, many Road and Highway Administrations are faced with two typical problems: (a) in designing new bridges, estimate their bearing capacity after a certain amount of years from construction time under given environmental and service condition; (b) for existing bridges, assess their residual bearing capacity in the damaged state, after a certain amount of years from construction time, their residual life-cycle and the possibility of a sustainable extension of their service life.

After having deepened the main requirements related to the problem of assessing the structural safety, the attention has been focused on the effects induced by the most frequent damaging causes on the overall structural performance of RC structures. Such a problem requires (I) a representative modeling of the damage diffusion inside the volume of the RC element; (II) a discretization technique fit for the actual structures and structural elements; (III) a reliable and synthetic tool in order to investigate the bearing capacity over time.

Aiming at proposing a methodology applicable to daily engineering practice, the structural modeling based on finite beam-column elements has been adopted because of their optimal balance between accuracy and computational efficiency. In the global structural framework, the matrix formulation of Limit Analysis has been at first reviewed and developed through ad hoc computer codes. Wide comparisons with reference to the Nonlinear approach have been carried out. Then, moving from the global level to the local one, a finite number of elementary "equivalent" frameworks or trusses of bars has been adopted in studying continuous systems.

The damage state can be assumed as a given data or can be modeled by means of a general technique handling the damage diffusion and based on the Cellular Automata algorithm. Depending on the given damage scenario, such a degradation of the mechanical properties has been incorporated in the structural analysis.

Thus, a procedure for a *virtual loading test* is proposed, consisting in the exam of a structure at different damage states and in the evaluation of the multiplier at the collapse of a given additional traffic load distribution. A synthesis of these results is given by examining the damage evolution and the loading capacity of the structure over time and associating to this evolution a robustness index, which obviously decreases with time. In addition, the data resulting from the Limit Analysis is useful to highlight the essential details of such an evolution, showing how the internal forces redistribute from the weakest structural parts to the undamaged elements.

We think that this approach may give a contribution in solving the aforementioned problems and in assessing the effectiveness of repairing and strengthening interventions.

Keywords: Existing Structures; Structural Safety; Robustness Assessment; Limit Analysis; Environmental Damage.

Contents

Abstract ix

List of Symbols xv

List of Figures xxii

List of Tables xxiv

1 Introduction 1
- 1.1 Motivation and Problem Statement 1
  - 1.1.1 Dealing with existing structures 2
    - 1.1.1.1 Influence of the structural modeling 2
    - 1.1.1.2 Influence of Materials modeling 3
    - 1.1.1.3 Influence of the loading conditions 4
    - 1.1.1.4 Concerning the Materials 5
- 1.2 Scope and objectives 6
- 1.3 Research significance 8
- 1.4 Contents of this document 9

2 Structural Safety versus Structural Weaknesses 11
- 2.1 Introduction 11
- 2.2 Safety and Safety Assessment of Existing Structures 12
- 2.3 Structural Safety Definitions 13
- 2.4 Structural Safety in being 14
  - 2.4.1 Cantilever Bridges 15
  - 2.4.2 Steel Bridges 15
  - 2.4.3 RC & PC Bridges 15
  - 2.4.4 Suspension & Cable-Stayed Bridges 20
  - 2.4.5 Repair interventions 20
- 2.5 Closing Remarks 20

3 About Structural Robustness 23
- 3.1 General Concepts 23
- 3.2 Failure Events 24
- 3.3 Definition of the most recurrent Terms 26
- 3.4 Robustness Measures and Assessment 28

3.4.1 Deterministic measures . . . 28
3.4.2 Reliability-based measures . . . 33
3.4.3 Risk-based measures . . . 35
3.4.4 A review of the different proposals . . . 35
3.5 Tools for a Robustness Assessment . . . 37
3.6 Closing Remarks . . . 39

4 A Review of Monodimensional Modeling for RC Structures 41
4.1 Introduction . . . 41
4.2 Global Framework . . . 42
4.3 State of the Structure . . . 43
4.4 State of the Element . . . 44
4.4.1 Stiffness Approach . . . 46
4.4.1.1 Distributed loads . . . 47
4.4.1.2 Geometric non linearities . . . 48
4.4.2 Flexibility Approach . . . 50
4.4.2.1 Static field . . . 50
4.4.2.2 Kinematic field . . . 51
4.4.2.3 Additional considerations . . . 52
4.4.2.4 Distributed loads . . . 54
4.4.3 Element state determination . . . 55
4.5 State of the Section . . . 56
4.5.1 Normal Forces . . . 57
4.5.2 Combined Normal and Tangential Forces . . . 58
4.6 State of the Fiber . . . 60
4.7 Conclusion . . . 61

5 Limit Analysis of RC Frame Structures 63
5.1 Introduction . . . 63
5.2 The matrix approach to the Limit Analysis . . . 64
5.2.1 Basic Hypothesis . . . 65
5.2.2 Equilibrium and compatibility conditions . . . 67
5.2.3 Yield condition and flow rule . . . 68
5.2.4 The static and the kinematic theorems . . . 70
5.3 Applicability of Limit Analysis on RC structures . . . 71
5.4 Input for an arbitrary RC Section . . . 73
5.4.1 Axial and Bending interaction Domain . . . 73
5.4.2 Bending and Torsion interaction Diagram . . . 74
5.4.2.1 Strength in pure torsion and pure bending . . . 75
5.4.2.2 Strength in torsion-bending . . . 76
5.5 A benchmark. The Corace Bridge . . . 77
5.5.1 Limit Analysis . . . 78
5.5.2 Nonlinear Analysis . . . 79
5.5.3 Comments of the results and Comparisons . . . 79
5.6 Closing remarks . . . 82

6 Assessment of a RC Existing Structure 85
6.1 Introduction 85
6.2 Sound RC Grillage Deck 86
6.2.1 Limit Analysis 90
6.2.2 Nonlinear Analysis 91
6.3 Damaged RC Grillage Deck 91
6.3.1 Corrosion scenario 91
6.3.2 Limit Analysis at different time instants 94
6.3.3 Nonlinear Analysis at different time instants 96
6.3.3.1 Dead loads effects 96
6.3.3.2 Combined action of self-weight and live load 99
6.3.4 Lifetime structural robustness estimation 101
6.4 Closing remarks 104

7 Limit Analysis of RC Structural Elements 105
7.1 Introduction 105
7.2 RC Structural Elements 106
7.3 Framework Modeling 107
7.4 Bresler & Scordelis A1 Beam 109
7.5 Deep beam WT2 112
7.6 RC Corbel 116
7.7 Comments on the results 120
7.8 Closing remarks 120

A Damage modeling in RC structures exposed to corrosion 121
A.1 Introduction 121
A.1.1 Modeling of the diffusion process 122
A.1.2 Modeling of the mechanical damage 123
A.1.3 Limit Analysis at different time instants 126
A.1.4 Nonlinear Analysis at different time instants 127

Conclusions 129

References 135

List of Symbols

The following is a list of the most important symbols and abbreviations that appear in the chapters of the thesis. Symbols not included in this list are defined when they first appear.

Latin Letters

a	rectangular element side (trusswork method)
$\mathscr{A}$	assembling process
A_c	area of concrete fiber
A_s	area of longitudinal steel bar
A_t	area of stirrup
A_d	area of diagonal truss in the elementary framework
A_x	area of horizontal truss in the elementary framework
A_y	area of verical truss in the elementary framework
$\mathbf{a}_s$	sectional interpolating matrix
b	rectangular element side (trusswork method)
$\mathbf{b}$	force's shape functions matrix
$\mathbf{B}$	displacement's shape functions matrix (derivatives)
C	concentration of the aggressive agent
C_0	initial concentration of the aggressive agent
$\mathbf{c}$	nodal coordinate vector
D_e	effective diffusion coefficient
E_c	concrete elastic modulus
E_s	steel elastic modulus
$\mathbf{e}_s$	generalized sectional strains vector
f_{cr}	tensile cracking stress
f_y	steel yielding stress
$\mathbf{f}_{ne}$	equivalent nodal forces vector
$\mathbf{f}_p$	distributed loads vector
$\mathbf{f}_s$	generalized sectional stresses vector

$\mathbf{f}_{s,r}$	sectional resisting force (complete RC section)
$\mathbf{f}_{s,\gamma}$	sectional resisting force (normal stress contribution)
$\mathbf{f}_{s,\epsilon}$	sectional resisting force (tangential stress contribution)
$\mathbf{F}_e$	structural external nodal forces vector
$\mathbf{F}_r$	structural restoring nodal forces vector

$\mathbf{h}_l$	beam element's compatibility matrix
$\mathbf{h}_0$	level arm
$\mathbf{h}_l^T$	beam element's equilibrium matrix
$\mathbf{H}$	structure's equilibrium matrix
$\mathbf{H}^T$	structure's compatibility matrix

$\mathbf{J}$	Jacobian matrix

$\mathbf{k}$	beam element's stiffness matrix
$\bar{\mathbf{k}}$	beam element's stiffness matrix (system without rigid body modes)
$\mathbf{k}_g$	geometric contribution to beam element's stiffness matrix
$\mathbf{k}_s$	section's stiffness matrix (complete RC section)

M	bending moment
M_p	plastic moment

N	axial force
N_p	plastic axial force
$\mathbf{N}$	displacements shape functions matrix

p_0	perimeter
$\mathbf{q}$	beam element's nodal displacements vector
$\bar{\mathbf{q}}$	beam element's basic displacements vector
$\mathbf{q}_t$	structural basic displacement vector
$\mathbf{Q}$	beam element's nodal forces vector
$\bar{\mathbf{Q}}$	beam element's basic forces vector
$\mathbf{Q}_g$	geometric contribution to beam element's nodal forces
$\mathbf{Q}_t$	structural basic forces vector

R	pitting factor
R_d	robustness

s	ratio between design and resistant value
s_i	state of the cellular automaton
$\mathbf{s}$	structural nodal displacements

t	time instant
$\mathbf{T}_\alpha$	beam element transformation matrix (local to global system)
T	torque moment
T_p	plastic torsional capacity

u	local horizontal displacement of the generic point
$\mathbf{u}$	displacements vector in the generic point $[u\ v]^T$
$\mathbf{u}_s$	sectional generalized displacements vector $[u_0\ v_0\ w_0\ \varphi]^T$
v	local vertical displacement of the generic point
V	shear force
w	crack width opening
W_e	external work
W_i	internal work
x	x axis
y	y axis
z	z axis

Greek Letters

α	reinforcing steel inclination
χ_z	curvature around z axis
χ_y	curvature around y axis
δ_s	dimensionless damage index
Δt	automaton time step
Δx	automaton grid dimension
ε_0	axial strain
$\boldsymbol{\varepsilon}$	strain tensor $[\varepsilon_x\ \gamma_{xz}\ \gamma_{xy}]^T$
ϕ	evolutionary rule of the automaton
$\boldsymbol{\phi}_s$	section flexibility matrix
$\bar{\boldsymbol{\Phi}}$	beam element's flexibility matrix (system without rigid body modes)
$\bar{\boldsymbol{\Phi}}_t$	plastic potential vector
λ_c	collapse multiplier
$\boldsymbol{\mu}$	flow parameters vector
ν_e	effectiveness factor
ϑ	angle between axis y and axis 1
$\rho_{s,i}$	performance index

σ_x	normal stress
$\boldsymbol{\sigma}$	stress tensor $[\sigma_x \ \tau_{xz} \ \tau_{xy}]^T$
τ	tangential stress
θ	torsional curvature

ABBREVIATIONS

LA	Limit Analysis
NLA	Non Linear Analysis
NLG	Non Linear Geometry
NLM	Non Linear Mechanic
PS	Plane Section hypothesis
RC	Reinforced Concrete
SILS	Structural Integrity Limit State
SLS	Serviceability Limit State
ULS	Ultimate Limit State

List of Figures

1.1 Famous Bridges Collapses in Italy. 1
1.2 Different structural modeling in a common structure. 3
1.3 Time-dependent effect on the structural behavior. 4
1.4 Development of loads model over time. 5
1.5 Examples of consequences of corrosion of steel in concrete (Bertolini *et al.*, 2016). 6
1.6 Scope of the Thesis. The proposed approach is the combination of three parts. 7

3.1 Collapse of Silver Bridge in 1967. 24
3.2 Mississippi River Bridge in Minneapolis and the gusset plate collapsed in 2007. 25
3.3 Robustness: structural property versus property of structure and environment (Cavaco *et al.*, 2013b). 27
3.4 Load measures needed to calculate redundancy of bridge systems proposed by (Ghosn and Moses, 1998) and (Liu *et al.*, 2001). 30
3.5 Damaged-based measure for robustness (Starossek and Haberland, 2008). The curve A represents the more robust structure and curve C the less robust structure. 31
3.6 Normalized structural response as a function of normalized damaged (Cavaco *et al.*, 2010). 33
3.7 Event Tree (Baker *et al.*, 2008). 36
3.8 Barrier Model, adapted from (Sorensen and Christensen, 2006). . . . 36

4.1 Comparisons between Finite Element Models. 42
4.2 general Framework for Global Analysis. 42
4.3 Beam-column element and its mechanical response under the generalized stresses. 43
4.4 Beam element notations. Static field. Nodal foces $\mathbf{Q}$. 45
4.5 Beam element notations. Kinematic field. Nodal displacements $\mathbf{q}$. . 45
4.6 Distributed loads on the beam element. 48
4.7 Second order geometrical non-linearity. 49
4.8 Static field of the *j-th* element *without* rigid body modes. 51
4.9 Kinematic field of the *j-th* element *without* rigid body modes. 52
4.10 Distributed loads and associated reaction forces. 54

4.11 Uniaxial $\sigma - \varepsilon$ constitutive law used to derive the generalized stresses N, M_y and M_z. 57
4.12 Torque-twist relationship under the hypothesis of uncoupling between torsional and flexural behavior. 58
4.13 Typical mechanical uni-axial response of steel and concrete materials. 61

5.1 Limit Analysis hypothesis: rigid perfectly-plastic behavior. 65
5.2 Limit Interaction Domains in the two distinct cases considered. . . . 66
5.3 Limit analysis: reference systems and conventions. 66
5.4 Yielding criterion for each *i-th* plastic domain, specialized according to the active generalized stresses. 69
5.5 Energy equivalence for the definition of the effectiveness factor. . . . 72
5.6 Interaction domain for a RC square section (Briccola *et al.*, 2013). . 74
5.7 Torsional resistance by the space truss model. 75
5.8 Interaction Torsion-Bending moment for a rectangular cross-section with different ratios r. 77
5.9 Corace Bridge (Calabria, Italy). 78
5.10 Limit Analysis. (a) Distribution of the plastic hinges which transform the structure into a mechanism. (b÷d) Points representing the ultimate values of the internal forces N and M on the linearized frontiers of the most relevant sections corresponding to plastic hinges in the arch and in the upper girder. 79
5.11 Axial force N diagram derived through both the analyses at incipient collapse. 80
5.12 Bending moment M diagram derived through both the analyses at incipient collapse. 80
5.13 Non Linear Analysis: deformed configuration until collapse. 81

6.1 An existing RC grillage deck in Italy. 86
6.2 RC grillage deck. Geometry and reinforcement of the characteristic sections. Details 1, 2 and 3 refer to the longitudinal beams section. Details 4 and 5 identify the cross-beams section (units in cm). 87
6.3 Reinforcements chracteristic and layout for the longitudinal beams. The encircled letters identify the type of stirrups. The letters c and v identify respectively the constant and variable segments of the longitudinal beam's section. 88
6.4 Structural model and loading conditions. The applied loads are composed of two parts: the fixed one, corresponding to dead loads and a variable part, distributed according to the traffic load arrangement. 88
6.5 Subdivision of longitudinal beam. 89
6.6 Limit Analysis of the sound grillage deck. Distribution of the plastic hinges in the structure and on the linearized frontiers of the most relevant sections. 90
6.7 Nonlinear Analysis of the sound grillage deck: progressive evolution of the whole deformed configuration until collapse (scale equal to 25). 90
6.8 Severe damage state in correspondence of the edge longitudinal beam. 91

6.9 Corrosion scenarios: longitudinal and sectional distribution of the aggressive agent. . . . 92
6.10 Maps of $C(x,t)/C_0$ concentration of the midspan section over time ($t = 0 \div 50$ years). . . . 93
6.11 Reduction of the steel area over time for the midspan damaged cross-section. . . . 93
6.12 Variation of the collapse multiplier and relative distribution of the plastic hinges on the deck at different time instants. . . . 94
6.13 Bending and torque moments along the edge longitudinal beam at incipient collapse for different sampling times ($t = 0 \div 50$ years). . . 95
6.14 Bending and torque moments along the central cross-beam at incipient collapse for different sampling times ($t = 0 \div 50$ years). . . . 95
6.15 Bending and torque moments along the end cross-beam at incipient collapse for different sampling times ($t = 0 \div 50$ years). . . . 95
6.16 Position of the point representing the ultimate values of the internal forces M_z and T on the linearized frontier of the midspan damaged cross-section over time corresponding to the plastic hinge in the edge longitudinal beam. . . . 96
6.17 Deformed shapes of the deck at different time instant under dead load only (scale factor equal to 180). . . . 97
6.18 Deformed shape under dead load only for different sampling times ($t = 0 \div 50$ years). . . . 98
6.19 Bending and torque moments along the longitudinal edge beam under dead load only for different sampling times ($t = 0 \div 50$ years). . 98
6.20 Bending and torque moments along the central cross-beam under dead load only for different sampling times ($t = 0 \div 50$ years). . . . 98
6.21 Deformed shapes of the deck at different time instant under the combined action of dead and traffic loads (scale factor equal to 25). . 99
6.22 The load-bearing capacity of the deck under the combined action of dead and traffic loads at different time instant. . . . 99
6.23 Distribution of the vertical reactions at the supports under the combined action of dead and traffic loads at different time instants. . . . 100
6.24 Comparison between collapse mechanism derived by LA and deformed shape obtained through NLA. . . . 101
6.25 Collapse multiplier over time by means of Limit and Nonlinear Analysis at certain damage state. . . . 101
6.26 Global measure of damage and robustness index at different sampling times. . . . 103
6.27 Robustness factor R estimation over time for the damaged grillage deck. . . . 103

7.1 Historical development of structural techniques for RC structures. . 106
7.2 Discretization technique in studying RC structural elements. . . . 107
7.3 Pattern of the Framework modelization for continuous systems. . . . 107
7.4 Bresler & Scordelis A1 Beam. Geometry and trusswork discretization. 109
7.5 Comparison between ultimate values in the resistant domains. . . . 110
7.6 Bresler & Scordelis A1 Beam. Limit Analysis results. . . . 111

7.7 Qualitative comparison for Bresler & Scordelis A1 Beam results. . . 111
7.8 Deep Beam WT2. Geometry and trusswork discretization. 112
7.9 Comparison between ultimate values in the resistant domains. 113
7.10 Deep Beam WT2. Results coming from Limit Analysis. 114
7.11 Qualitative comparison for WT2 Deep Beam results. 115
7.12 RC Corbel. Geometry and trusswork discretization. 116
7.13 Comparison between ultimate values in the resistant domains. 118
7.14 Qualitative comparison for the results of RC Corbel. 118
7.15 RC Corbel. Plasticized elements in tension (red) and compression (blue) and corresponding collapse mechanism (left). The sketch in the right side highlights location and direction of these elements, where the color intensity is proportional to their bearing capacity. . 119

A.1 Neighbourhoods for 2D Cellular Automata with radius $r = 1$. 123
A.2 Modeling of cross section reduction of a steel bar, adapted from (Titi, 2012). 124
A.3 Model. 125
A.4 Modeling of mechanical damage: (a) time evolution of the damage index during diffusion process; (b) linear relationship between rate of damage and concentration of the aggressive agent. 126

List of Tables

2.1 Main requirements for structural safety, EN 1990 (2001). 14
2.2 Common weaknesses in RC continuous cantilever bridge. 16
2.3 Common weaknesses in RC and PC decks. 16
2.4 Common weaknesses in steel cantilever bridge. 17
2.5 Common weaknesses in truss bridges. 17
2.6 Common weaknesses in arch bridges. 18
2.7 Common weaknesses in cable-stayed bridges. 18
2.8 Common weaknesses in suspended bridges. 19
2.9 Common weaknesses after repairing interventions. 19

3.1 Adopted approach to characterize the robustness of existing structures. 38

5.1 Limit Analysis Theorems: Input & Output variables. 71
5.2 Different analysis for the Corace Bridge. N.L.G. = Non Linear Geometry, N.L.M. = Non Linear Mechanics. 81
5.3 Comparisons among different Different Limit Analysis for the Corace Bridge. N.L.G. = Non Linear Geometry, N.L.M. = Non Linear Mechanics. 82
5.4 Comparisons among different Nonlinear Analysis for the Corace Bridge. N.L.G. = Non Linear Geometry, N.L.M. = Non Linear Mechanics. . 82

6.1 Distribution of stirrups in the beams. 89
6.2 Material's characteristics 89

7.1 A1 Bresler & Scordelis Beam: materials characteristics. 109
7.2 Resistant domains in the equivalent trusses made by concrete only. . 110
7.3 Resistant domains in the equivalent trusses made by concrete and steel. 110
7.4 Deep Beam WT2: materials characteristics. 112
7.5 Resistant domains in the equivalent trusses made by concrete only. . 113
7.6 Resistant domains in the equivalent trusses made by concrete and steel. 113
7.7 RC Corbel: materials characteristics. 117
7.8 Resistant domains in the equivalent trusses made by concrete only. . 117

7.9 Resistant domains in the equivalent trusses made by concrete and steel. 117

1

Introduction

The objectives of the thesis are presented and outlined with the aim of proposing a synthetic methodology handling the robustness assessment of reinforced concrete structures based on time-variant capacity that account for environmental hazards. Focus is given to the main reasons for which a study on existing structures has been carried out.

1.1 Motivation and Problem Statement

Structural design and assessment criteria must evolve over time in order to cope with new challenges and solve, thanks to a better understanding, drawbacks emerging from previous mechanical and technological approaches.

During the last decades many studies have been carried out to better investigate the deterioration processes of existing structures, due to inadequate design, aggressive environmental causes, fatigue and increased traffic loads. A special attention has been given to reinforced concrete (RC) structures. In addition to deepening the understanding of the damaging causes, aim of these studies is to guarantee an adequate structural safety during the residual service life of aged structures.

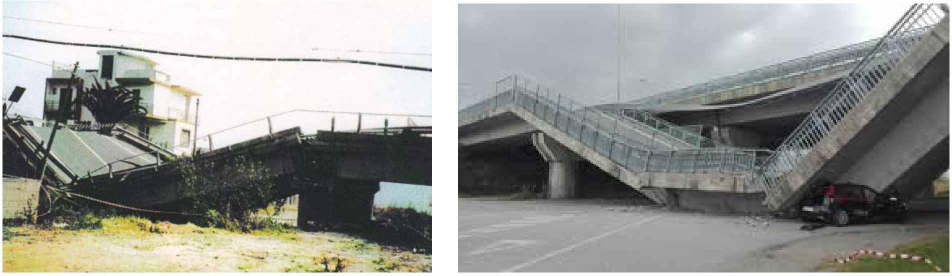

(a) Santo Stefano Viaduct.

(b) Fossano Bridge.

Figure 1.1: Famous Bridges Collapses in Italy.

Part of the aforementioned shortcomings was due to lack of knowledge or to excessively simplified computations; another was due to a naïve confidence in apparently well-known materials. The combination of these factors has resulted in several structures having an actual service life rather shorter than the one expected, usually 100 years, with consequent impacts on the functionality, inspection and maintenance costs of the infrastructural systems. Moreover, the need of researches in this field is periodically pushed by the occurrence of catastrophic collapses, as in Fig. 1.1.

In this context, many Road and Highway Administrations are faced with two typical problems:

(a) when designing new bridges, the capacity to estimate their bearing capacity and safety level after a certain amount of years from construction and under given environmental and service conditions;

(b) for existing bridges, the capacity of assessing (1) their residual bearing capacity in their actual damaged state, (2) their residual life-cycle and (3) the possibility of a sustainable extension of their service life.

Object of the thesis is to propose a methodology that can be applied to assess the existing structures. Core of the Thesis is the Limit Analysis of frames, with the whole structure or selected parts of it subjected to a certain damage state. Aim of the analysis is to highlight the collapse mechanism and the redistribution capacity of the internal forces, in order to detect the weakest parts, to assess the influence of a certain type of damage and to explore the effectiveness of repair hypotheses.

In particular, a procedure for *a virtual loading test* is proposed, consisting in the exam of a structure at different damaged states and in the evaluation of the multiplier at collapse of a given additional traffic load distribution. The search for these limit behaviors may be seen as a lifetime structural robustness estimation, tailored on the actual or supposed damaging characteristics of a given structure. Moreover, such an approach allows to outline the consequences due to different damage factors and the modes which lead to sudden collapses, when neither weakness signals nor intermediate anomalous behaviours appear.

1.1.1 DEALING WITH EXISTING STRUCTURES

Dealing with existing structures, we cannot avoid framing them into the context of their time. The major aspects that must be taken into consideration usually regard: the concepts which led to choosing that specific shape for the structure, the theories and methods used for design and safety checks, the models assumed for characterizing the material properties, the nominal loading conditions and the role of the environmental conditions.

1.1.1.1 INFLUENCE OF THE STRUCTURAL MODELING

Up until fifty years ago, structural analyses were based mainly on elastic computations and the algebraic difficulties were overcame by means of special methods like the Hardy Cross Method or, for the case of the arch bridges, the Theory of the Ellipse of Elasticity.

The modern computational tools are based on wider mechanical bases and are able, potentially, to solve any kind of structural problem, linear and/or nonlinear, coping with thousands degrees of freedom. However, each structural system involves different scales of analyses. For a given structure, it is possible to identify a dominant behaviour, characterizing the essential structural response in terms of end support reactions, maxima and minima internal forces, maxima and minima displacements. Then there are the local problems, regarding, for instance, nodes at which the structural members are connected, presence of geometrical singularities, sudden changes of thickness or limited areas on which intense loads are transmitted.

One of the more relevant achievements of the actual assessment and design methods is a clear distinction between global and local behaviours. The first one can be detected with basic modellization of the whole structure, with a limited number of degrees of freedom, but still suitable to derive the most important parameters governing the main structural checks or provide the data allowing a preliminary design of the structure. The local behaviours are the object of separated local analyses. Conventionally, for frame-like structures (Fig. 1.2), slender members are defined B-regions (B for Bernoulli), while the others, involving local stress diffusion states, are defined D-regions (Schlaich and Schafer, 1991).

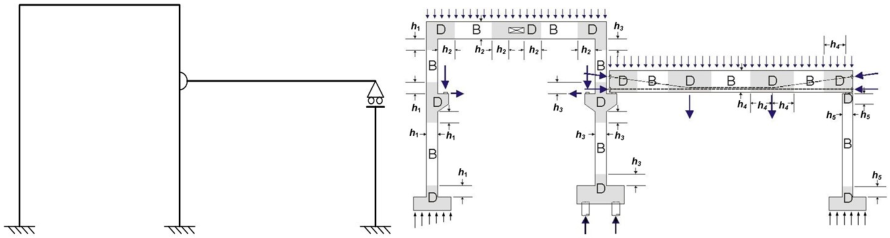

(a) 1D modeling. **(b)** B and D regions subdivision.

Figure 1.2: Different structural modeling in a common structure.

In this Thesis, the structural modeling is based on the finite beam-column element (1D model). The main reasons that justify this choice are:

1. Monodimensional modeling (1D) works through generalized stresses (axial force and shear forces, bending and torsional moments) and generalized displacements (elongations and curvatures), that is with the same reference quantities at the basis of the sectional checks;
2. 1D modellization allows a quick and thorough interpretation of the results;
3. 1D modellization may be extended also to study continuous systems, by means of "equivalent" frameworks, similar to Hrennikoff frame models.

1.1.1.2 INFLUENCE OF MATERIALS MODELING

Before the advent and diffusion of computational methods, structural analyses were based mainly on elastic calculations and safety checks were referred to allowable stress levels, usually assumed as a fraction of the ultimate stress. For this type of analyses, the only characteristic of the structural material that needed to be known was the elastic modulus, and the safety assessment was based on conventional assumptions, without a true measurement of the level of safety.

Actual analyses and actual sectional checks need reliable constitutive models both for concrete and steel, as well as for any other structural material that may be involved in the construction. A particular problem concerns the time dependent effects of reinforced and prestressed concrete structures, due to creep and shrinkage. These phenomena may induce quite different behaviours: in some cases, they have little relevance with respect to both the serviceability and ultimate states, while, in other cases, they play a crucial role for meeting the required performances both at the beginning and at the end of the expected service life of a structure.

The experiences of the last decades showed significant serviceability drawbacks, like, for example, wrong estimations of prestress losses, excessive vertical displacements, slope discontinuities and longitudinal displacements greater than the design values used for dimensioning of joints and bearing supports (Kristek *et al.*, 2006). Such shortcomings cause severe reductions of durability and of ride comfort and may represent a triggering cause of serious mechanical damages, as shown in Fig. 1.3.

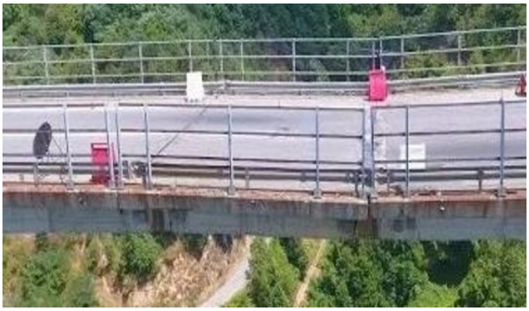

Figure 1.3: Time-dependent effect on the structural behavior.

Modern analyses may be based on reliable creep and shrinkage models, as well as validated numerical methods for long time predictions of delayed behaviours.

1.1.1.3 INFLUENCE OF THE LOADING CONDITIONS

Existing bridges were designed for the nominal loads prescribed by the codes of the time of construction (Fig. 1.4): for instance, 100 years ago, the load train for road bridges was made of a row of 16 metric ton carts, 6 m long, pulled by a team of four couples of horses, 10 m long and ($4x1.4$) ton heavy. The maximum rail bridge loads were $30 \div 60\, kN/m$. It must be remembered that, in those times, the speed was also lower and that usually only two lanes were sufficient (Malerba, 2014).

From those times, speed and traffic intensity, as well as the loads for axle, have gradually increased and today there is demand for heavier and heavier overloads. Moreover, nowadays a specific attention must be paid to seismic and wind actions.

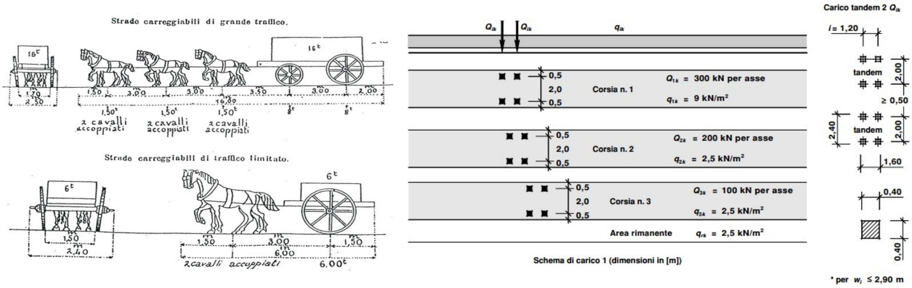
Strado carreggiabili di grande traffico.
16t
1,50t
2 cavalli accoppiati
2 cavalli accoppiati
2 cavalli accoppiati
Strado carreggiabili di traffico limitato.
6t
2 cavalli accoppiati
6.00t
Carico tandem 2 Q_{ik}
Q_{ik}
Q_{ik}
q_{ik}
Corsia n. 1
Q_{1k} = 300 kN per asse
q_{1k} = 9 kN/m²
Corsia n. 2
Q_{2k} = 200 kN per asse
q_{2k} = 2,5 kN/m²
Corsia n. 3
Q_{3k} = 100 kN per asse
q_{3k} = 2,5 kN/m²
Area rimanente
q_{rk} = 2,5 kN/m²
Schema di carico 1 (dimensioni in [m])
tandem
tandem
* per $w_l \leq 2{,}90$ m

(a) After Italian DM 06.05.1916.

(b) Model 1 recommended by Italian Code.

Figure 1.4: Development of loads model over time.

1.1.1.4 Concerning the Materials

The effects of the environmental aggressiveness are shown by clear signals, like:

- wear of the surfaces and microcracking patterns, which signal a probable incubation of corrosive phenomena. Carbonation and chlorides may foster the penetration of aggressive agents towards the rebars;

- visible deformation and/or alteration of the structural geometry, mainly due the time-dependent effects;

- visible cracking patterns, both in main and secondary elements. At this stage, the corrosive action has begun and is signaled by the expulsion of concrete covers and the formation of stains and visible rust;

- generalized corrosion. Without remedial interventions and restoration, the state of degradation increases until integrity is lost (De Sitter, 1984).

The presence of a certain degree of damage changes the analysis criteria. The simplest approach assumes an approximated reduction of capacity of the damaged elements (typically a reduction of the steel area) or even that the most severely damaged elements are neglected in the model. Recent experimental and numerical researches lead to numerical approaches suitable to accurately model the damage diffusion for different types of aggressive agents, like carbonation, chloride attack, icing and de-icing cycles and ice abrasion. Such approaches allow to follow the damage diffusion in the volume of structural the members over time. On the bases of surveys, measurements and the signs detected on steel bars and on the surface of the element, these algorithms allow to model the damage effects into the element volume and upgrade the mechanical and/or geometrical characteristics used in the analysis.

In this work the diffusion process at the macroscopic level is carried out through a special evolutionary technique called Cellular Automata.

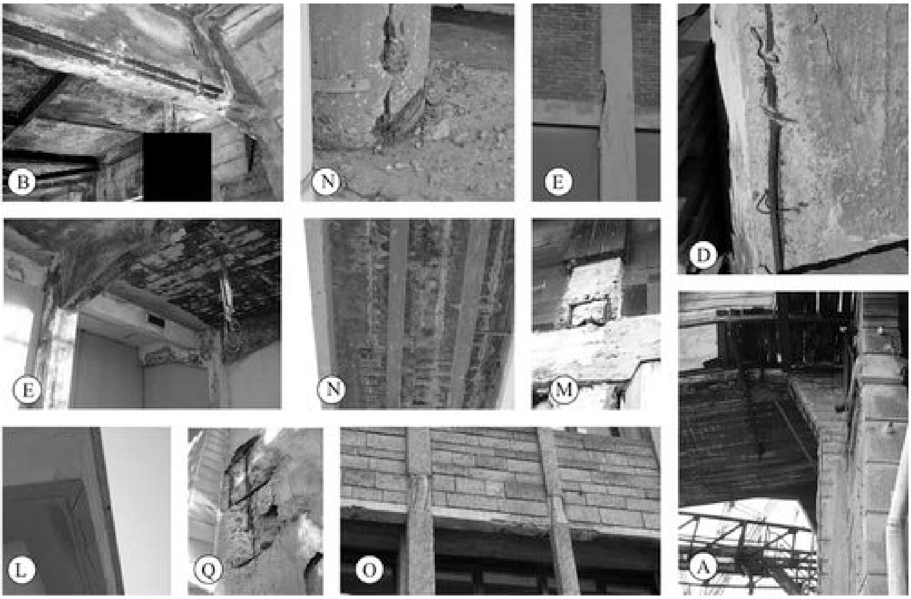

Figure 1.5: Examples of consequences of corrosion of steel in concrete (Bertolini *et al.*, 2016).

1.2 SCOPE AND OBJECTIVES

Main goal of the Thesis is to present an effective and direct approach to evaluate the actual bearing capacity of a structure subjected to a given or simulated damage scenario. We will then apply this tool to qualitatively estimate its structural robustness.
The Thesis is composed of three parts:

(1) a review of the factors which condition the durability of a structure and a collection of the most frequent defects depending on the weakening of structural details;

(2) the study of the behaviour of the structure as a whole. Starting from the definition of the structural integrity limit state (SILS), the objective is to characterize the robustness at the global level, investigating the time-variant evolution of the structural performances;

(3) the study of elements belonging to the so-called D regions by means of the Limit Analysis and an equivalence method, in order to investigate, with the same approach, the diffusion zones as well.

These three parts are initially completely independent. In particular, the first one addresses the general criteria to meet the requirements at the different limit states. The second and third parts concern mainly the structural analysis and the computational aspects in modeling monodimensional RC elements and RC structures. The structural analyses are based on the Limit Analysis (LA) approach, taking into account iether axial-bending or bending-torque interaction. We consider such an approach the most synthetic and effective for the purposes of this work. Comparisons between the results given by the Limit Analysis and those given by the Non Linear Analysis are presented.

A development of the proposed study concerns the modelization of diffusion zones by reducing membrane elements, like deep beams, corbels, irregular walls, to networks of beam or truss elements, to be analyzed with the same basic Limit

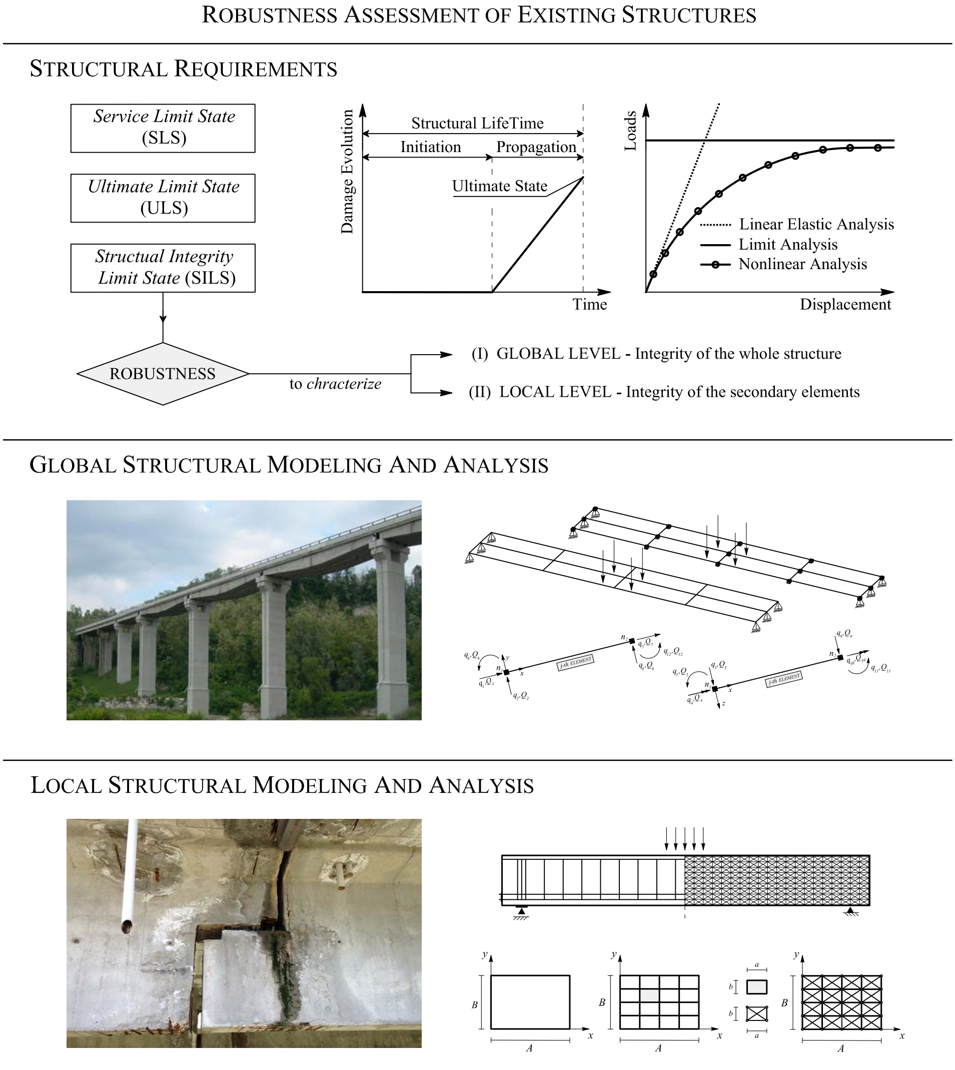
ROBUSTNESS ASSESSMENT OF EXISTING STRUCTURES
STRUCTURAL REQUIREMENTS
Service Limit State (SLS)
Ultimate Limit State (ULS)
Structual Integrity Limit State (SILS)
Damage Evolution
Structural LifeTime
Initiation
Propagation
Ultimate State
Time
Loads
Linear Elastic Analysis
Limit Analysis
Nonlinear Analysis
Displacement
ROBUSTNESS
to chracterize
(I) GLOBAL LEVEL - Integrity of the whole structure
(II) LOCAL LEVEL - Integrity of the secondary elements
GLOBAL STRUCTURAL MODELING AND ANALYSIS
j-th ELEMENT
LOCAL STRUCTURAL MODELING AND ANALYSIS
y
x
B
A
a
b

Figure 1.6: Scope of the Thesis. The proposed approach is the combination of three parts.

Analysis tools.

Finally, these methods will be used to investigate the structural lifetime performance of existing structures. For each damaged state, the structure is subjected to a *virtual loading test* under the most severe loading conditions for that state. The partial results under different damage states are used to carry out a robustness estimation of the particular structure studied.
The principal results will concern:

1. the role played by the main structural elements in the redistribution process studied by the analyses;
2. the effects due to localized damages;
3. the characterization of the progressive reduction of structural performances;
4. the warnings deriving from a mechanical deterioration process, which may lead to a sudden collapse.

Such results may give a contribution in assessing the performances of the existing structures and in answering to the basic questions concerning the safety of critical infrastructures, in particular bridges, as well as to guide the decisions in terms of proper maintenance actions and/or rehabilitation interventions.

1.3 RESEARCH SIGNIFICANCE

This Thesis proposes a methodology able to outline how the consequences due to different deterioration factors may lead to a loss of structural integrity end/or to a sudden collapse, without showing neither signals of weakness nor intermediate static equilibria.

Two approaches are used: the *Limit Analysis* and the Non Linear Analysis. As highlighted through the case studies, the Nonlinear Analysis gives us the evolution of the structural behaviour, in terms both of displacements and internal forces, all along the load path until the collapse, while the Limit Analysis presents in a more synthetic way the ultimate behaviour. Limit Analysis seems to be most effective in judging the capacity of a structure to assume, or not, alternative load paths.

Thus, a procedure for a *virtual loading test* is proposed, consisting in the exam of a structure at different damage states and in the evaluation of the multiplier at the collapse of a given additional traffic load distribution. A synthesis of the results is given by examining over time the damage evolution, the internal forces redistribution, the loading capacity of the structure and by associating to this evolution a robustness index, which obviously decreases with time. Thus, the data resulting from the Limit Analyses is useful to highlight the essential details of such an evolution, showing how the internal forces redistribute from damaged to undamaged structural parts.

All the numerical procedures proposed in this Thesis have been coded in specific computer programs written in MatLab(1), by using some basic techniques from object oriented programming methodologies. The so-obtained codes interact with other structural tools and are open to future improvements.

---

(1) Matlab is a registered trademark of The MathWorks Inc., 24 Prime Park Way, Natick, MA 01760-1500, U.S.A. Web: `http://www.mathworks.com`.

In addition to safety and robustness assessments, the present methodology may be useful in evaluating the effectiveness of repairing interventions.

1.4 CONTENTS OF THIS DOCUMENT

The Thesis is composed of these parts:

1. Structural Requirements - concerns the main requirements related to the limit states that need to be met. The main aim of this part is to discuss the methodologies and procedure for the assessment of existing structures. In particular:

   - Chapter 2 reviews the problem of structural safety, focused on the identification of common weaknesses in bridge structures, aimed to find solutions to extend their performance and service life;
   - Chapter 3 outlines the robustness evaluation with respect to RC structures exposed to an aggressive environment. It recalls previous deterministic, probabilistic and risk-based robustness measures for different types of structures. Among many indexes, we prefer to propose a new methodology based on a *virtual loading test*, used to estimate the robustness at the global and local level;

2. Global Structural Modeling and Analysis - presents the methods of structural analysis suitable to deal with nonlinear behavior of RC structures. The main aim of this part is to study the structural performance of the whole structure, according to its actual state. In particular:

   - Chapter 4 deals with the review of monodimensional modeling for frame structures. Dual formulations are applied in order to define the beam element, while the determination of the section state depends on the interaction mechanism between normal and tangential stresses;
   - Chapter 5 presents the Limit Analysis formulation for a RC beam element. After reminding the main hypotheses of the Upper and Lower Bound Theorems, the definition of the resistant domains according to the active generalized stresses is recalled. A thorough benchmark is carried out, by analyzing an arch bridge and comparing the results to those obtained from the nonlinear approach;
   - Chapter 6 studies an existing RC grillage deck with severe damages. By using the Limit Analysis, the results lead to a robustness assessment of the structure and the complementary information are derived through the nonlinear analysis. The main conclusions provide an answer to the basic questions concerning the safety and robustness level of a structure and guide the decisions in terms of maintenance interventions;

3. Local Structural Modeling and Analysis - after recalling previous contributions to frame analyses, a coupling of Limit Analysis and Framework Modeling is proposed for the study of RC membrane elements. Such a discretization technique, in addition to the determination of the load multiplier and the mechanism of collapse of the structure, allows also to provide useful indications on the position and orientation of the compressed struts and on the distribution of the plasticization in the tensioned elements, with results comparable with those of conventional strut and tie models;

4. Appendix A - presents the damage process and its modeling through a diffusivity equation. The problem is solved through the Cellular Automata algorithm. The effects of the damage are then specialized to the case of RC elements. The damage indexes, concerning both steel and concrete, are introduced and then tested for different reinforcement layouts. For its generality, the so-obtained damage models can be jointed with any structural analysis procedure.

Finally, the main conclusions and possible future developments are outlined.

2

Structural Safety versus Structural Weaknesses

This chapter focuses on the general aspects and the main requirements related to the assessment of the existing structures, which are reaching their ultimate lifetime and require increasing inspection and maintenance costs. A great attention is given to the factors causing damage, which lead to identify the common weaknesses of the most representative bridge schemes.

2.1 INTRODUCTION

All over the world, RC and PC bridges and viaducts with more than 40-60 years of service life exhibit more or less severe damage states, which reduce their structural reliability and require increasing inspection and maintenance costs. As concerns the safety assessment, such a situation leads to two typical problems:

(a) in designing new bridges, estimating their bearing capacity and safety after a certain amount of years from construction time and under given environmental and service condition;

(b) for existing bridges, assessing (1) their residual bearing capacity in their actual damaged state, (2) their residual life-cycle and (3) the possibility of a sustainable extension of their service life.

As concerns the interventions to be adopted, we must choose among several solutions, different in terms of performance, duration and cost. Typically:

- the structure can be repaired aiming to restore conditions close to the initial ones;

- the structure can be repaired removing past drawbacks and eliminating weaknesses emerged during its service life, but also strengthening selected structural members or details and increasing its whole performance;

- respecting the original layout of the bridge (ends connections with the approaching sides, span distribution, clearance under/over the bridge) one can choose to change the original static scheme. Typical solutions are: make continuous articulated spans, adjoin external prestressing cables, insert diagonal struts, which, starting from the body of the piers, contribute to support the deck. Obviously, these radical changes which must be justified and motivated by unavoidable infrastructural needs.

Between the problems statement and their solutions, we have to definite a set of criteria and methods in order to guide judgments and decisions. These criteria and methods concern:

1. the damage detecting methodology, the surveying reliability, the interpretation of the survey reported data;
2. the level of knowledge reached on the basis of the original documentation and on the inspection results, or, in other words, the awareness of the actual integrity/damage state of the bridge;
3. the safety criteria to be assumed in assessing structures under time variant damaging states;
4. the measurement of structural improving of the structure performance after the intervention.

At the end one must know if its structure is safe and for how many years, or better if its structure has been improved, not only recovering its original characteristics, but also becoming more robust.

From the methodological point of view, a first problem consists in modeling in a rational way the damage states. Such states may be assumed as described by the direct results of the surveys, or they may be modelled by means of numerical techniques, able to predict degradation of mechanical properties, or, in the end, may be derived from suitable matching of surveying and theoretical/numerical results. After the quantification of the mechanical damage, the second problem involves the assessment of the structural performance in the damage state at a given time of its life.

In this work we try to solve both problems through a unified approach, consisting of an analysis of the diffusion of the deterioration processes induced by aggressive agents, accompanied by the analysis of the damaged structure. This allows, at a certain instant, the direct evaluation of the load bearing capacity and the detection of the collapse mechanism. Organizing such an analytical tool according to predefined damage scenarios and timing sequences we shall qualitatively characterize the structural robustness in the assessment framework, both at global and local level.

2.2 SAFETY AND SAFETY ASSESSMENT OF EXISTING STRUCTURES

In assessing existing structures, old codes and regulations assumed the same rules as for the new ones. Since the two last decades only, the most important modern codes contain special chapters dedicated to existing structures and special rules, differentiated in function of the construction and material typologies.

In truth, the approach to an existing or old structure involves wider perspectives, which must consider also the effective sustainability of the restoring operations and the advantages or disadvantages in prolonging its service life.

(Vrouwenvelder, 1996) synthesizes the differences between the two problems as follow:

1. Increasing safety levels usually involves more costs for an existing structure than for structures that are still in the design phase. The safety provisions embodied in safety standards have also to be set off against the cost of providing them, and on this basis, improvements are more difficult to justify for existing structures.

2. The remaining lifetime of existing structures is often less than the standard reference period of 50 or 100 years that applies to new structures. The reduction of the reference period may lead to reductions in the values of representative loads as for instance indicated in the Eurocode for Actions.

3. For an existing building or bridge structure, actual measurements with respect to geometry, material properties and behavior under normal or design circumstances (e.g. settlements, cracks, corrosion, survival of certain loads, etc.) may be made in order to reduce uncertainty.

2.3 STRUCTURAL SAFETY DEFINITIONS

At the basis of any safety criteria, there is the problem of the uncertainties which affect geometrical and material characteristics, type, intensity and distribution of the loading conditions. For the existing structures, we must add the need of actual knowledge the structure, in the hidden parts also.

As outlined by (Casciati *et al.*, 2014), the "data" are more or less "imprecise". Hence, the structural safety has become a problem of defining the probability of collapse of a structure, which has to account for the aleatory nature of the variables.

The effects of collapse must be referred to the safety of the people affected by the structural failure. In defining such probabilities SIA 260 Building Code states that:

"A structure can be declared safe if during a critical event, like impact, fire downfall, safety of people is granted".

As pointed out by (Giuliani, 2009), accordingly to this definition safety could be provided also by means of non-structural measures aimed at reducing the exposure of the structure to critical events. In ISO 2394 the safety is put in relation to the structural integrity of the structure. This code specifies:

"Structures and structural elements should be designed, built and maintained in such a way to be proper for their use during the structure's design life in an economical way. Particularly they should, with a proper level of reliability:

a. *safety exercise ultimate state requirements;*

b. *safety load ultimate state requirements;*

c. *safety structural integrity requirements."*

A synthetic frame of the requirements to be accounted for a safety checks is given in Tab. 2.1, with the following meaning of the notations:

- *SLS* means Serviceability Limit State;
- *ULS* means Ultimate Limit State;
- *SILS* means Structural Integrity Limit State.

Limit State	*SLS*	*ULS*	*SILS*
Main requirements	STIFFNESS	RESISTANCE	ROBUSTNESS
Verification level	Fibre(stresses) Element(displacem.)	Section(solicitation) Element(buckling)	Structural System

Table 2.1: Main requirements for structural safety, EN 1990 (2001).

In a more detail, the safety requirements can be classified as follows:

- safety with regard to Serviceability Limit States (SLS) means that all the requirements which can guarantee the performance levels laid down for the operating conditions are satisfied;
- safety with regard to Ultimate Limit States collapses, requires avoiding loss of equilibrium and serious total or partial instability which may endanger persons or result in the loss of goods, or cause serious environmental and social harm or put the structure out of service.
- robustness with regard to accidental actions represents the ability to avoid damage disproportionate to the scale of the triggering cause such as fire, explosion, impact or the consequences of a human error.

In the last definition, the safety associated to the impossibility to overcome of the predeterminated levels of resistance and functionality is well documented by the modern codes and related to the assessment of individual elements or components. Acceptable levels of structural integrity and related concepts are not addressed in the codes. In this case, SILS refers mainly to the overall behavior of the structure after the occurrence of a critical event: this limit state has to be assumed as possible, in order to restrict the consequences.

2.4 STRUCTURAL SAFETY IN BEING

Sometimes there is a strong contrast between the reassurances derived from theoretical assessments and the direct view of the damaged parts of a bridge. In many cases such a bad sensation derives from the state of the surfaces, without a true relationship with the actual weakness of the member examined, but, in other cases, the visual inspections allow an effective and sound signal of misfunctioning. Moreover, many types of bridges exhibit recurrent and typical misfunctioning situations or damage states. Many of these damages concern localized parts frequently considered as secondary. On the contrary, the experience is showing that many dramatic collapses started from the breakage of apparently meaningless detail.

The following tables summarize the most frequent cases conditioning both the local and global integrity of a bridge structure.

2.4.1 CANTILEVER BRIDGES

As shown in Tab. 2.2, the Gerber type bridge is a continuous bridge, hinged at certain sections, typically at the points of reversion of flexure. These structures are statically determined and don't feel the influence of settlements of foundations. Moreover, there is the possibility of arranging special equipment for the intermediate construction stages, without the need of falseworks that would obstruct rivers during construction. Cantilever bridges have given a fundamental contribution to the bridge development and many of them are still in service. The long period of use of the Gerber bridges allows us to ascertain their performances over time and to highlight, also, their major drawbacks. Joints and articulations must work as hinges. For the same geometry and loading conditions, articulated girders are statically/kinematically equivalent to continuous ones, if the articulations are placed at the sections with zero bending moment in the corresponding continuous scheme. But these hinges allow also a relative rotation between the two ends of the cantilevers. Such a local discontinuity fosters the dynamic effects in the neighborhood of the hinges and causes severe damages both at these devices and at their interfaces with the main structure. Moreover, the increase of the dynamic effects on the cantilever beams induces fatigue stresses in upper reinforcing bars and tendons for negative moments. In RC and PC structures the arise of cracks may favor the corrosion of the reinforcement.

2.4.2 STEEL BRIDGES

Steel bridges (Tabs. 2.4 and 2.5) built at the beginning of the twentieth century are characterized by less resistant materials and construction techniques very different with respects to the current ones. Typical of that era was the use of structural elements composed by riveting elementary steel shapes (angles and sheets) placed side by side and without gaps among their surfaces. After decades of service, we are seeing dangerous distortions of such composed members, due to rust grown inside the interstices and to the swelling of this rust layer over time. Rust expansion causes distortions of the steel profiles and may induce member instabilities.

2.4.3 RC & PC BRIDGES

Common damages observed on RC and PC medium-long span bridges are mainly due to the aging of the construction and lack of maintenance, as shown in Tabs. 2.3 and Tab. 2.6. They can be resumed as surface wearing carbonated surfaces, spalling

Structure	Weak Signals	
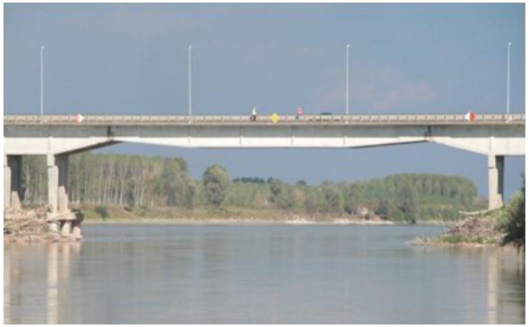	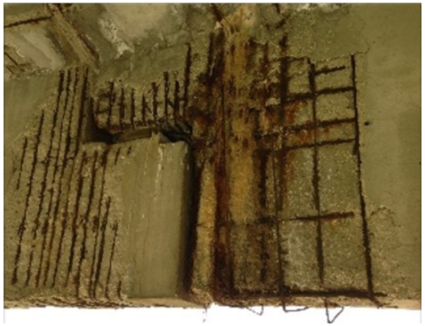	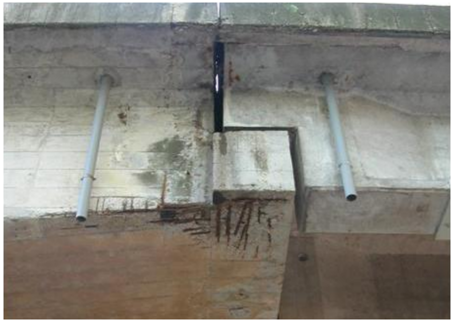

Table 2.2: Common weaknesses in RC continuous cantilever bridge.

Structure	Weak Signals	
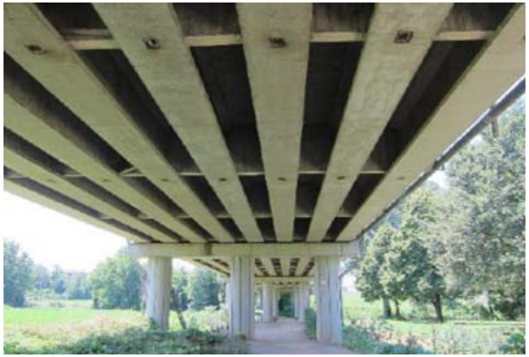	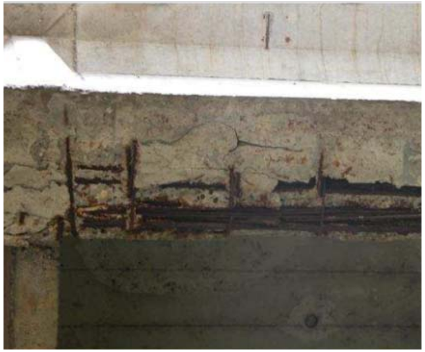	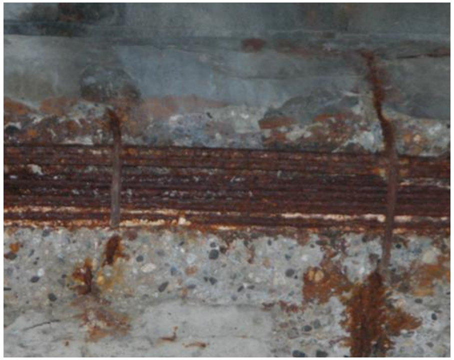

Table 2.3: Common weaknesses in RC and PC decks.

Structure	Weak Signals	
	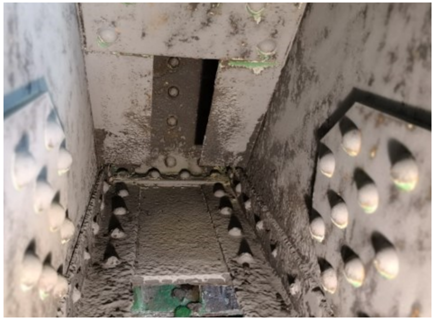	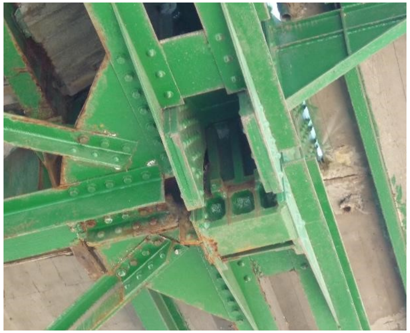

Table 2.4: Common weaknesses in steel cantilever bridge.

Structure	Weak Signals	
	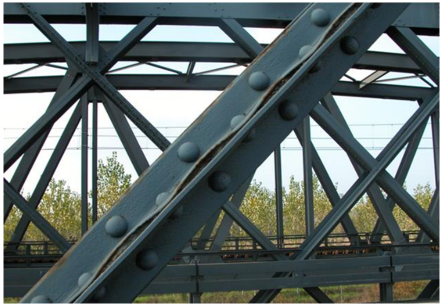	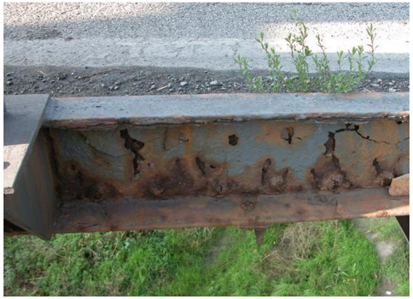

Table 2.5: Common weaknesses in truss bridges.

Structure	Weak Signals	
	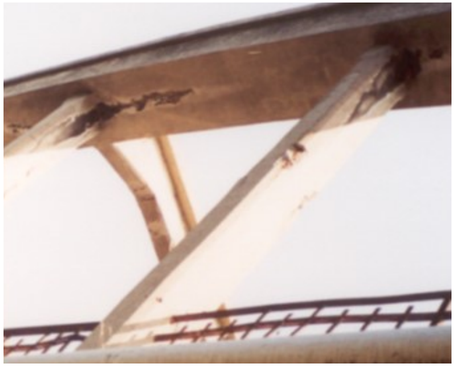	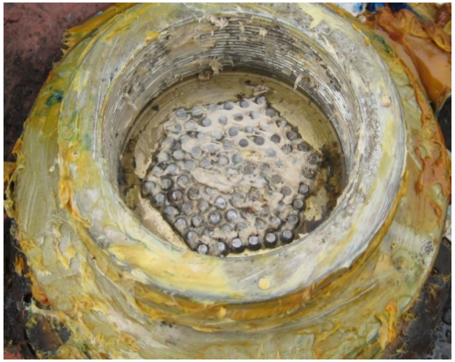

Table 2.6: Common weaknesses in arch bridges.

Structure	Weak Signals	
	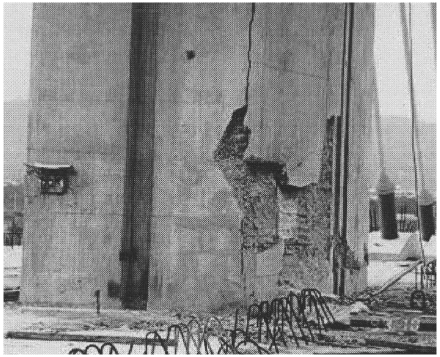	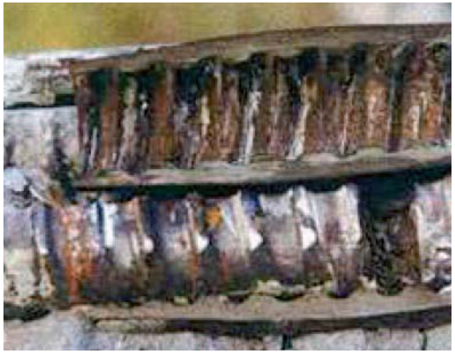

Table 2.7: Common weaknesses in cable-stayed bridges.

Structure	Weak Signals	
	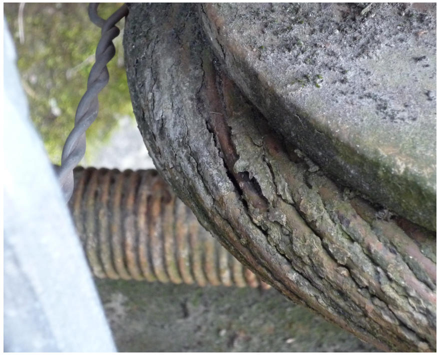	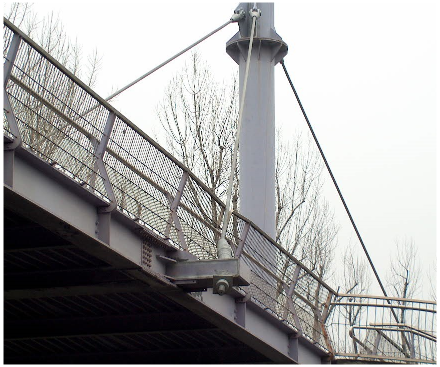

Table 2.8: Common weaknesses in suspended bridges.

Structure	Weak Signals	
	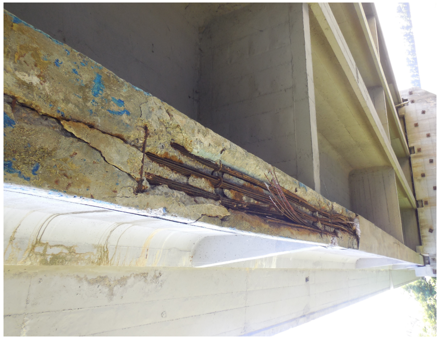	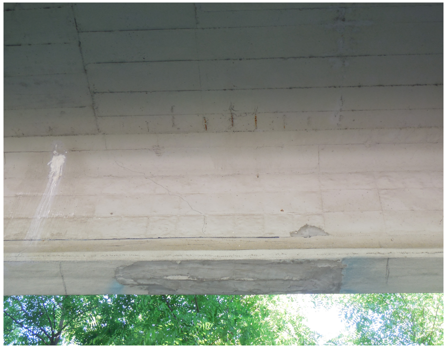

Table 2.9: Common weaknesses after repairing interventions.

at the corners of beams and columns and at the bottom of the slabs and onset and diffusion of steel corrosion. It is important to outline how the majority of these damages are due to inefficient drainage systems. In long cantilever girders, both articulated and continuous, typical malfunctions are due to insufficient analysis of the time-dependent effects, causing excessive shortening and/or excessive deflections. Another cause is the incorrect use of prestressing in governing the static and deformed configuration of the structure.

2.4.4 SUSPENSION & CABLE-STAYED BRIDGES

The most frequent drawbacks are damages in the hangers and risk of detachment of the hangers from the collars connecting them to the main cables; excessive slackness of a stay due to loss of pretensioning; breakage of a stay due to fatigue or corrosion (Tab. 2.8).

2.4.5 REPAIR INTERVENTIONS

Dealing with existing bridges, the repair interventions are generally carried out on *(i)* the foundation systems (piers, basements and piles), *(ii)* the main structures of the bridges and *(iii)* their complementary or special devices. For example, the need for an intervention on the foundations arises mainly after their stability has been checked according to new codes and regulations, which lead to higher depths of the estimated scour holes and higher values of the acting forces. This brings to strengthening the original foundation systems in order to obtain a suitable safety level. However, a common problem of these type of interventions is the accomplishment of a robust connection between new parts and old structures (Malerba, 2014). Differently, the main interventions needed on the structures of a bridge concern the strengthening of the carrying structure due to some lack in their load-bearing capacity, refurbishment and adjustment of the structure to new codes prescriptions and the need of widening the road platform. A lack of efficiency of the interventions may cause a weakness in the structure, as shown in Fig. 2.9.

Special sensitivity of the weak parts is connected with the structures itself, with an improper design of the sub-systems, with the growing of loads, and with the weather and environmental aggressiveness. Such a posteriori evaluation is not intended as a critic of a praiseworthy past, but rather as an opportunity for examining the common weaknesses of these structures, so as to conceive practical solutions to extend their service life.

2.5 CLOSING REMARKS

In this chapter, general aspects and the main requirements related to the problem of assessing the structural safety have been recalled. Safety and structural integrity must be assessed checking both global and local behaviours and fixing suitable levels for service (SLS), ultimate (ULS) and structural integrity ($SILS$) Limit States.

Recurrent weaknesses of the bridge structures have been highlighted both in relation to their static scheme and of typical damages at the detail level.

Identification of these weaknesses during the lifetime of the structure may be carried out by means of methods suitable to detect the mechanism according to which the structure evolves toward the collapse and to specialize such research to the actual damage state physically detected or theoretically modeled with reference to a given environmental exposition.

3 About Structural Robustness

In this chapter, some definitions for robustness concept as well as for other related characteristics are recalled. In order to assess and quantify structural robustness, measures and tools are here reviewed with reference to the latest advances in the research. In the end, the adopted philosophy for the assessment of existing structures is presented, aimed to provide a lifetime structural robustness estimation.

3.1 GENERAL CONCEPTS

Recent tragic events have shown catastrophic collapses. In many cases, the total loss of structural integrity was caused by a local failure in some critical element. A *disproportionate collapse* occurs when an initial local failure, that is produced by some small triggering event, leads to widespread failure of other structural components such that a major part of the structure collapses (Starossek, 2007b), (Ellingwood and Dusenberry, 2005). Such a phenomenon is also referred to as *progressive collapse.* Progressive collapse can be produced by different mechanisms which depend on the type and form of a structure and its orientation in space, as well as the type, location and magnitude of the triggering abnormal event. In literature, a large number of terms with various meanings are used in connection with progressive collapse.

The term *collapse resistance*, a short form of resistance against progressive collapse, is defined as the insensitivity of a structure to accidental circumstances, which comprise unforeseeable or low-probability events (Starossek, 2006). Collapse resistance is a property that is influenced by both structural features as well as possible causes of initial failure. Resistance against progressive collapse is a structural property that is influenced by a number of conditions.

The property of resisting to collapse is the *structural robustness.* In a robust structure, no damage disproportionate to the initial failure will occur. Usually, robustness is associated with explosions, terrorist attacks and other extreme events. However, a robustness evaluation is of current interest also in the context of more probable environmental exposures, where the structures are working for the design loads but may be prone to severe deterioration scenarios. In fact, many collapses had triggered by local breakages, induced in apparently secondary parts by localized damage phenomena.

In the following, a short review of the most famous bridge failures is recalled.

3.2 FAILURE EVENTS

Descriptions and investigations of structural failures is a fundamental reference in order to improve the methods for the safety measurements.

The *Silver Bridge*, collapsed in Virginia in 1967 (Fig. 3.1), represents an example of progressive collapse due to environmental aggressiveness. It was a two-lane eye-bar suspended bridge measuring 681 m including the approaches. There were small cracks that started as corrosion pits in the eye-bar of the suspension bridge. Once the eye-bar failed, the pin fell out unpinning the suspension chain. The tragedy killed 46 people and seriously injured nine. The cause of failure was from stress corrosion and corrosion fatigue. Years before the collapse, a tiny crack appeared in a suspension chain on the bridge, and the crack grew bigger as time went on. However, it went unnoticed by bridge inspectors because the technology did not allow inspectors to see the crack.

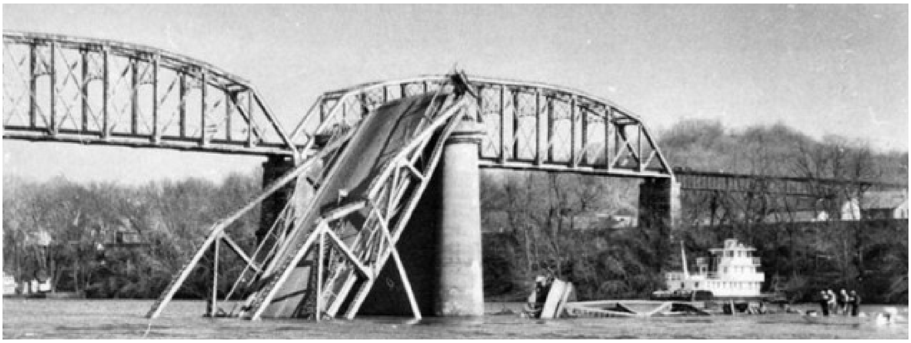

Figure 3.1: Collapse of Silver Bridge in 1967.

The *Viadotto Cannavino* (Cosenza, Italy) collapsed during construction in 1972 (Wittfoht, 1983). The triggering event seemed to be a formwork failure. (Wittfoht, 1983) said that "...an unscheduled procedure during erection caused overloading of the tip of the cantilever, which resulted in crack formation in the critical section. Since the tensile reinforcement and the concrete were not yet bonded at this point, the crack was able to open and 'collect' the entire strain of all the free tendon lengths. This led to constriction of the concrete compression zone to the point of explosive failure".

In 1983, the *Mianus River Bridge* in Connecticut lost a whole span after the failure of a pin-and-hanger connection. The bridge deck was supported by two main beams and the spans were connected by the pin-and-hanger assemblies. Corrosion of the connection provoked the slip pf the pin from its hanger. By knocking out the beam it was supporting, the system could not redistribute the load to the remaining part of the structure, which in this case consisted of the other main beam. The collapse was thus initiated by the local nonductile failure of a connection in the nonredundant two-girders superstructures topology.

Another progressive collapse of a bridge occurred during the construction of *Haeng-Ju Grand Bridge* in Seoul in 1992. After the failure of a temporary pier, an 800 m section of the bridge collapsed. In fact, the continuous prestressing tendons in the superstructure of the bridge played a particular and disastrous role. When the Haeng-Ju Grand Bridge collapsed, most tendons resisted the enormous stresses caused by the rupture of the encasing concrete and the collapse of structural elements. The high degree of robustness of the material coupled with the continuity of the tendons over the length of the bridge worked against the robustness of the structure. A chain reaction ensued where the forces transmitted by the tendons led to the collapse of all eleven continuous spans. The collapse did not stop until it reached the transition joints on both ends of the bridge.

The *Santo Stefano Viaduct*, across the homonymous river, is part of the road in the Messina town (Italy) and it was designed in July 1954. The viaduct is constituted of four-span 18.5 m long, resting on three piers and two abutments, for a total length equal to 78 m. Since viaduct was located on the Ionian coast a few meters from the shoreline, in some periods of the year it was cyclically invested by marine aerosols. Visual inspections had revealed the presence of numerous areas of corrosion relatively to the transversal rebar and accentuated in correspondence of the beam of shore seaside. The prestressing reinforcement was visible from the outside of the concrete cross-section because it was subjected to widespread corrosion, due to the small thickness of the cover. Such a state of disrepair, although present on the entire structure, it became more severe on the beam exposed to the sea than the other ones. After 40 years of service, in 1999, one of the four spans of the viaduct, with no vehicles and/or pedestrians, collapsed.

Another key event was the collapse of the *Mississippi River Bridge* in Minneapolis (Minnesota) in 2007, in which the whole bridge, classified as non-load-path redundant, catastrophically collapsed after the failure of a gusset plate connection. The initiating event in the collapse of the bridge was the lateral shifting instability of the upper end of a diagonal member and the subsequent failure of gusset plates on the center portion of the deck truss, as in Fig. 3.2.

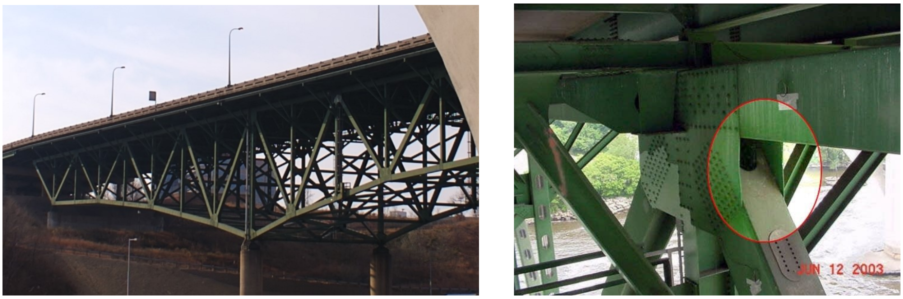

Figure 3.2: Mississippi River Bridge in Minneapolis and the gusset plate collapsed in 2007.

These dramatic events have in common the occurrence of consequences disproportionate to the initial cause or damage. It is clear that standards cannot absolutely avoid their risks, but new provisions seem to provide some requirements for the robustness against system failure. Often, the stated requirement is that structural systems should be robust, but a precise definition of structural robustness still does not exist. This limitation is more important as most structural failures are due to unexpected loads, design errors, errors during execution, unforeseen deterioration and poor maintenance which cannot be prevented using the conventional component-based code checking formats, for example verifying if a design is acceptable with regard to individual failure modes (Bontempi, 2006), (Canisius *et al.*, 2007), (Arangio and Bontempi, 2010).

3.3 DEFINITION OF THE MOST RECURRENT TERMS

One of the main issues related to the robustness of structural systems is that its description varies and it is very difficult to present a thorough and ordered presentation. The most used definitions of *robustness* are quite similar to each other, especially those provided by the design codes, and terms like structural robustness, structural integrity or vulnerability but also prevention of progressive collapse phenomenon, sometimes appear used in an interchangeable manner.

Several proposed definitions for robustness concept can be classified according to two different adopted points of view. According to the first point of view, robustness is considered as a structural property only and is related to the structural behavior after damage occurs. Such a definition is independent of the environment where the structure is inserted. This concept seems more simple and can be quantified exclusively considering the structural engineering domain (Fig. 3.3). In this meaning, robustness is defined by some authors as follows:

(1.a) "Insensitivity against small deviations in the assumptions" (Huber, 1996).

(1.b) "Bridge robustness, ability to carry loads after the failure of one of its members" (Wisniewski *et al.*, 2006).

(1.c) "The robustness of a structure, intended as its ability not to suffer disproportionate damages as a result of a limited initial failure, is an intrinsic requirement, inherent to the structural system organization" (Bontempi *et al.*, 2007).

(1.d) "Insensitivity of a structure to local failure. It's a property of the structure alone and independent of the possible causes and probabilities of the initial local failure" (Starossek, 2008).

If one considers both the structure and the environment, the robustness represents a more complex and wide property. A structure that has been considered as robust, may not become robust due to the potential changes in the environment. For example, let's consider a viaduct over a highway. If the traffic increases or if the bridge is subjected to a progressive damage state, the structure may maintain a sufficient bearing capacity, but its robustness decreases. According to this second point of view, Literature suggests for robustness the following definitions, slightly different from the previous ones:

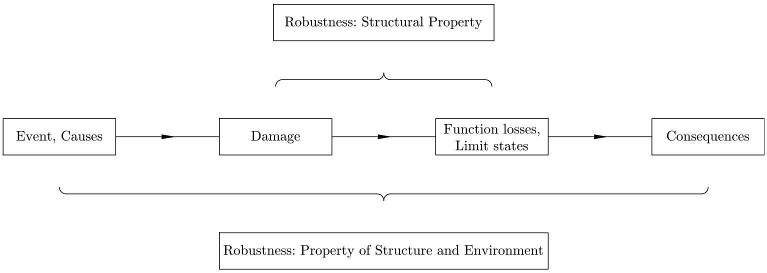
Robustness: Structural Property
Event, Causes
Damage
Function losses, Limit states
Consequences
Robustness: Property of Structure and Environment

Figure 3.3: Robustness: structural property versus property of structure and environment (Cavaco *et al.*, 2013b).

(2.a) "The degree to which a system is insensitive to effects that are not considered in the design" (Slotine *et al.*, 1991).

(2.b) "The ability to react appropriately to abnormal circumstances (i.e. circumstances "outside of specifications"). A system may be correct without being robust" (Meyer, 1988).

(2.c) "The ability of a system to maintain function even with changes in internal structure or external environment" (Callaway *et al.*, 2000).

(2.d) "The ability of a structure to withstand extreme events without being damage to an extent disproportionate to the original cause" (Agarwal *et al.*, 2003).

(2.e) "We call a system robust if it can withstand an arbitrary damage, for example, the loss of a member or degradation in the quality of a member" (Agarwal *et al.*, 2003).

(2.f) "Robustness is taken to imply tolerance to damage from extreme loads or accidental loads, human error and deterioration" (Baker *et al.*, 2008).

(2.g) "Structural robustness can be viewed as the ability of the system to suffer an amount of damage not disproportionate with respect to the causes of the damage itself" (Biondini *et al.*, 2008).

It's also another point of view that when talking about maintaining structural function after damage, it can be referred to the preservation of all kind of functions a structure is designed for. Previous definitions go in this direction, by not reducing damage and functions spectrum.

From the definitions presented, it can be observed that *robustness* is a property involving causes, events and damage with consequences and structural functions. Notions as disproportionate or abnormal consequences are used by several authors in order to quantify the relationship between the reported key concepts.

In conclusion, *robustness* can be defined as the ability of a structure to resist without disproportionate damage to their abnormal events or initial damage. To assess structural robustness, it is necessary to take into account the possible scenarios which may lead to collapse, their probability of occurrence as well as their consequences.

3.4 ROBUSTNESS MEASURES AND ASSESSMENT

The quantification of robustness tries to give the answers to some questions such as *What is a measure for robustness?* and *What is the purpose of quantification?* (Starossek and Haberland, 2008). As previously stated, a precise definition for robustness still not exist. This ambiguity borns not only from the two distinct ways about the definition but also because there is a diffused tendency to compare the proposed frameworks to measure it or the other concepts when they give a measure of different things.

In this paragraph, the proposed measures for assessing robustness and other related indicators of this property are reviewed according to three board categories, with increasing complexity: *(A)* deterministic, *(B)* probabilistic and (C) risk-based measures. On the one hand, deterministic measures are simpler to be implemented and seem very practical in engineering fields (especially for bridges). They are based on the comparison between the properties of the damaged and undamaged structures. On the other hand, probabilistic and risk-based quantification approaches explicitly consider the many uncertainties associated with the structure and environment. This kind of measures have the potential to provide a more detailed description of structural robustness, but they are generally to complex to be useful in typical design situations. The validity and usefulness of robustness measures are linked to a series of general requirements, which cannot be satisfied to the same level at the same time (Lind, 1995),(Haberland, 2007), (Starossek, 2009):

1. *expressiveness*, a measure should express all aspects of robustness or collapse resistance and should not be influenced by other aspects, it should allow a clear distinction between structures that are robust and non-robust or, between structures collapse-resistant and collapse-susceptible;
2. *objectivity*, the measure should be independent on the designer's decisions, i.e. under unchanged conditions, the values of the measures should be reproducible;
3. *simplicity*, the definition of the measure should be as simple as possible;
4. *computability*, it should be possible to derive the measure from the properties or the behavior of the structure (all required input parameters must be quantifiable) and a sufficiently accurate numerical evaluation should be possible with limited computational effort;
5. *generality*, the measure should as far as possible be applied to any kind of structure.

3.4.1 DETERMINISTIC MEASURES

In relation to deterministic approaches, (Frangopol and Curley, 1987) measured the *structural redundancy* as the reserve strength between damaged components and system's collapse, which can be estimated as follows:

$$R = \frac{L_{intact}}{L_{intact} - L_{damaged}} \tag{3.1}$$

where L_{intact} is the overall collapse load of the structure without damage and can be computed through plastic methods of structural analysis. $L_{damaged}$ is the overall collapse load of the structure considering some damage in one or more members. The redundancy factor is equal to 1 when the damaged structure has no reserve strength and is infinite when the damage has no influence on the reserve strength of the structure.

According to (Ghosn and Moses, 1998) and (Liu *et al.*, 2001), *structural redundancy* is defined as the capability of the system to continue to carry the load after the failure of one main member. Seeking simple methods that can be implemented in bridge engineering practice, they defined three different measures. As shown in Fig. 3.4, two measures are related to the overloading of the originally intact bridge configurations of the structure and are defined as the ability of the structural system to resist collapse and/or avoid the loss of structural functionality. The third measure is calculated for a damaged configuration of the structure and leads to the evaluation of the capability of the system to carry some emergency load after the damage of one main member. These measures are given as:

$$\begin{aligned} R_u &= \frac{LF_u}{LF_1} \\ R_f &= \frac{LF_f}{LF_1} \\ R_d &= \frac{LF_d}{LF_1} \end{aligned} \tag{3.2}$$

where LF_1 is the load that causes the failure of the first member, LF_u is the load that causes collapse of the system, LF_f is the load that causes the functionality limit state of the initially intact structure to be exceeded and LF_d is the load factor that causes the collapse of a damaged structure that has lost one main member. These measures compare the system's capacity to the capacity of the system to resist first member failure, making them applicable for evaluating alternative designs. The criteria were developed to match the redundancy levels of bridges that have historically shown adequate levels of redundancy and robustness. The measures of redundancy are practical and have been implemented during the design of new bridges, as demonstrated by (Hubbard *et al.*, 2004), and thus can also be incorporated in structural codes. Following the same approach, (Wisniewski *et al.*, 2006) proposed a technique to include redundancy in the assessment of bridge's robustness and its overall system capacity.

A simple and practical measure of *structural redundancy* used in the offshore industry is based on the so-called RIF value (Residual Influence Factor), (Faber, 2006), (BS, 2007). A Reserve Strength Ratio (RSR) is computed as:

$$RSR = \frac{R_C}{S_C} \tag{3.3}$$

where R_C denotes the characteristic value of the base shear capacity of an offshore platform (typically a steel jacket) and S_C is the design load corresponding to the ultimate limit state. In order to measure the effect of full damage (or loss of functionality) of *i-th* structural member on the structural capacity, the so-called

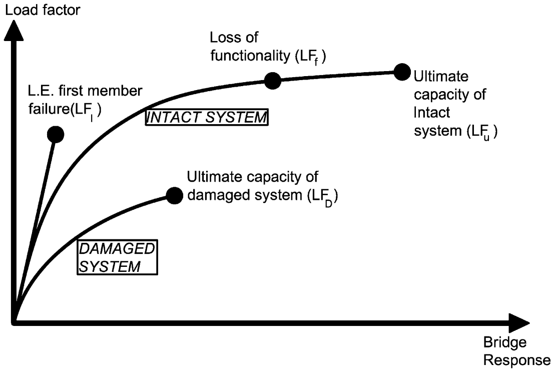
Load factor
Loss of functionality (LF_f)
L.E. first member failure(LF_I)
INTACT SYSTEM
Ultimate capacity of Intact system (LF_u)
Ultimate capacity of damaged system (LF_D)
DAMAGED SYSTEM
Bridge Response

Figure 3.4: Load measures needed to calculate redundancy of bridge systems proposed by (Ghosn and Moses, 1998) and (Liu *et al.*, 2001).

RIF value (sometimes referred to as the Damaged Strength Ratio) is defined by:

$$RIF_i = \frac{RSR_{fail,i}}{RSR_{intact}} \tag{3.4}$$

where RSR_{intact} is the RSR value of the intact structure and $RSR_{fail,i}$, is the RSR value of the structure where the i-th member has either failed or has been removed. The RIF takes values between zero and one, with larger values indicating larger redundancy, i.e. RIF tends to one if the Reserve Strength Ratio of the structure in the damaged state approaches the Reserve Strength Ratio of the intact structure (the structure, in this case, is robust because the damage is localized and it does not modify significantly the resistance of the overall system). A combination of the RSR and RIF can be considered to provide an indication of the robustness of the structure, with RSR reflecting more a situation similar to "Key Element Design" for buildings, because if a key element has been damaged, the resistance of the overall system is probably reduced and the RSR of the structure in the damaged state is much lower than in the intact state.

Differently, (Restelli, 2007) evaluates *robustness* using indicators that are related to the global displacement of a structure composed of parallel members, using the following expression:

$$\rho = \frac{s_0}{s_d} \tag{3.5}$$

where s_0 and s_d are the displacement of the intact and damaged system respectively. This index decreases from 1 and approaches to 0 as damage spreads within the system. The aim of this measure is to evaluate the system's susceptibility to degrading damages spreading through the structural elements. The index is therefore calculated for each damage state up to system collapse.

Another option to measure *structural robustness* was proposed firstly by (Haberland, 2007) and then by (Starossek, 2007a), which is related to the global stiffness matrix of a linear elastic structural model and is given as:

$$R_S = min_j \frac{det\mathbf{K}_j}{det\mathbf{K}_0} \tag{3.6}$$

where $det\mathbf{K}_0$ is the determinant of the stiffness matrix of the intact system and $det\mathbf{K}_j$ is the determinant obtained when the j-th member is assumed to be damaged and removed from the system. This damage index is highly dependent on the structural model and may not adequately reflect the robustness property of the structure itself. In fact, (Haberland 2007) concluded that R_S is not an adequate measure of structural robustness but is more an indicator of the cross-linkage of the system. Based on the description of mechanisms and types of collapse presented by Starossek (2007), it can, therefore, be concluded that this approach is in principle suitable for structures that are susceptible to zipper-type collapse.

In 2007, (Starossek, 2007a) also proposed other non probabilistic measures for robustness. The first *robustness* measure based on damage extent is given by the expression:

$$R_d = 1 - \frac{p}{p_{lim}} \tag{3.7}$$

where p is the maximum total damage resulting from the assumable initial damage and p_{lim} is the acceptable total damage. A value of one indicates perfect robustness and negative values indicate that the design objectives are not met. To account for the possible damage intensity and direct consequences with the initial damage, a measure of robustness based on the structural performance is formulated (Starossek and Haberland, 2008):

$$R_{d,int} = 1 - 2\int_0^1 [d(i) - i]\, di \tag{3.8}$$

where $d(i)$ is the maximum total damage resulting from and including initial dimensionless damage of extent i. A value of one indicates maximum possible robustness and a value of zero indicates a total lack of robustness. As shown in Fig. 3.5, which gives a schematic representation of possible relationships between $d(i)$ and i, the damage index in 3.8 is very sensitive to these relationships. These damage based measures are very expressive, but the overall damage is difficult to assess and sometimes is not well correlated with structural performances.

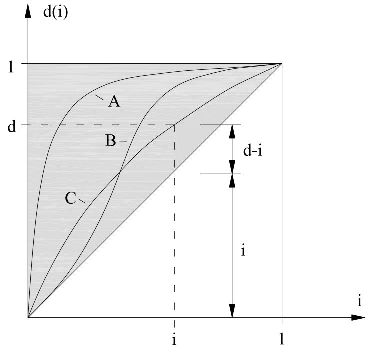

Figure 3.5: Damaged-based measure for robustness (Starossek and Haberland, 2008). The curve A represents the more robust structure and curve C the less robust structure.

More appropriated to impact type progressive collapses, (Starossek and Haberland, 2009) proposed an energy based *robustness* measure R_e given by:

$$R_e = 1 - max_j \frac{E_{r,j}}{E_{f,k}} \tag{3.9}$$

where $E_{r,j}$ is the energy released during initial failure of *j-th* structural element and contributing to damaging a subsequently affected *k-th* element, while $E_{f,k}$ is the energy required for failure of subsequently affected element k. A value equal to 1 indicates perfect robustness and negative values indicate failure progression. According to the authors, the term $E_{r,j}$ is difficult to calculate since it can be both under or over assessed.

According to (Biondini *et al.*, 2008), *robustness* evaluations are usually related to damage suddenly provoked by accidental actions, like explosion or impacts. However, damage could also arise slowly in time from aging of structures, as induced, for example, by environmental aggressive agents, as addressed in this work. In this context, they develop suitable life-cycle measures of structural robustness with respect to a progressive deterioration of the structural performance. (Biondini *et al.*, 2008) considered in particular the deterioration of cross-section members by chloride-induced corrosion, specified by means of the damage index δ. To assess robustness, the authors compared several structural performance indicators on initial and on damage state. The indicators used were several stiffness matrix properties, displacements at certain points, internal energy measures and pseudo-loads. For each level of corrosion, the deterministic measure of robustness is defined as:

$$\rho = \frac{f_0}{f_d} \tag{3.10}$$

where f_0 and f_d are the structural performance indicators of the undamaged and deteriorated states respectively. In this case, a single value for robustness not exists because for different levels of corrosion and for a given type of damage many robustness values exist.

Finally, (Cavaco *et al.*, 2010) proposed a modified version of the damage-based index 3.8 to evaluate the robustness for corroded members. The *robustness index* is defined from the following expression:

$$R_d = \int_{d=0}^{d=1} f_d(x)dx \tag{3.11}$$

where $f_d(x)$ is the ratio between the structural performance of a system in the original intact state and in its damage state and d is the ratio of actual and maximum possible damage. R_d represents the area below the curve $f_d(x)$ in the domain of normalized damage. The approach is very flexible because it allows for the use of different performance indicators. As a more complex performance index is used, the complexity in the model increases. The idea of this deterministic approach is to compare specific performance indicators F with the structure intact ($D = 0$) and damaged ($D = d$). As shown in Fig. 3.6, the robustness index would vary from zero to one with correspondence with extreme cases A and E respectively.

For curve A, minimum damage would lead to total performance lost, and for curve E only the maximum damage possible would cause some difference on structural response. The curve C would represent reference robustness of 1/2. All cases in Fig. 3.6 represented the maximum damage leads to the total loss of structural performance. This methodology is also valid in other situations where the maximum damage does not correspond to the total loss in performance or in situations where the collapse happens before maximum damage occurs (Cavaco *et al.*, 2010).

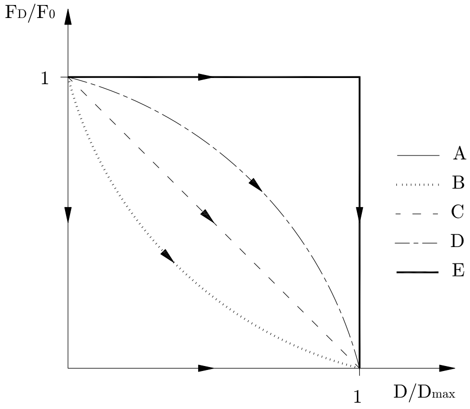

Figure 3.6: Normalized structural response as a function of normalized damaged (Cavaco *et al.*, 2010).

3.4.2 RELIABILITY-BASED MEASURES

To account for the uncertainties associated with the behavior of structural systems and their redundancies, several measures of structural redundancy and bridge redundancy in particular have been proposed in Literature, which also indicates a level of robustness.

The first reliability measures of robustness were suggested by (De *et al.*, 1989), who defined *redundancy* by comparing the probability of system collapse to the probability of member failure. The robustness was defined by comparing the probability of collapse of the system in its damaged state with the probability of collapse of the originally intact system. The two indices are expressed as:

$$R_{red} = \frac{P_{f(intact)}}{P_{f(member)}} \qquad R_{red} = \frac{P_{f(damaged)}}{P_{f(intact)}} \tag{3.12}$$

where P_f represent the failure probability.

Related to 3.1, (Frangopol and Curley, 1987) proposed a probabilistic *redundancy factor*, based on reliability index β:

$$\beta_R = \frac{\beta_{(intact)}}{\beta_{(intact)} - \beta_{(damaged)}} \tag{3.13}$$

Despite its simplicity, the index β_R may have a large range of values, causing difficulties in appreciating the effect of damage on different systems with different $\beta_{(intact)}$. By normalizing the reliability index, one loses a perspective on the inherent level of safety.

(Lind, 1995) proposes similar quantitative measures of *vulnerability* and *damage tolerance* of a system. In his point of view, vulnerability and damage tolerance are complementary concepts. If a system is vulnerable it is not damaged tolerant and vice-versa. (Lind, 1995) defined the vulnerability V as the damage tolerance, what was defined as robustness:

$$V = \frac{P(r_d, S)}{P(r_0, S)} \tag{3.14}$$

where r_d is the resistance of the damaged system, r_0 is the resistance of the intact system and S is the loading. $P(r, S)$ is the probability of system failure as a function of both effects of loading and resistance. The vulnerability V of a system can vary from zero to infinite, if the damage has a null or huge impact on system resistance, respectively. On the other hand, the damage tolerance T_d is defined as the reciprocal of V:

$$T_d = \frac{P(r_0, S)}{P(r_d, S)} \tag{3.15}$$

Lind's indicators to assess robustness is very similar to the one suggested by (Frangopol and Curley, 1987). They represent a form to measure robustness as a property of the structure with the advantage that can be applied to any kind of damage and structural performance.

The deterministic measures 3.2 introduced by (Ghosn and Moses, 1998) and (Liu *et al.*, 2001) were found to be consistent with probabilistic models expressed in terms of reliability index. In particular, (Ghosn and Moses, 1998) proposed three reliability measures of *redundancy* that are defined in terms of relative reliability margins expressed as:

$$\begin{aligned} \Delta\beta_u &= \beta_{ult} - \beta_{member} \\ \Delta\beta_f &= \beta_{func} - \beta_{member} \\ \Delta\beta_d &= \beta_{damaged} - \beta_{member} \end{aligned} \tag{3.16}$$

where β_{member} is the reliability index related to the failure of one member and β_{ult}, β_{func}, $\beta_{damaged}$ refers respectively to collapse of intact system, loss of functionality and collapse of the damaged structure. These measures have been used to evaluate the redundancy of bridge systems by a probabilistic model. The advantage of using the reliability index for members as the benchmark is because most bridge codes and practices were calibrated to achieve a target reliability β_{member}.

According to (Ellingwood and Dusenberry, 2005), (Starossek and Haberland, 2008), (Starossek and Haberland, 2009), progressive collapse resistance can be introduced in various ways. One possibility is through the structural robustness. In a robust structure, no damage disproportionate to the initial failure will occur. In probabilistic terms, *progressive collapse* may be represented as a chain of partial probabilities:

$$P(F) = P(E) \times P(D|E) \times P(F|D) \tag{3.17}$$

where $P(F)$ is the probability of progressive collapse occurrence due to an event E and D represents any kind of damage. In particular, Starossek defines robustness as a property of structure and associated it with the term $P(F|D)$. If a structure is robust, the probability of failure will not be too much affected by damage occurrence.

Finally, the *robustness measure* proposed by (Cavaco, 2013) can be easily extended into probabilistic terms, if for example the reliability index is selected as a performance indicator (Cavaco *et al.*, 2013b). In this case, the robustness index R_d is similar to one of (Frangopol and Curley, 1987). If the performance indicator is selected as the probability of failure and damage is only assumed a single value, $f_d(x)$ can be expressed as $f_d(x) = P(F|D=0)/P(F|D=d)$, becoming the damage tolerance index proposed by (Lind, 1995).

3.4.3 RISK-BASED MEASURES

Risk-based approaches provide the most complete framework for evaluating the robustness of structures by accounting for the probability of structural collapse and simultaneously for the economic, political, and societal consequences of collapse. The model can be summarized by:

$$R = \sum P(C|D) \cdot P(D|H) \cdot P(H) \cdot Cost(C) \tag{3.18}$$

where R respresents the total risk of the structure, $Cost(C)$ the cost of collapse (in monetay values), D and H are the damage and the hazard respectively.

Based on risk approach, (Baker *et al.*, 2008) proposed a quantification of *robustness* as:

$$I_{rob} = \frac{R_{Dir}}{R_{Dir} + R_{Ind}} \tag{3.19}$$

where R_{Dir} and R_{Ind} refer to the direct and indirect consequences due to the system collapse. Larger values of I_{rob} indicates larger robustness. Fig. 3.7 shows the decision analysis theory and event tree formulation at the base of his proposed approach. It starts out with the consideration and modeling of hazard (H) that can damage the components of the structural system. After an extreme event has occurred, all the components of the structural system either remain in an undamaged state ($\bar{D}$) as before or change into a damaged state (D). For this last state, there is a probability that system partial or complete fails (F) or its survival without any further damage ($\bar{F}$). Consequences are associated with each of the possible damage and failure scenarios, and classified as either direct (C_{dir}) or indirect (C_{ind}). This risk approach and robustness index I_{rob} may be considered as the most complete approaches to robustness. The index accounts not only for the characteristics of the structural performance, but also for the performance of the system after damage and all relevant consequences.

3.4.4 A REVIEW OF THE DIFFERENT PROPOSALS

Although there are many proposals for measuring and quantifying structural robustness, only qualitative instead of quantitative recommendation can be found

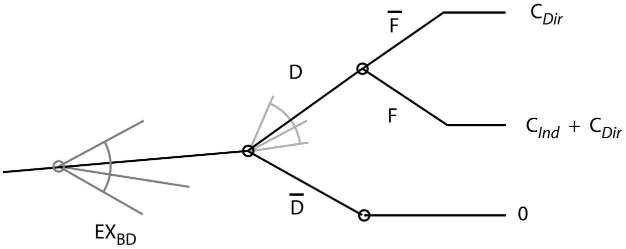
$\overline{F}$
C_{Dir}
D
F
$C_{Ind} + C_{Dir}$
$\overline{D}$
0
EX_{BD}

Figure 3.7: Event Tree (Baker *et al.*, 2008).

in the Literature as well as in the regulations. From the summary of the main quantitative approaches, it has been emerged that the deterministic measures have two main advantages:

1. their simple mathematical formulation, such that they could be evaluated with few numerical efforts;

2. their general definition, such that they could be applied to standard type structure.

On the other hand, they cannot be considered as general methods, because they are oriented to specific cases.

Risk-based and reliability-based quantification approaches may address the shortcomings of the deterministic ones, by explicitly considering the uncertainties associated with the problem. These approaches have the potential to provide a more exhaustive picture of a system's robustness, but they are generally too complex to be useful in typical assessment situations. As it can be seen in (3.18), the robustness definition proposed by (Baker *et al.*, 2008) depends on the environment and so cannot be considered only as a structural property, but it may vary depending on changes on the environment. Thus, the same structure may have different robustness in different contexts.

An interesting point of view and different level of approach is the so-called *Barrier Model*, as shown in in Fig. 3.8. It has been introduced by (Haddon, 1980), (Ersdal, 2005), (Sorensen and Christensen, 2006) and can be helpful in understanding the significance of each measure of robustness.

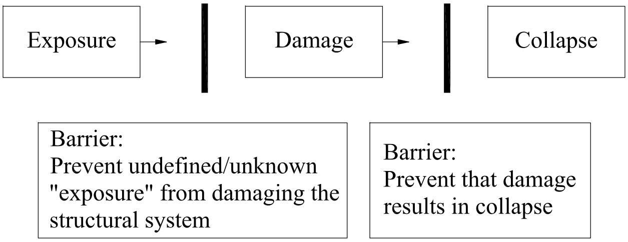
Exposure
Damage
Collapse
Barrier:
Prevent undefined/unknown "exposure" from damaging the structural system
Barrier:
Prevent that damage results in collapse

Figure 3.8: Barrier Model, adapted from (Sorensen and Christensen, 2006).

The first barrier protects the structure from environment aggressions and may consist of more general measures including detailed and independent quality control of both design and construction, assessment of loads and design parameters and modeling. The second barrier deals with how the structure reacts after a damage occurrence. The way to enhance this barrier is to design structures robustly and more damage tolerant. Baker's robustness index allows for both barriers and goes further by making possible a third barrier between collapse and indirect consequences. According to this distinction, (Ghosn and Moses, 1998) do not account for consequences and robustness is defined as an environment property: their proposal reflects the first barrier. (Frangopol and Curley, 1987), (Lind, 1995), (Biondini *et al.*, 2008) and (Starossek and Haberland, 2009) measures are more concerned with structural performance not significantly affected by damage. This concept is related to the second barrier, which means that the authors consider robustness as a structural property. Damaged-based measure proposed by (Starossek and Haberland, 2008) measures the relation between the initial damage and the total damage resulting from it. Since total damage accounts for the damage occurred on the structure environment, robustness becomes a property of the structure and its environment (second barrier).

As seen, the identification of a universal index to quantify and assess the structural robustness, among the different proposed measures, is still controversial and a matter of debate.

3.5 TOOLS FOR A ROBUSTNESS ASSESSMENT

In the following paragraph, a *new approach* is proposed, not to quantify but to characterize the structural robustness. The basic tool of such an approach is the *Limit Analysis*, which has the following properties:

- easy to implement into numerical codes;
- applicable to any kind of framed structures;
- able to account the effects of the structural damaging;

In this work the analyses are developed within a deterministic approach, i.e. defined assuming, a priori, the load distribution and the damage scenarios, but they are extendible also to a probabilistic one.

In the context of existing structures, in particular bridges, instead of identifying significant cases which lie in a specific and assigned definition of robustness (ad hoc index), we consider a series of problems for which *characterize the robustness.* To do this, the robustness is defined through filters, according to two different main levels:

1. GLOBAL LEVEL - Integrity of the *overall structure.*
   At the global level, the structure is considered as a whole. The attention is focused on the load multiplier versus the applied loads, the redistribution of internal forces far from the loss of structural integrity and the investigation of the structural performance over time.

2. LOCAL LEVEL - Integrity of the *secondary elements*.
   At the local level, the interest moves towards the secondary elements such as nodes and joints (D-regions). The layout of the load path and the plasticization distribution may be useful in assessing and validating the bearing schemes assumed in the design practice.

VIRTUAL LOADING TEST		
Damage State	&	*Limit Analysis*
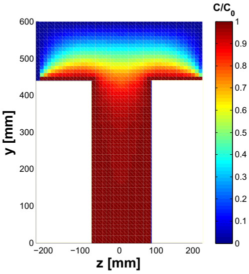 c/c$_0$ y [mm] z [mm] 600 500 400 300 200 100 0 −200 −100 0 100 200 1 0.9 0.8 0.7 0.6 0.5 0.4 0.3 0.2 0.1 0		
Output: reduction of cross-section of bars; ductility reduction of reinforcing steel; reduction of concrete strength; spalling of the concrete cover.		Output: load collapse multiplier; redistribution of internal forces; collapse mechanism; plasticization distribution.

Table 3.1: Adopted approach to characterize the robustness of existing structures.

It is important to note that the choice of the structural method and the level of accuracy is strictly related to the specific phase of the life-cycle and to the complexity and the importance of the structure (Bontempi, 2006).

The most efficient method to characterize the robustness assessment of existing structures is the one based on plastic theory (Zwicky, 2010). Thus, the robustness characterization can be carried out at the global and local level by means the Upper and Lower Bound Theorems, as well reported in chapter 5.
For each level, the Limit Analysis process is based on a *monodimensional modeling*, as described in chapter 4.

In the present approach, the robustness assessment of existing structures consists of two phases. It starts typically with the evaluation of the current state of the structure, on the basis of the results of the inspections (visual surveys, physical-chemical analyses, experimental measurements, syntheses from condition rating procedures, etc.). Since in some cases information about deterioration and its mechanical effect is not available, the damage state can be artificially simulated through suitable numerical techniques, like those discussed in Appendix A. If the numerical simulation is representative of the current state, the simulation could provide a more detailed and deepen description of the deterioration process.

Then, the assessment of the structure is based on a *virtual loading test* under the most severe loading conditions at each time instant corresponding to its damage state is carried out. By means of a set of Limit Analyses, the response of structural systems and sub-systems is intended as the ability of damaged structures to carry out the increase of internal forces derived from the redistribution mechanism without developing weakness signals. The obtained results provide a reference to develop a *judgment on the robustness* of the structure.

3.6 Closing Remarks

The assessment of existing structures with the traditional methods check the satisfaction of the standards limit states, but pay few attention to requirements like the structural integrity.

Robustness has been recognized as a desirable measure of the effects of unpredictable damage to structural safety. Although robustness has mostly been used to evaluate the consequences of triggering events, a similar framework can be used to investigate the time-variant structural performances due to deterioration. From the presented state of the art, the following comments arise:

- a unique definition of the term cannot be found in the literature;
- a set of definitions are proposed by several authors, in order to distinguish the if robustness is a property of the structure or property of its environment;
- the quantitative definition is a challenging problem that is currently open;
- no approach has emerged as distinctly superior or preferable so far;

Despite many contributions in this field, it is clear that more work is still needed at all levels to further facilitate the consideration of robustness during the design of new structures and the safety evaluation of existing ones.

In reaching the main object of the thesis - a robustness assessment of existing structures - a procedure for *a virtual loading test* is proposed, consisting in the exam of a structure at different damaged states and in the evaluation of the multiplier at the collapse of a given additional traffic load distribution. The assessment is be carried out at the global and local level by means the *Limit Analysis*, as well reported in the following chapters. The search for these limit behaviors may be seen as a *lifetime structural robustness estimation*, tailored on the actual or supposed damaging characteristics of a given structure. Moreover, such an approach allows outlining the consequences due to different damage factors and the modes which lead to sudden collapses, when neither weakness signals nor intermediate anomalous behaviors appear.

4

A Review of Monodimensional Modeling for RC Structures

This chapter provides a general presentation of the global framework in monodimensional modeling and a review of its nested state. The nonlinear problem is presented by considering two dual approaches in formulating finite beam-column elements. In dealing with the state of a RC section, the attention is focused on how to treat normal and tangential stresses. By using the standard finite technique, the problem is outlined with respect to frame structures.

4.1 INTRODUCTION

Modelization of reinforced concrete structures by means of beam elements is the most used tool of analysis in Civil Engineering design. Several models can be proposed (Fig. 4.1), but in design or assessment of the real frame structures, the use of complex 2D or 3D FE programs can turn to be impracticable, not only for the high computational cost, but also for the huge amount of generated data from which a difficult results interpretation process descends. For this reasons, 1D modeling with distributed nonlinearity seems a good compromise because of the optimal balance between accuracy and computational efficiency they offer. In fact, for skeleton analyses the frame modelization perfectly fits the actual structure and plane and spatial frames are used also to discretize continuous systems, like shear walls and bridge decks, made of orthotropic grillages.

Frame analysis possesses many relevant characteristics. First of all, it is characterized by simplicity and geometrical effectiveness in modeling the actual structure. These properties make the planning of the analyses easy to do and simple to be verified. Moreover, it works through generalized stresses (i.e. axial force N, shear forces V, bending moments M and torque moment T) and not with local stresses (σ_{ij}). Such synthetic representation of the internal stresses conforms to that, based on N, V, M, T, establishing the basic theory of the reinforced and prestressed concrete. In fact, concrete structure design is currently based on the so-called "capacity design", through which the the problem is formulated in terms of normal stresses and shear and torsional failure must be avoided a priori. This has led to formulate new 1D models with distributed nonlinearity that can adequately address not only the problem of normal forces, but also the one of shear force and torsion.

In dealing with RC frame systems, this chapter hence presents a short description and discussion of each module included in the global structural framework. In particular, in formulating the finite beam-column element, all the expressions referred to the generalized stresses N, M and T and the work due to V is not included.

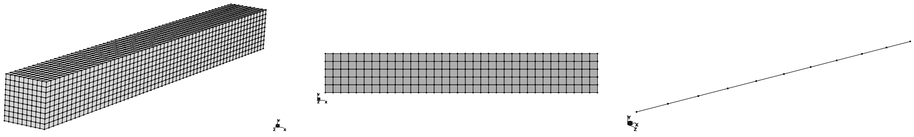

(a) 3D model. **(b)** 2D model. **(c)** 1D model.

Figure 4.1: Comparisons between Finite Element Models.

4.2 GLOBAL FRAMEWORK

The global structural framework is explained with reference to Fig. 4.2. The real generic structure of Fig. 4.2a is discretized in monodimensional elements as Fig. 4.2b shows. The Finite Element Method (FEM) works through nested modules that goes from the structure to the material point (fibre). In particular, four nested states must be evaluated:

1. the state of the *structure*, that is made of elements;
2. the state of the *element*, that is made of sections;
3. the state of the *section*, that is made of fibers;
4. the state of the *fiber*, on which constitutive laws are assumed and/or evaluated by using specific techniques.

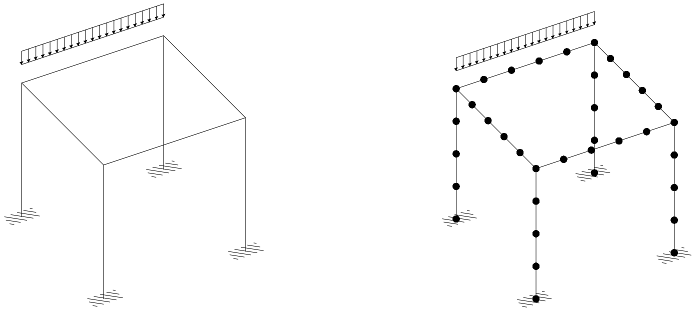

(a) Real structure. **(b)** 1D mesh.

Figure 4.2: general Framework for Global Analysis.

Although all real structural elements are 3D, the discretization of each member of the structure is made by one or more *beam-column elements*, whose behavior is represented by a collection of cross-sections orthogonal to a straight (or a curved) segment, usually indicated as element axis (x axis) as in Fig. 4.3a. As a consequence, all the mechanical information of the cross-sections, according to the beam's theory adopted, are condensed in that reference axis. Considering this assumption, the mechanical response of the beam-column element must be described accounting the effects due to the basic actions (Fig. 4.3b). In case of linear elastic material, the De Saint-Venant beam theory provides accurate solutions. However, if the response is non-linear (as in reinforced concrete), the effects of the actions cannot be easily superimposed and more refined theories are preferred for the definition of numerical elements model.

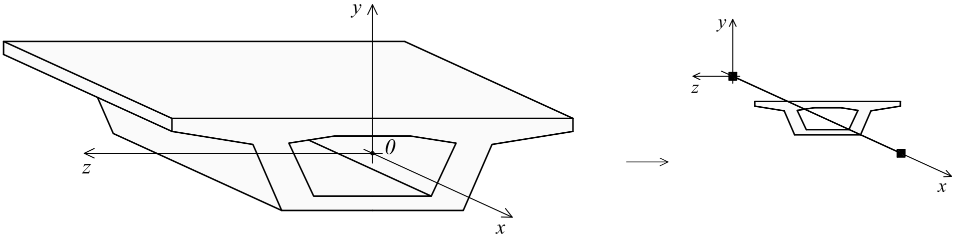

(a) From the real RC element towards beam-column element.

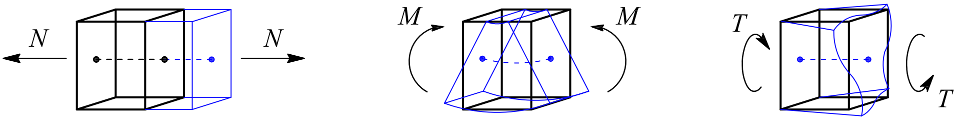

(b) Basic force and deformation behaviors on a general beam portion.

Figure 4.3: Beam-column element and its mechanical response under the generalized stresses.

4.3 STATE OF THE STRUCTURE

The *State of the Structure* is obtained by assembling the states of the elements in which it is subdivided. For example, by using a global displacement approach, the unknowns of the problem are the global displacements $\mathbf{s}$. The external loads acting on the system are transformed in equivalent nodal forces that can be collected in a vector $\mathbf{F}_e$. Aim of the finite element analysis is to find the *State of the Structure* so that the resisting structural forces $\mathbf{F}_r$ are equal to the external ones:

$$\mathbf{F}_r\left(\mathbf{s}\right) = \mathbf{F}_e\left(\mathbf{s}\right) \tag{4.1}$$

This is, in general, a nonlinear system of equations since both the external and the resisting forces may depends on the solution itself, represented by the nodal structural displacements $\mathbf{s}$. The system shows in (4.1) is obtained by assembling *weighting* the state of the elements in which the structure is discretized.

4.4 STATE OF THE ELEMENT

The structural theory of the beam-column elements requires, at first, the definition of sectional kinematics. The simplest one is the well-known Navier-Bernoulli beam theory, which assumes that cross-sections remain plane under deformation and orthogonal to the element axis. Due to the shear and torsional actions, the cross-sections undergo warping deformations and, in case of shear only, the orientation of the plane changes with respect to the axis. Thus, the drawback of the Navier-Bernoulli's theory is its incapability to account for shear forces and torsion moments in a general way.

To overcome these limitations, the Timoshenko beam theory allows considering the effects of the generalized shear strains in a simplified manner, by means of a constant shear strain distribution along the section. The main statement of this theory is that cross-sections remain plane after deformation but not orthogonal to the beam's axis. Other proposals, in which the complexity of the sectional kinematics progressively grow, are focused on the aim of enhance the available beam theory. Between them, by extending the standard Timoshenko model and by accounting for the warping deformation of the cross-sections, (Bairán García, 2005) has proposed a generalized beam model that describes non-uniform shear strain/stress distributions through an enhanced cross-section model, ensuring the equilibrium conditions between the fibers composing the element. The model adopts an accurate 3D material model to describe the brittle behavior of concrete and a 1D model to represent the transversal reinforcements, which are numerically described as embedded in the element volume.

When a proper choice of the sectional kinematic is done, the beam formulation can be based on the application of the Virtual Work Principle or on the Hu-Washizu Variational Theorem (Taylor *et al.*, 2003). Hence, the beam-column elements are usually classified according to the dual formulations used: displacement-based beam element, if we have to apply the Virtual Displacement Principle, and a force-based beam element if the formulation derives from the Virtual Force Principle. What happen on the section is not a problem related with the formulation of the beam, because the section is only a sub-module, as exposed in the next paragraph.

In order to define the *State of the Element* for standard 3D finite elements analysis program, the element's nodal quantities are showed in Figs. 4.4 and 4.5. The element's nodal displacements are collected in vector $\mathbf{q}$, as follow:

$$\mathbf{q} = \begin{bmatrix} q_1 & q_2 & q_3 & q_4 & q_5 & q_6 & q_7 & q_8 & q_9 & q_{10} & q_{11} & q_{12} \end{bmatrix}^T$$

and the element's nodal forces are grouped in vector $\mathbf{Q}$:

$$\mathbf{Q} = \begin{bmatrix} Q_1 & Q_2 & Q_3 & Q_4 & Q_5 & Q_6 & Q_7 & Q_8 & Q_9 & Q_{10} & Q_{11} & Q_{12} \end{bmatrix}^T$$

By imposing boundary conditions at the elements end, we have to evaluate the nodal forces $\mathbf{Q}$ associated to the nodal displacement $\mathbf{q}$. This can be carried out either by the displacement-based approach or by the force-based approach.

Through the Principle of Virtual Displacements (PVD), by assigning the nodal displacements $\mathbf{q}$, the internal work produced by a variation of the real kinematic

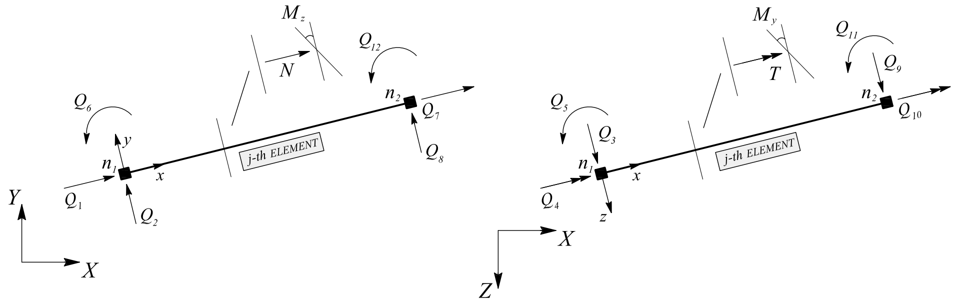

(a) Plane x-y.   **(b)** Plane x-z.

Figure 4.4: Beam element notations. Static field. Nodal foces **Q**.

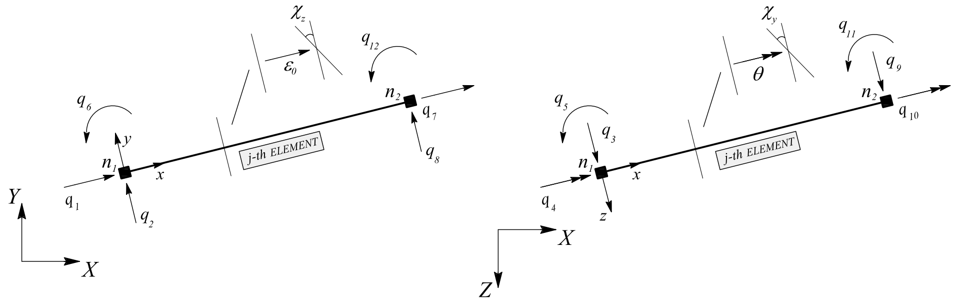

(a) Plane x-y.   **(b)** Plane x-z.

Figure 4.5: Beam element notations. Kinematic field. Nodal displacements **q**.

field with the real static field is computed. In general, we don't know the kinematic quantities in a generic section of the element as a function of **q**. However, it is possible to interpolate them by using specific shape functions ordered in a matrix called $\mathbf{B}(x)$. The element formulated in this way is called a *displacement-based element* and it will be presented in par. 4.4.1. On the contrary, if we apply the Principle of Virtual Forces (PVF), we have to compute the internal work produced by a variation of the real static field with the real kinematic field, by assigning the nodal forces **Q**. Similar to the previous case, in order to compute the internal work, the static quantities in a generic section of the element have to be expressed as a function of **Q** by using equilibrium statements. As a result, we can find exact shape functions $\mathbf{b}(x)$ and as a consequence, intrinsic approximations are not present. In this case, some benefits derive from the fact that models with force interpolation functions, that reproduce the variation of internal element forces in a strict sense, yield the exact solution of the governing equations in the absence of geometric nonlinearity (Neuenhofer and Filippou, 1997). The element formulated in this way is a *force-based element*, as discussed in par. 4.4.2. However, the major drawback of the flexibility formulation is its numerical implementation in a standard finite element analysis program that imposes kinematic, rather than static, boundary conditions at the element ends (Spacone *et al.*, 1995). These aspects produce an *Element State Determination* process that is more complex with respect to the displacement based elements. Since the input are nodal displacements and the corresponding output both nodal forces and element stiffness matrix, a flexibility based element does not interpolate the nodal displacements (known terms), but the nodal forces (unknown terms). There is the so-called *lack-of-fit* and additional calculations are needed.

4.4.1 STIFFNESS APPROACH

In the stiffness method, the displacement field of the 3D finite element is described by the displacement components $u = u(x, y, z)$, $v = v(x, y, z)$, $w = w(x, y, z)$ and it can be fully defined by means of the center of mass displacement components and by torsional rotation. At the section of abscissa ($0 \leq x \leq l$), the displacement field $\mathbf{u}(x)$ is discretized and interpolated in terms of generalized displacement degrees of freedom $\mathbf{q}$ such that:

$$\mathbf{u}(x) = \begin{bmatrix} u_0(x) \\ v_0(x) \\ w_0(x) \\ \varphi_x(x) \end{bmatrix} = \mathbf{N}(x)\mathbf{q} \tag{4.2}$$

In conventional frame elements, the matrix of displacement functions $\mathbf{N}(x)$ is defined by adopting the cubic Hermitian polynomials for the transverse displacement fields and linear Lagrangian shape functions for the axial displacement and torsional rotation, defined as follows:

$$\begin{aligned}
N_1(x) &= 1 - \left(\frac{x}{l}\right) = N_4(x) \\
N_2(x) &= 1 - 3\left(\frac{x}{l}\right)^2 + 2\left(\frac{x}{l}\right)^3 = N_3(x) \\
N_5(x) &= -l\left[\left(\frac{x}{l}\right) - 2\left(\frac{x}{l}\right)^2 + \left(\frac{x}{l}\right)^3\right] = -N_6(x) \\
N_7(x) &= \left(\frac{x}{l}\right) = N_{10}(x) \\
N_8(x) &= 3\left(\frac{x}{l}\right)^2 - 2\left(\frac{x}{l}\right)^3 = N_9(x) \\
N_{11}(x) &= l\left[\left(\frac{x}{l}\right)^2 - \left(\frac{x}{l}\right)^3\right] = -N_{12}(x)
\end{aligned} \tag{4.3}$$

The matrix of displacement functions $\mathbf{N}(x)$ results:

$$\begin{bmatrix}
N_1 & 0 & 0 & 0 & 0 & 0 & N_7 & 0 & 0 & 0 & 0 & 0 \\
0 & N_2 & 0 & 0 & 0 & N_6 & 0 & N_8 & 0 & 0 & 0 & N_{12} \\
0 & 0 & N_3 & 0 & N_5 & 0 & 0 & 0 & N_9 & 0 & N_{11} & 0 \\
0 & 0 & 0 & N_4 & 0 & 0 & 0 & 0 & 0 & N_{10} & 0 & 0
\end{bmatrix} \tag{4.4}$$

The expression for the deformation fields $\mathbf{e}_s(x)$ is then:

$$\mathbf{e}_s(x) = \begin{bmatrix} \varepsilon_0 \\ \chi_z \\ \chi_y \\ \theta \end{bmatrix} = \mathbf{B}(x)\mathbf{q} \tag{4.5}$$

where $\mathbf{B}(x)$ contains the derivatives of the shape functions previously introduced. According to the Principle of Virtual Displacements, the internal work is:

$$\begin{aligned} \delta W_i &= \int_0^l \delta \mathbf{e}_s^T(x) \cdot \mathbf{f}_s(x)\, dx = \\ &= \int_0^l \delta \mathbf{q}^T \mathbf{B}^T(x) \cdot \mathbf{f}_s(x)\, dx \\ &= \delta \mathbf{q}^T \int_0^l \mathbf{B}^T(x) \cdot \mathbf{f}_s(x)\, dx \\ &= \delta \mathbf{q}^T \mathbf{Q} \end{aligned} \tag{4.6}$$

in which we can recognize the element resisting forces $\mathbf{Q}$.

$$\mathbf{Q} = \int_0^l \mathbf{B}^T(x)\ \mathbf{f}_s(x)\, dx \tag{4.7}$$

Being this problem nonlinear, a tangent approach is used. The Jacobian matrix involved in the iterations is equal to the tangent stiffness matrix $\mathbf{k}$ of the element and it is defined by:

$$\mathbf{k} = \int_0^l \mathbf{B}^T(x)\ \mathbf{k}_s(x)\ \mathbf{B}(x)\, dx \tag{4.8}$$

in which $\mathbf{k}_s(x)$ is the tangent stiffness matrix of the section at the abscissa x of the element.

4.4.1.1 DISTRIBUTED LOADS

In a displacement-based element, distributed loads in Fig. 4.6 can be included by means of equivalent nodal forces. By defining the load vector $\mathbf{f}_p$:

$$\mathbf{f}_p = \begin{bmatrix} f_x & f_y & f_z & m_t \end{bmatrix}^T \tag{4.9}$$

the virtual external work δW_e produced by the displacements $\mathbf{u}$ and the distributed forces $\mathbf{f}_p$ is computed in all the sections of the element as follow:

$$\delta W_e = \int_0^l \delta \mathbf{u}^T(x) \cdot \mathbf{f}_p(x)\, dx \tag{4.10}$$

By introducing (4.2) in (4.10) we obtain:

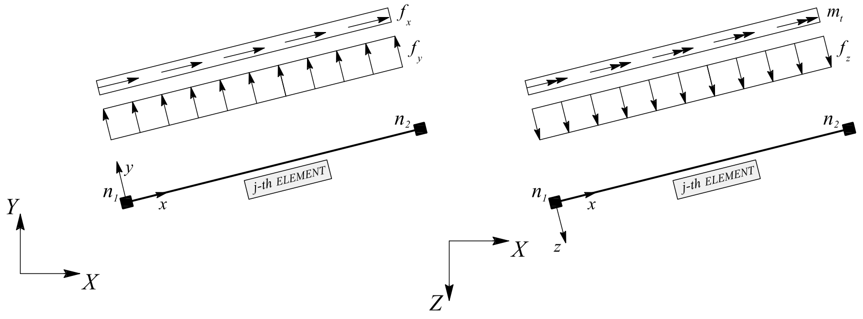

(a) Plane x-y. **(b)** Plane x-z.

Figure 4.6: Distributed loads on the beam element.

$$
\begin{aligned}
\delta W_e &= \int_0^l \delta \mathbf{u}^T(x) \cdot \mathbf{f}_p(x)\, dx = \int_0^l \delta(\mathbf{N}(x)\mathbf{q})^T \cdot \mathbf{f}_p\, dx = \\
&= \int_0^l \delta \mathbf{q}^T \mathbf{N}(x)^T \mathbf{f}_p\, dx = \\
&= \delta \mathbf{q}^T \int_0^l \mathbf{N}(x)^T \cdot \mathbf{f}_p\, dx \\
&= \delta \mathbf{q}^T \;\; \mathbf{f}_{ne}
\end{aligned}
\tag{4.11}
$$

from which we can define the equivalent nodal forces $\mathbf{f}_{ne}$:

$$
\mathbf{f}_{ne} = \int_0^l \mathbf{N}(x)^T \cdot \mathbf{f}_p\, dx \tag{4.12}
$$

These nodal forces depends on the shape functions $\mathbf{N}(x)$ used to discretize and interpolate the displacement field in terms of generalized displacement degrees of freedom $\mathbf{q}$.

4.4.1.2 GEOMETRIC NON LINEARITIES

In the beam element formulation, the geometrical nonlinearities, due to the second-order effects, also contribute to both the element stiffness matrix $\mathbf{k}$ and the vector of resisting forces $\mathbf{Q}$. Let P be an axial force applied to the ends of the beam element, and let Δ be the corresponding displacement (Fig. 4.7), (Malerba and Bontempi, 1989), (Biondini *et al.*, 2004a). This displacement is congruent with the deformed shape and equals the difference between the length of the bent beam, assumed as axially rigid, and the length of the cord of its deformed axis:

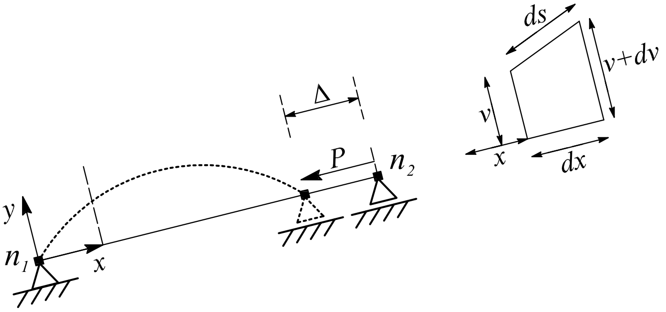

Figure 4.7: Second order geometrical non-linearity.

$$\begin{aligned}
ds - dx &= \sqrt{(dx^2 + dy^2 + dz^2)} - dx = \\
&= dx \left\{ 1 + \frac{1}{2} \left[\left(\frac{dv}{dx} \right)^2 + \left(\frac{dw}{dx} \right)^2 \right] - \frac{1}{8} \left[\left(\frac{dv}{dx} \right)^4 + \left(\frac{dw}{dx} \right)^4 \right] + \cdots \right\} = \\
&= \frac{1}{2} \left[\left(\frac{dv}{dx} \right)^2 + \left(\frac{dw}{dx} \right)^2 \right] + \cdots
\end{aligned} \tag{4.13}$$

By neglecting the higher order terms, Δ became:

$$\Delta = \int_0^l (ds - dx)\; dx = \frac{1}{2} \int_0^l \left[\left(\frac{dv}{dx} \right)^2 + \left(\frac{dw}{dx} \right)^2 \right] dx \tag{4.14}$$

and adopting the beam's displacement functions in the following form:

$$\begin{bmatrix} \dfrac{dv}{dx} \\ \dfrac{dw}{dx} \end{bmatrix} = \mathbf{G} \cdot \mathbf{q} \tag{4.15}$$

where the matrix **G** is defined as:

$$\begin{bmatrix}
0 & 0 & 0 & 0 & 0 & 0 & 0 & 0 & 0 & 0 & 0 & 0 \\
0 & N_{2,x} & 0 & 0 & 0 & N_{6,x} & 0 & N_{8,x} & 0 & 0 & 0 & N_{12,x} \\
0 & 0 & N_{3,x} & 0 & N_{5,x} & 0 & 0 & 0 & N_{9,x} & 0 & N_{11,x} & 0 \\
0 & 0 & 0 & 0 & 0 & 0 & 0 & 0 & 0 & 0 & 0 & 0
\end{bmatrix} \tag{4.16}$$

the displacement and his virtual variation can be written as:

$$\begin{aligned}
\Delta &= \frac{1}{2} \mathbf{q}^T \int_0^l \mathbf{G}^T(x) \cdot \mathbf{G}(x)\, dx \cdot \mathbf{q} \\
\delta\Delta &= \delta \mathbf{q}^T \int_0^l \mathbf{G}^T(x) \cdot \mathbf{G}(x)\, dx \cdot \mathbf{q}
\end{aligned} \tag{4.17}$$

The external virtual work can be hence written as:

$$\delta W_G = P \cdot \delta\Delta = \delta\mathbf{q}^T \int_0^l P\ \mathbf{G}^T(x) \cdot \mathbf{G}(x)\, dx \cdot \mathbf{q} \tag{4.18}$$

By using the same notation introduce before, we can find a geometric contribution to the element resisting forces $\mathbf{Q}$:

$$\begin{aligned} \mathbf{Q}_g &= \delta\mathbf{q}^T \left(\int_0^l P\ \mathbf{G}^T(x) \cdot \mathbf{G}(x)\, dx \right) \mathbf{q} = \\ &= \delta\mathbf{q}^T \qquad\qquad \mathbf{k}_g \qquad\qquad \mathbf{q} \end{aligned} \tag{4.19}$$

in which $\mathbf{k}_g$ is the geometric stiffness matrix of the element. In general, however, also the effects due to geometric nonlinearities must be evaluated by numerical integration since axial forces derive from variable sectional states. Through (4.19), the equilibrium equations (7.11b) implicitly take into account the so-called $P - \Delta$ effect.

4.4.2 FLEXIBILITY APPROACH

In a force-based element the static field is defined by using equilibrium equations, derived with the direct stiffness method. Then, the application of the Virtual Force Principle gives compatibility equations. However, due to the so-called *lack-of-fit*, the scope of a flexibility approach is to determine the nodal forces and the element stiffness matrix in order to write global equilibrium equations. In order to do that, a *mixed approach* as reported in (Taylor *et al.*, 2003) is adopted and the definition of two reference systems is required. Thus, the quantities referred to the system without rigid body modes are conventionally over-lined while the ones referred to the system with rigid body modes follow the notation as in Fig. 4.4 and Fig. 4.5 .

4.4.2.1 STATIC FIELD

Let's considered the generic *j-th* element of the structure, as reported in Fig. 4.4. Since the element is free in the space, this system is indicated as element "with rigid body modes". The nodal forces $\mathbf{Q}$ act in nodes n_1 and n_2.
By writing equilibrium, a system of six equations in twelve unknowns can be obtained:

$$\begin{aligned} Q_1 + Q_7 &= 0 \\ Q_4 + Q_{10} &= 0 \\ Q_2 + Q_8 &= 0 \\ Q_3 + Q_9 &= 0 \\ Q_6 + Q_{12} - Q_2 \cdot l &= 0 \\ Q_5 + Q_{11} - Q_9 \cdot l &= 0 \end{aligned} \tag{4.20}$$

In other words, between twelve nodal forces only six of them are independent: these are the so-called *basic forces*, collected in the vector $\bar{\mathbf{Q}}$. They act on a system that can be viewed as the element "without rigid body modes", as shown in Fig. 4.8.

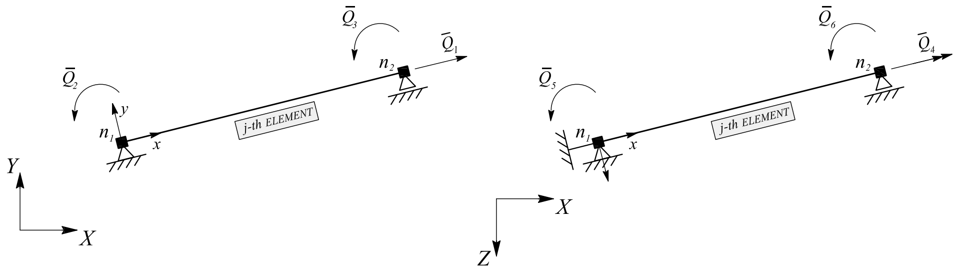

(a) Plane x-y. **(b)** Plane x-z.

Figure 4.8: Static field of the *j-th* element *without* rigid body modes.

By choosing as basic forces in the plane x-y the force in the second node Q_7 and the two nodal moments Q_6 and Q_{12}, and in the plane x-z the three nodal moments Q_{10}, Q_5 and Q_{11}, we define:

$$\begin{matrix} \bar{Q}_1 = Q_7 & \bar{Q}_2 = Q_6 & \bar{Q}_3 = Q_{12} \\ \bar{Q}_4 = Q_{10} & \bar{Q}_5 = Q_5 & \bar{Q}_6 = Q_{11} \end{matrix} \tag{4.21}$$

and

$$\bar{\mathbf{Q}} = \begin{bmatrix} \bar{Q}_1 & \bar{Q}_2 & \bar{Q}_3 & \bar{Q}_4 & \bar{Q}_5 & \bar{Q}_6 \end{bmatrix} \tag{4.22}$$

The relation between the nodal forces $\mathbf{Q}$ and the basic forces $\bar{\mathbf{Q}}$ can be obtained by using equilibrium. In matrix form we have:

$$\underset{\mathbf{Q}}{\begin{bmatrix} Q_1 \\ Q_2 \\ Q_3 \\ Q_4 \\ Q_5 \\ Q_6 \\ Q_7 \\ Q_8 \\ Q_9 \\ Q_{10} \\ Q_{11} \\ Q_{12} \end{bmatrix}} \underset{=}{=} \underset{\mathbf{h}_l^T}{\begin{bmatrix} -1 & 0 & 0 & 0 & 0 & 0 \\ 0 & 1/l & 1/l & 0 & 0 & 0 \\ 0 & 0 & 0 & 0 & -1/l & -1/l \\ 0 & 0 & 0 & -1 & 0 & 0 \\ 0 & 0 & 0 & 0 & 1 & 0 \\ 0 & 1 & 0 & 0 & 0 & 0 \\ 1 & 0 & 0 & 0 & 0 & 0 \\ 0 & -1/l & -1/l & 0 & 0 & 0 \\ 0 & 0 & 0 & 0 & 1/l & 1/l \\ 0 & 0 & 0 & 1 & 0 & 0 \\ 0 & 0 & 0 & 0 & 0 & 1 \\ 0 & 0 & 1 & 0 & 0 & 0 \end{bmatrix}} \underset{\bar{\mathbf{Q}}}{\begin{bmatrix} \bar{Q}_1 \\ \bar{Q}_2 \\ \bar{Q}_3 \\ \bar{Q}_4 \\ \bar{Q}_5 \\ \bar{Q}_6 \end{bmatrix}} \tag{4.23}$$

where l is the length of the element.

4.4.2.2 KINEMATIC FIELD

In a similar way, for the kinematic field it is possible to define two types of nodal displacements: the ones that act on the element "with rigid body modes" (Fig. 4.5),

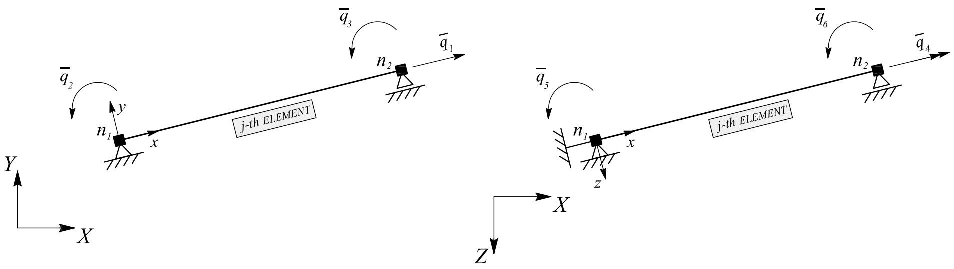

(a) Plane x-y. **(b)** Plane x-z.

Figure 4.9: Kinematic field of the *j-th* element *without* rigid body modes.

marked with $\mathbf{q}$, and the ones that act on the element "without rigid body modes", marked with $\bar{\mathbf{q}}$.

The relation between the two vector of nodal displacements can be obtained by using the Virtual Work Principle. The following condition holds:

$$\underbrace{\begin{bmatrix} \bar{q}_1 \\ \bar{q}_2 \\ \bar{q}_3 \\ \bar{q}_4 \\ \bar{q}_5 \\ \bar{q}_6 \end{bmatrix}}_{\bar{\mathbf{q}}} = \underbrace{\begin{bmatrix} -1 & 0 & 0 & 0 & 0 & 0 & 1 & 0 & 0 & 0 & 0 & 0 \\ 0 & 1/l & 0 & 0 & 0 & 1 & 0 & -1/l & 0 & 0 & 0 & 0 \\ 0 & 1/l & 0 & 0 & 0 & 0 & 0 & -1/l & 0 & 0 & 0 & 1 \\ 0 & 0 & 0 & -1 & 0 & 0 & 0 & 0 & 0 & 1 & 0 & 0 \\ 0 & 0 & -1/l & 0 & 1 & 0 & 0 & 0 & 1/l & 0 & 0 & 0 \\ 0 & 0 & -1/l & 0 & 0 & 0 & 0 & 0 & 1/l & 0 & 1 & 0 \end{bmatrix}}_{\mathbf{h}_l} \underbrace{\begin{bmatrix} q_1 \\ q_2 \\ q_3 \\ q_4 \\ q_5 \\ q_6 \\ q_7 \\ q_8 \\ q_9 \\ q_{10} \\ q_{11} \\ q_{12} \end{bmatrix}}_{\mathbf{q}} \tag{4.24}$$

in which we can observe that the transformation matrix is the transpose of the one relative to the static field (see (4.23)).

4.4.2.3 ADDITIONAL CONSIDERATIONS

By using a flexibility approach, if we know the he nodal forces $\mathbf{Q}$, the element stiffness matrix $\mathbf{k}$ can be computed by inverting the element flexibility matrix. It's clear that the flexibility matrix in the system with rigid body modes is rank deficient (6 times in space) and so that development can not be performed. However, we can at first work in the reference system without rigid body modes (in which matrices have full rank), and than we can move the information in the reference system with rigid body modes. The following passages are required:

1. by working in the element without rigid body modes, we can find the static quantities $\mathbf{f}_s(x)$ in a generic section by using the static shape functions matrix

$\mathbf{b}(x)$:

$$\mathbf{f}_s(x) = \mathbf{b}(x)\bar{\mathbf{Q}} \tag{4.25}$$

2. by using the section forces in (4.25), we can find the sectional deformations $\mathbf{e}_s(x)$ in *indirect way*:

$$\mathbf{e}_s(x) = (\mathbf{k}_s)^{-1}\,\mathbf{f}_s(x) = \boldsymbol{\phi}_s\ \mathbf{f}_s(x) \tag{4.26}$$

   where $\mathbf{k}_s$ is the section stiffness matrix and $\boldsymbol{\phi}_s$ is the section flexibility matrix;

3. according to the Principle of Virtual Forces the internal work is:

$$\begin{aligned} \delta W_i &= \int_0^l \delta\mathbf{f}_s^T(x)\cdot\mathbf{e}_s(x)\,dx = \\ &= \int_0^l \delta\mathbf{Q}^T\mathbf{b}^T(x)\cdot\mathbf{e}_s(x)\,dx \\ &= \delta\mathbf{Q}^T\int_0^l \mathbf{b}^T(x)\cdot\mathbf{e}_s(x)\,dx \\ &= \delta\mathbf{Q}^T\bar{\mathbf{q}} \end{aligned} \tag{4.27}$$

   in which we can recognize the element nodal displacements $\bar{\mathbf{q}}$, associate to the nodal forces $\bar{\mathbf{Q}}$, as the integral of section deformations $\mathbf{e}_s(x)$ (produced by section forces $\mathbf{f}_s(x)$, interpolated from $\mathbf{Q}$ in an exact way):

$$\bar{\mathbf{q}} = \int_0^l \mathbf{b}(x)^T\ \mathbf{e}_s(x)\ dx \tag{4.28}$$

   whose derivatives gives the flexibility matrix $\bar{\boldsymbol{\Phi}}$:

$$\bar{\boldsymbol{\Phi}} = \int_0^l \mathbf{b}(x)^T\ \boldsymbol{\phi}_s\ \mathbf{b}(x)\ dx \tag{4.29}$$

4. flexibility matrix defined in (4.29) is referred to the system without rigid body modes. For that reason, matrix $\bar{\boldsymbol{\Phi}}$ has full rank and it can be inverted in order to obtain the stiffness matrix $\bar{\mathbf{k}}$:

$$\bar{\mathbf{k}} = \left(\bar{\boldsymbol{\Phi}}\right)^{-1} \tag{4.30}$$

5. matrix $\bar{\mathbf{k}}$ is the operator that gives:

$$\bar{\mathbf{k}}\ \bar{\mathbf{q}} = \bar{\mathbf{Q}} \tag{4.31}$$

   However, what is necessary is the stiffness matrix referred to the system with rigid body modes $\mathbf{k}$, so that:

$$\mathbf{k}\ \mathbf{q} = \mathbf{Q} \tag{4.32}$$

   We can define that matrix through the following developments:

(a) we introduce in (4.31) the expression given by (4.24):

$$\bar{\mathbf{k}}\ \mathbf{h}_l\ \mathbf{q} = \bar{\mathbf{Q}} \tag{4.33}$$

(b) we pre-multiply by $\mathbf{h}_l^T$:

$$\mathbf{h}_l^T\ \bar{\mathbf{k}}\ \mathbf{h}_l\ \mathbf{q} = \mathbf{h}_l^T\ \bar{\mathbf{Q}} \tag{4.34}$$

(c) for the right term, by remembering (4.23), we can write:

$$\left(\mathbf{h}_l^T\ \bar{\mathbf{k}}\ \mathbf{h}_l\right)\ \mathbf{q} = \mathbf{Q} \tag{4.35}$$

(d) and we have find the definition of matrix $\mathbf{k}$:

$$\mathbf{k} = \mathbf{h}_l^T\ \bar{\mathbf{k}}\ \mathbf{h}_l \tag{4.36}$$

4.4.2.4 Distributed loads

In a force-based element, the inclusion of distributed forces is straightforward. In comparison to the stiffness approach, in this case we don't interpolate the displacement field, but the static field is interpolated in an exact way by using equilibrium statements. In fact, the distributed loads represented in Fig. 4.10 provide additional contribution to the formulation presented in par. 4.4.2.3.

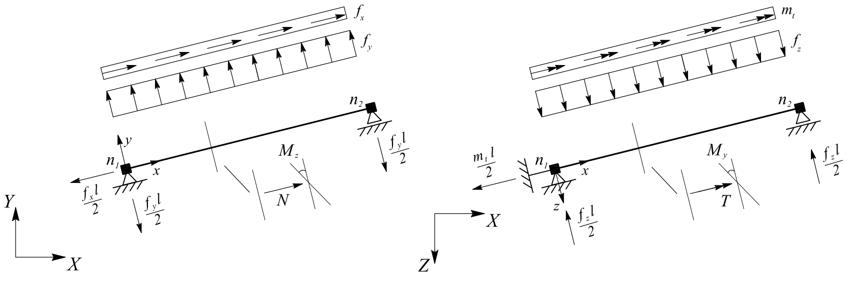

(a) Distributed load in x direction. **(b)** Distributed load in y direction.

Figure 4.10: Distributed loads and associated reaction forces.

In particular, (4.23) became:

$$\mathbf{Q} = \mathbf{h}_l^T \bar{\mathbf{Q}} + \mathbf{h}_f \mathbf{f}_p \tag{4.37}$$

and through (4.25), the following relation can be derived:

$$\mathbf{f}_s(x) = \mathbf{b}(x)\bar{\mathbf{Q}} + \mathbf{b}_f(x)\mathbf{f}_p \tag{4.38}$$

These additional terms enter in the element state determination algorithm and the restoring displacements (4.41) became:

$$\begin{aligned}
\bar{\mathbf{q}}_r &= \int_0^l \mathbf{b}(x)^T \mathbf{e}_s(x)\ dx \\
&= \int_0^l \mathbf{b}(x)^T \boldsymbol{\phi}_s(x)\, \mathbf{f}_s(x)\ dx \\
&= \int_0^l \mathbf{b}(x)^T \boldsymbol{\phi}_s(x)\ \big(\mathbf{b}(x)\, \bar{\mathbf{Q}} + \mathbf{b}_f(x)\, \mathbf{f}_p(x)\big)\ dx \\
&= \left(\int_0^l \mathbf{b}(x)^T \boldsymbol{\phi}_s(x)\, \mathbf{b}(x)\ dx\right) \bar{\mathbf{Q}} + \int_0^l \mathbf{b}(x)^T \boldsymbol{\phi}_s(x)\, \mathbf{b}_f(x)\, \mathbf{f}_p(x)\ dx \\
&= \qquad\qquad \bar{\boldsymbol{\Phi}} \qquad\qquad \bar{\mathbf{Q}} + \qquad\qquad \bar{\mathbf{q}}_{r,f}
\end{aligned} \tag{4.39}$$

4.4.3 ELEMENT STATE DETERMINATION

As discussed in par. 4.4.1 and par. 4.4.2, the *State of the Element* is obtained starting from its nodal displacements $\mathbf{q}$ and the results are the nodal restoring forces $\mathbf{Q}$ and the element stiffness matrix $\mathbf{K}$.

For a displacement-based element, the Element State Determination results direct and straightforward. In fact, it follows two steps:

1. for each section, in direct form:
    - calculate the section deformations $\mathbf{e}_s$ by using (4.5);
    - calculate the section forces $\mathbf{f}_s$ as the integral over the section domain of the stresses produced by $\mathbf{e}_s$;
    - calculate the section stiffness matrix $\mathbf{k}_s$;
2. weighting the section states to obtain the state of the element:
    - resisting forces $\mathbf{Q}$ by using (4.7);
    - element stiffness matrix $\mathbf{k}$ by using (4.8).

On the other hand, in the force-based element the nodal forces $\mathbf{Q}$, which are unknowns, are the terms to be interpolated. As a result, the corresponding element state definition is more complex with respect to the displacement-based approach. This produces a system of non-linear equations to be solved at the element level, due to the *lack-of-fit* between the force-based approach and the displacement-based element. The main steps are:

1. given the nodal displacement in the element with rigid body modes $\mathbf{q}$, calculate the displacements in the system without rigid body modes:

$$\bar{\mathbf{q}} = \mathbf{h}_l\ \mathbf{q} \tag{4.40}$$

2. determine $\bar{\mathbf{Q}}$ so that: $\bar{\mathbf{q}}_r = \bar{\mathbf{q}}$ with:

$$\bar{\mathbf{q}}_r = \int_0^l \mathbf{b}(x)^T \mathbf{e}_s(x)\, dx \tag{4.41}$$

   Such a condition, which represent a system of non-linear equantions, can be solved by adopting the Newton-Raphson approach. Since the integral of $\bar{\mathbf{q}}_r$ depends on the sectional deformations $\mathbf{e}_s(x)$, another system of non-linear equations must be solved at the sectional level.

3. once in the previous step the solution is achieved, we move to the system with rigid body modes in order to calculate:

   - the element resisting forces:

$$\mathbf{Q} = \mathbf{h}_l^T\ \bar{\mathbf{Q}} \tag{4.42}$$

   - the element stiffness matrix:

$$\mathbf{k} = \mathbf{h}_l^T\ [\bar{\mathbf{\Phi}}_i]^{-1}\ \mathbf{h}_l = \mathbf{h}_l^T\ \bar{\mathbf{k}}\ \mathbf{h}_l \tag{4.43}$$

   and the Element State Determination process is consequently completed.

It can be point out that the procedure here recalled is not the unique way to deal with the lack-of-fit problem. In fact, several procedures exist, as reported in detail in (Quagliaroli, 2014).

4.5 STATE OF THE SECTION

The element behavior, according to the procedures in par. 4.4, is determined through the numerical integration of the response of key sections that are monitored through the analysis. In the specific case of fibre beam-column element, the definition of the sectional state is obtained by the *State of the Fibers* that compose it. Here, the section must be viewed as a module able to solve two types of problems:

- Type 1 Problem (direct):
  given a strain state (the sectional strains) $\mathbf{e}_s$, determine the stress state (the resultant, or restoring, or resisting section forces) $\mathbf{f}_{s,r}$:

$$\mathbf{e}_s \quad \rightarrow \quad \mathbf{f}_{s,r} \tag{4.44}$$

- Type 2 Problem (indirect):
  given a stress state $\mathbf{f}_{s,e}$, determine the sectional strain state $\mathbf{e}_s$:

$$\mathbf{f}_s \quad \rightarrow \quad \mathbf{e}_s \tag{4.45}$$

In RC sections, it's clear that we have to deal with two materials: (1) the concrete, that is described by a continuum sectional domain, and (2) the reinforcing steels, that is described by discrete quantities arbitrary positioned in the sectional domain.

This paragraph deals with the definition of the state of a RC section, by recalling the sectional models that can then applied in formulating the beam-column elements. In fact, the applicability of beam elements for the analysis of frame systems, using fibers subjected to uniaxial stress states, is basically limited to those cases in which shear and torsion are not determinant on their behavior and ultimate capacity. Since the fibers account only the axial-bending interaction (pure normal stresses), the process can be considered straightforward. However, in 3D case, beams cross-sections can be subjected to a total of six internal forces: three normal - axial force and two bending moments - and three tangential - torsion and two shear forces. When tangential forces acting in the cross-section, the fiber-element approaches rely on material isotropy assumptions to decouple normal and tangential stresses. Nevertheless, if concomitant shear forces and torsional are relevant, as in the case of RC material, a generalized coupling between normal and tangential forces takes place. The complexity of the fully-coupled problem of RC sections under the total six forces is considered higher than for solely normal stresses and it is still today an object of several researches. In the following, the treatment of normal and tangential stresses is briefly addressed and discussed.

4.5.1 NORMAL FORCES

Dealing with an arbitrary RC cross-section under the interaction between axial force and bending moments, the sectional state is derived by subdividing the section into sub-domains called fibers. In the corresponding fiber's centroid the function that has to be integrated is evaluated and then weighted by its area (Riemann Mid-Point Integration Rule). Thus, the integral is mathematically evaluated through the summation of each fiber's contribution. Among the different techniques proposed (Quagliaroli *et al.*, 2015), the so called "fiber approach" is considered the simpler particular case.

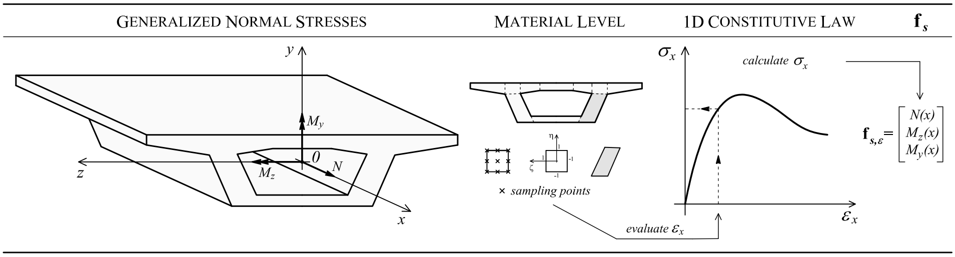

Figure 4.11: Uniaxial $\sigma - \varepsilon$ constitutive law used to derive the generalized stresses N, M_y and M_z.

In general, the Navier-Bernoulli hypothesis - plane section (PS) - has proved to be a suitable approximation of the sections' kinematics in all range of loadings (Bairan, 2005). Uniaxial longitudinal strain ε_x at each sub-domain is computed from the generalized strains by means the PS hypothesis. As a consequence, the corresponding longitudinal stresses σ_x are computed by using a non-linear uniaxial constitutive model $\sigma_x = \sigma_x(\varepsilon_x)$ and their integral, over the sectional domains, gives the generalized stresses (axial force and two bending moments), as shown in Fig. 4.11.

These formulations have been successfully employed to study complex non-linear and time-dependent phenomena on RC elements, such as those proposed by (Kang and Scordelis, 1980), (Buckle and Jackson, 1981), (Chan, 1982), (Mari and Scordelis, 1984), (Ulm *et al.*, 1994), (Cruz *et al.*, 1998) and (Ketchum, 1988). When the section discretization into sub-domains is coupled with a force-based element, a virtual *exact* solution of the problem is obtained, which represent the higher degree of accuracy at the current state of knowledge (Baron, 1961), (Bäcklund, 1976), (Carol and Murcia, 1989), (Spacone *et al.*, 1995), (Spacone *et al.*, 1996) and (Petrangeli and Ciampi, 1997a).

However, the main limitations of this formulation are related to the coupled interaction between the normal forces and the tangential ones. It has been recognized in (Ranzo and Petrangeli, 1998) that in a beam model the main assumptions, such as PS hypothesis, are more important than the details on more specific aspects in the element's formulation of material behavior.

4.5.2 Combined Normal and Tangential Forces

Traditionally, the analysis of concrete structures under shear and torsion has performed separately from normal forces, mostly through empirical or semi-empirical formulations. Some design codes include a-posteriori checks to take into account the interaction effects in a simplified form. Although rational sectional analysis models for shear and torsion exist, they are rare and are either limited to some particular load combinations.

Fiber elements, as described above, are not capable of considering shear stresses, as in the form $\tau = \tau(\gamma)$, therefore shear forces and torsion cannot be integrated as is done with normal forces. As in Fig. 4.12, sectional response to torque moment is sometimes considered in uncoupled fashion from the bending one, by means of a given generalized force-deformation curve or simply as perfect-elastic. In this case, the level of accuracy achieved results less that the one obtained with the concomitant normal stresses.

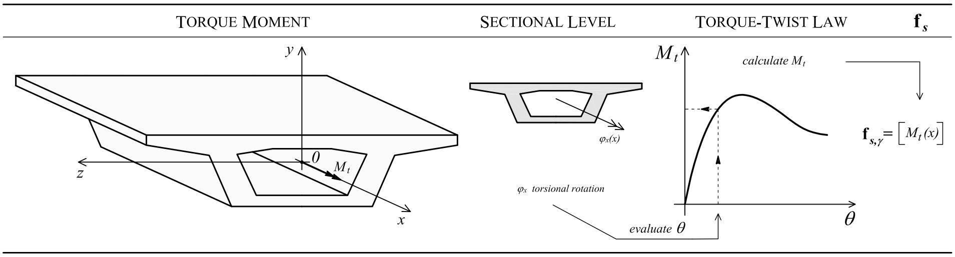

Figure 4.12: Torque-twist relationship under the hypothesis of uncoupling between torsional and flexural behavior.

Despite it results a difficult task, in case of RC sections, the σ-τ interaction has a relevant importance. If the load produces shear stresses, both a constitutive model of the materials (which must be multi-axial) and a suitable representation of kinematics in order to obtain the distribution of strains along the section are needed. Among the variety of constitutive models reported in literature in the last decades, the *smeared-crack models* seem to be the most suitable for cross-sectional analysis. In fact, the reinforcing concrete is treated as a continuum material with anisotropic characteristics, in which a crack is a discontinuity in the material and provides enough information for the directionality of the response. Some of the more extended smeared-crack models for concrete applications have been developed by two main groups: the group at University of Toronto (Vecchio and Collins, 1993), (Vecchio, 2000) and the group of University of Houston (Hsu, 1998), (Pang and Hsu, 1995), among others.

When a constitutive model is defined, some difficulties arise in the adoption of valid hypotheses for computing the coupling response under the applied six internal forces. As mentioned, it cannot be possible to derive the response of the cross-section in presence of tangential forces by direct integration over all material points under the PS hypothesis. In other word, in RC sections, the distribution of shear stresses and strain is not only more complex but also *state dependent.* This is the main problematic of modeling non-linear response of RC sections in presence of shear forces and torsion.

In the last two decades there have been considerable efforts in extending the capabilities of beam elements to correctly deal with load combinations more general than bending moments and axial force. Therefore, some models for integrating the sectional response in RC sections with shear forces or torsion have been proposed in this period. As a necessity, these models require some procedures for estimating the shear stress or strain distribution. In general, the approaches available can be classified into two groups:

1. *Fixed pattern approaches.* These approaches, equivalent to displacement-based sectional model, investigate tangential internal forces by a-priori stating of some constrained relationships between the section's tangential deformation and shear strain distribution, the section's internal forces and the distribution of shear stresses. This means that the shear strain and stress patterns are taken constant during the whole loading process. Despite these approaches exhibit a very fast performance, inter-fiber equilibrium cannot be verified as well as the compatibility among among fibres cannot be guaranteed. In addition, choosing the correct pattern is not always an easy task: it depends on section's shape, reinforcement arrangement and material's state. Models based on these approaches are detailed in the work of (Guner, 2008), (Ceresa *et al.*, 2007) and (Ferreira, 2013). Some sectional formulations that use these approaches for general 3D loading can be found in the works of (Onsongo, 1978), (Rahal and Collins, 1995), (Recupero *et al.*, 2005), (Gregori *et al.*, 2007) and (Capdevielle *et al.*, 2014). These models result less accurate than the second ones.

2. *Inter-Fiber Equilibrium approaches.* In an element built with a nonlinear material, such as reinforced concrete, stress and strain distribution must have a state-dependent property to satisfy the internal equilibrium requirements

among fibers. Therefore, the shapes of both stress and strain distribution change during loading. These models, equivalent to force-based sectional models, present a very hight accuracy and complexity, but also a demanding implementation. The works of (Vecchio and Collins, 1988), (Bentz, 2000), (Ranzo, 2000), (Bairan and Mari, 2007) and (Mohr, 2012), among others belong to this group. In the model called TINSA (Total Interaction Nonlinear Sectional Analysis) developed at the UPC University (Barcelona, Spain), (Bairán García, 2005) proposes an accurate model that solves the problem of the six internal force interactions at the section level. This is the most elegant and complete sectional model proposed to date. An extending version can be found in (Mohr *et al.*, 2010). This model has been readopted and improved by (Saritas, 2006) and Le Corvec (2012), in dealing with torsion effects and shear-lag problem in steel beams.

4.6 STATE OF THE FIBER

The Material State Determination is aimed at computing the stresses $\boldsymbol{\sigma}_p(x,y,z)$ in order to determine the section stiffness matrix $\mathbf{k}_s(x,y,z)$ and the vector of restoring forces $\mathbf{f}_s$ for a given strains $\varepsilon_p(x,y,z)$ at a specific material point used to perform the numerical integration required. In dealing with a general 3D element, the six-component stress vector $\boldsymbol{\sigma}(x,y,z)$ and the full stiffness matrix for a given six-component strain vector $\boldsymbol{\varepsilon}(x,y,z)$ have to be evaluated.
However, the evaluation depends on the specific model adopted to describe the behavior of the material point.

In the last decades, many studies are available on the behavior of both structural steel and concrete, aiming to develop numerical models to reproduce their response in structural analysis. Relevant formulation can be found in (Lemaitre and Chaboche, 1994) and (Chen and Saleeb, 2013). However, to incorporate 3D material models in the finite beam element is a challenging problem, given the complex phenomena governing their mechanical behavior. In the field of engineering structures, another option consists on selecting the relevant stress components from the six ones involved in the 3D model.

As described in Par. 4.11, the presented finite beam element assumes only three strain variables $\boldsymbol{\varepsilon}_p(x,y,z) = [\varepsilon_x \gamma_{xy} \gamma_{xz}]^T$ under the plane sections hypothesis. The contribution of the corresponding stress components $\boldsymbol{\sigma}_p(x,y,z) = [\sigma_x \tau_{xy} \tau_{xz}]^T$ is assumed to be uncoupled: the problem dealing with the normal stresses is studied at the material level (Fig. 4.11) while the torque moment is treated at the sectional level (Fig. 4.12).

For a matter of clarity, in RC structures the typical stress-strain relationships are the ones reported in Fig. 4.13. For example, the curve resulting from an uniaxial test on a reinforcing bar usually shows an initial elastic branch, corresponding to the reversible deformation of the material, and a subsequent nonlinear plastic one, corresponding to the formation of permanent strains and starting when the stress exceeds the elastic limit f_y (Fig. 4.13a). Moreover, the plastic branch is often characterized by strain hardening phenomena, i.e. the increase of the material strength produced by the plastic strain growth.

On the contrary, the mechanical response of concrete materials in Fig. 4.13b is influenced by more complex phenomena and it presents a brittle behavior. In compression the stress-strain relationship show a linear behavior up to almost the 30% of the peak compressive strength. For higher stresses, instead, the material can show a hardening response. In tension, the tipical curve presents an initial elastic branch up to a peak stress taht is 10 times smaller than the the compressive peak one. Above this level, a softening behaviour due to the propagation of microcracks in direction orthogonal to the applied load, leading to an abrupt failure of the material can be present.

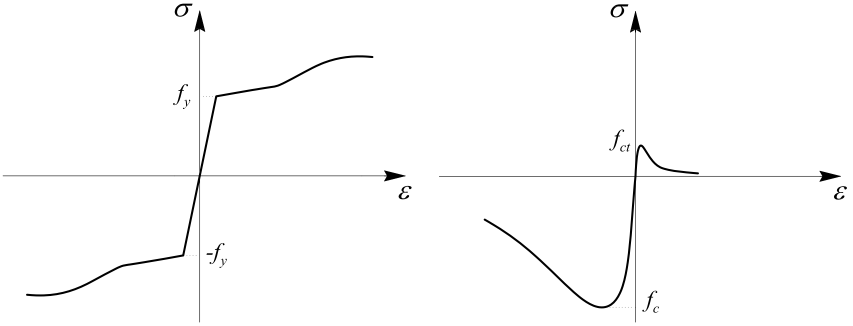

(a) Steel. **(b)** Concrete.

Figure 4.13: Typical mechanical uni-axial response of steel and concrete materials.

4.7 CONCLUSION

In this chapter, a review of the the monodimensional modeling has been presented. At first, the global structural framework is explained with respect to RC frame structures. The generic structure is subdivided into beam-column elements, which are composed by sections. Each section is made by fibers, on which the material state determination is computed.

According to the beam's theory adopted, a dual formulation has been applied in formulating 3D finite beam-column elements: the displacement-based element and the force-based element. The exposed formulations are referred to the generalized stresses N, M and T and the work due to V is not included, as a consequence of plane section hypothesis. It has been shown that the state of the element is obtained by weighting the state of the sections that compose it. In RC sections, the definition of the sectional state results straightforward if we deal with normal stresses, by integrating the state of the fibers in which the section is subdivided. On the contrary, the problem in which a coupling between normal and tangential is present results today still open and object of many researchers.

Concerning the state of the element, the force-based formulation has been here recalled to present in chapter 5 the matrix formulation of the Limit Analysis.

5 Limit Analysis of RC Frame Structures

In this chapter a force-based finite element for the Limit Analysis of three-dimensional RC framed structures is presented. Following the theorems of plastic theory, the complete solution of the problem - i.e. the collapse loads, the stress distribution at the incipient collapse and the collapse mechanism - is obtained and then compared with the Nonlinear Analysis results derived through the displacement-based approach explained in the previous chapter.

5.1 INTRODUCTION

In the usual design approach RC structures are studied as linear elastic systems. The linear elastic analyses (LEA) require only the modulus of elasticity and the gross dimensions of the member composing the skeleton. The resulting internal forces can be immediately used for proportioning the structural element, that is for refining the sectional dimensions and for computing the amount of the reinforcement. However, not only for ultimate loading levels, but also for low ones, this hypothesis may be violated because of the real material properties and sometimes the magnitude of the displacements and strains, which not always result small. Since structural design requires to satisfy both safety and serviceability conditions, a structure has to be properly modeled and analyzed in its whole service life considering the actual loads in order to accurately predict displacements, internal forces and deformations. Consequently, all inelastic and ultimate ranges should be taken into account (Bontempi and Malerba, 1998). Among several computation methods, suitable to solve the structural problem, the formulation of monodimensional beam-column element (as in chapter 4), used to study frame structures, is adopted in this thesis as powerful and efficient tool. According the adopted modelization, two distinct approaches come out.

A effective tool to analyze the behavior of a RC frame structure and to assess its bearing capacity, determining the collapse load, is the *Limit Analysis* (LA), based on the plastic theory (Prager, 1955b), (Dorn and Greenberg, 1957), (Massonnet and Save, 1965), (Nielsen and Hoang, 1984). Limit analysis works with rigid perfectly-plastic constitutive laws of the materials (concrete and steel) and requires the dimensions and reinforcement of the member composing the structure and a loading configuration, which can be composed of a fixed contribution and of a variable part, to be increased by a loading multiplier λ. The results are expressed in terms of the kinematic of the mechanism activated at the collapse (collapse mode) and of the collapse multiplier λ.

Differently, in *Nonlinear Analysis* (NLA) presented in chapter 4, both concrete and steel reinforcement contribute to defining the internal work which leads to the iterative research of the equilibrium. Basic mechanisms are those based on axial-bending interaction only (Kang and Scordelis, 1980), (Bontempi *et al.*, 1995a), but there are beam elements which allow to take into account also the membrane effects and model the shear and torsional behavior, as mentioned in the par. 4.5.2. In fact, Nonlinear Analysis give a more deepen assessment of the interaction mechanisms between concrete and steel reinforcement. They require the material constitutive laws and a failure criterion, the dimensions and reinforcement of the member composing the structure and a loading history. The results allow a thorough description of the structural behavior (displacements and internal stresses, onset and conventional extension of cracking) and identify the ultimate load when the equilibrium is no longer satisfied. Of common interest are the load displacements curves of certain characteristic control nodes, which help to understand the behavior of the structure till the collapse.

Hence, considering the same structure, the NLA represents the evolution of its behavior, in terms both of displacements and internal forces, all along the load path until the collapse. The LA highlights the mechanism of collapse as well as the internal forces diagrams and determines the ultimate value of the load multiplier.

This chapter, after short recalls of the Limit Analysis formulation, studies an existing RC bridge and compares the relevant results. Two aspects are highlighted: the complementary of the information given by the two methods (the load history versus the collapse mode) and the intensity of the ultimate loads. In an ideal comparison, the ultimate load given by the two different analyses is the only common and comparable result and one expects that, apart truncation and rounding approximations, it is unique. In truth, some differences may exist. The sources of these differences, referred to the case studied, are analyzed and discussed and may result a useful reference in approaching analogous problems.

5.2 THE MATRIX APPROACH TO THE LIMIT ANALYSIS

Based on the classical plastic theory, which assumes an ideal rigid perfectly-plastic behavior of the materials, the *Limit Analysis* provides a powerful tool for the assessment of the structural load-bearing capacity. A general formulation of a complete theory for perfectly plastic materials was given by (Gvozdev, 1938), but his work was not known in the Western world until the 1950s, where previously, mainly in works of Prager while at Brown University (Drucker and Prager, 1952) and (Prager, 1955a), a very similar theory had been developed (Nielsen and Hoang, 1984). One of the most important improvements in the development of the plastic theory was undoubtedly the establishment of the *upper* and *lower* bound theorems that, when the first computer based calculations became possible, can be translated in linear mathematical programming problems. Some of the first works in that direction has been done by (De Donato and Maier, 1972) and (Maier, 1973), in which also the geometrical non linearities are considered.

Other applications of limit analysis by mathematical programming can be found in (Cocchetti and Maier, 2003), (Ardito, 2004) and (Ardito *et al.*, 2008), in which also softening plastic-hinge models are considered in the elastic-plastic analyses of frames and critical thresholds on deformations are introduced by solving a non-convex nonsmooth constrained optimization problem usually referred to in the literature as "mathematical program under equilibrium constraints" (Ardito *et al.*, 2010).

5.2.1 BASIC HYPOTHESIS

In this thesis, a force-based finite element for the Limit Analysis of three-dimensional RC framed structures is proposed. The approach neglects shear failures and considers two distinct situations according to the interacting generalized plastic stresses assumed:

1. only axial force N and bending moment M_z;
2. only bending moment M_z and torque moment T.

Thus, a rigid perfectly-plastic constitutive law is adopted to relate the active stresses to the corresponding generalized plastic strains, represented by the cross-sectional quantities respectively:

1. axial elongation Δl and bending rotation θ_z;
2. bending rotation θ_z and twisting θ_x.

In this way, the behavior of the discrete cross-sections where the plastic strains tend to develop, can be represented by a plastic hinge which makes this kinematic behavior possible and, at the same time, fully transfers the corresponding plastic values of the active stresses. The plastic collapse is reached when a set of generalized plastic hinges is able to activate a kinematic mechanism for which the equilibrium can no longer be satisfied (Biondini and Frangopol, 2008).

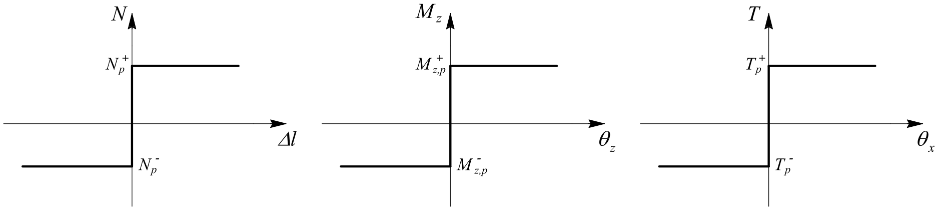

(a) Axial force-displacement. **(b)** Bending moment-rotation. **(c)** Torsion-twisting.

Figure 5.1: Limit Analysis hypothesis: rigid perfectly-plastic behavior.

In both cases, the hypotheses used are: (1) small displacements and stable structure before collapse; (2) rigid perfectly-plastic behavior (Fig. 5.1); (3) either

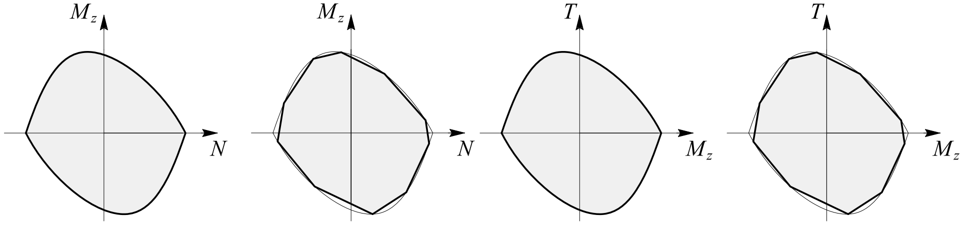

(a) $M_z - N$ domain: the real and linearized one. **(b)** $T - M_z$ domain: the real and linearized one.

Figure 5.2: Limit Interaction Domains in the two distinct cases considered.

only axial force and bending moment or, alternatively, bending moment M_z and the torque moment T active and interacting; (4) ultimate value of active stresses correlated through a curve, which bounds a convex interaction domain containing the origin of the axis (Fig. 5.2) and that can be idealized by a stepwise approximation; (5) the formation of plastic hinges occurs at the ends of the elements.

The proposed approach considers concentrated or distributed applied loads constant or proportionally variable. In the discretization, distributed loads are replaced by equivalent concentrated loads applied in an appropriate number of cross-sections, no distributed loads are considered acting on the element. The approximations, implicit in these assumptions, can be improved by increasing the number of the sides of the linearized yielding curve and/or the number of the beam elements which subdivide the whole structure.

Starting from these introductory concepts, the *upper* and *lower* bound theorems of Limit Analysis must be formulated. Forces, displacements and generalized stresses are assumed with reference to the conventions and the local and global reference systems shown in Fig. 5.3.
For a sake of clarity, to generalize the approach for the two distinct situations (N-M_z or M_z-T), in presenting the matrix formulation of Limit Analysis the active stress components are indicated with the capital letter A and B, as well as the corresponding plastic strains with the lowercase a and b.

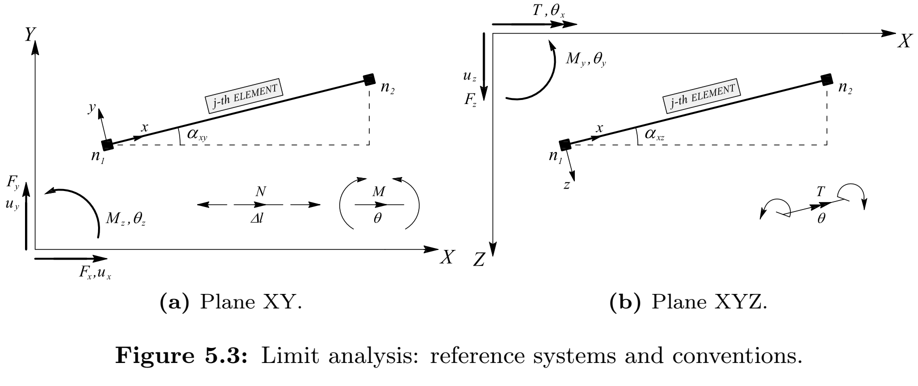

(a) Plane XY. **(b)** Plane XYZ.

Figure 5.3: Limit analysis: reference systems and conventions.

5.2.2 EQUILIBRIUM AND COMPATIBILITY CONDITIONS

For the generic *j-th* element of the structure, the equilibrium conditions are set in accordance to the force method presented in par. 4.4.2.1. In the local coordinate system, by removing the rigid body motions, the active internal forces at the sections ($x = 0, l$) are expressed in function of the basic forces $\bar{\mathbf{Q}}_j$ at the end nodes n_1, n_2 from simple equilibrium equations $\mathbf{r}_i = [A, B] = \mathbf{h}_b \bar{\mathbf{Q}}_j$ (Fig. 4.8).
In the same way, the end global forces $\mathbf{Q}_j$ are derived from $\bar{\mathbf{Q}}_j$ as:

$$\mathbf{Q}_j = \mathbf{h}_l \bar{\mathbf{Q}}_j \tag{5.1}$$

By introducing the transformation matrix $\mathbf{T}_\alpha$:

$$\mathbf{T}_\alpha = \begin{bmatrix} \mathbf{T}_0 & \mathbf{0} & \mathbf{0} & \mathbf{0} \\ \mathbf{0} & \mathbf{T}_0 & \mathbf{0} & \mathbf{0} \\ \mathbf{0} & \mathbf{0} & \mathbf{T}_0 & \mathbf{0} \\ \mathbf{0} & \mathbf{0} & \mathbf{0} & \mathbf{T}_0 \end{bmatrix} \tag{5.2}$$

with

$$\mathbf{T}_0 = \begin{bmatrix} c_{x,X} & c_{x,Y} & c_{x,Z} \\ c_{y,X} & c_{y,Y} & c_{y,Z} \\ c_{x,Z} & c_{y,Z} & c_{z,Z} \end{bmatrix} \tag{5.3}$$

the end global forces $\mathbf{Q}_j$ are rewritten in the global coordinate system as:

$$\begin{aligned} \mathbf{Q}_{g,j} &= \mathbf{T}_\alpha \ \mathbf{Q}_j \\ &= (\mathbf{T}_\alpha \ \mathbf{h}_l)\, \bar{\mathbf{Q}}_j \\ &= \quad \mathbf{H}_{g,j} \ \bar{\mathbf{Q}}_j \end{aligned} \tag{5.4}$$

where $\mathbf{H}_{g,j}$ is the transformed equilibrium matrix, for the element *j-th*. By assembling over all the *ne* elements, we obtain the *global equilibrium equations* which correlate the vector containing all the element basic forces $\mathbf{Q}_t$, to the external nodal forces vector $\mathbf{F}_e$, by means of the the equilibrium matrix $\mathbf{H}_{g,j}$ of the whole structure.

$$\begin{aligned} \mathbf{F}_e &= \sum_{j=1}^{ne} \mathscr{A} \left(\mathbf{Q}_{g,j}\right) \\ &= \sum_{j=1}^{ne} \mathscr{A} \left(\mathbf{H}_{g,j} \cdot \bar{\mathbf{Q}}_j\right) \\ &= \mathbf{H} \cdot \mathbf{Q}_t \end{aligned} \tag{5.5}$$

Compatibility conditions are derived through the Virtual Force Principle (VFP), by equating the virtual internal work δW_i to the external one δW_e. The external and the internal works are:

$$\delta W_e = \delta \mathbf{F}^T \mathbf{s} \qquad\qquad \delta W_i = \delta \mathbf{Q}_t^T \ \mathbf{q}_t \tag{5.6}$$

From (5.5), we have $\delta \mathbf{F}_e = \mathbf{H} \delta \mathbf{Q}_t$ and stating $\delta W_e = \delta W_i$, we obtain:

$$\delta \mathbf{Q}_t^T \, \mathbf{H}^T \, \mathbf{s} = \delta \mathbf{Q}_t^T \, \mathbf{q}_t \tag{5.7}$$

Since such an equation is valid for any choice of $\delta\mathbf{Q}_t^T$, the *global compatibility equations* are finally derived as:

$$\mathbf{q}_t = \mathbf{H}^T\,\mathbf{s} \tag{5.8}$$

The compatibility matrix $\mathbf{H}^T$ is the transposed of the equilibrium matrix $\mathbf{H}$. In these correspondences, the vector of the forces $\mathbf{F}_e$ works for that of the displacements $\mathbf{s}$ in the global reference system, as the vector of the basic forces $\mathbf{Q}_t$ works for that of the basic displacements $\mathbf{q}_t$, as shown in Fig. 4.9.

It has been show that the equilibrium matrix is the transpose of the compatibility matrix. Such a results can be used in order to classify a structure:

- if matrix $\mathbf{H}$ has full rank, with equilibrium equations we can find the vector of basic forces and hence the internal forces: this is the case of a *statically determined structure*;

- if matrix $\mathbf{H}$ has more columns than rows, equilibrium states that infinite solutions can be possibile. This is the case of a *statically undetermined structure*;

- if matrix $\mathbf{H}$ has more rows than columns, equilibrium states that there are not solutions. This is the case of a *kinematic undetermined structure.*

5.2.3 YIELD CONDITION AND FLOW RULE

The constitutive law for a *perfectly-plastic* material must include: *(i)* a *yielding criterion*, which defines the stress state corresponding to the starting of the plastic flow (the yield function curve is convex) and *(ii)* an *associated flow rule*, through which the increments of the plastic strains are correlated to the actual stress state.

In the present case, where the only active generalized plastic stresses for the *i-th* critical cross-section are A and B, the yielding criterion has the shape shown in Fig. 5.4, which can be defined by the equation:

$$f_i(A_i, B_i) = 0 \tag{5.9}$$

Such a criterion defines, in the A-B plane, a domain that can be reasonably idealized by a stepwise approximation which is, for the sake of safety, inscribed within the convex yielding criterion:

$$f_i(A_i, B_i) \leq 0 \tag{5.10}$$

By assuming a stepwise linearization with q sides for each *i-th* plastic domain, with reference to Fig. 5.4 we can define:

- a matrix $\mathbf{N}_i$, in which each row contains the components with respect the axis of the normal vector $\mathbf{n}_j^i$ to the *j-th* side of the curve (n_{j1}^i, n_{j2}^i);

- a vector $\mathbf{k}_i$, with inside the k_j distance between the side of the domain and the origin of the axis.

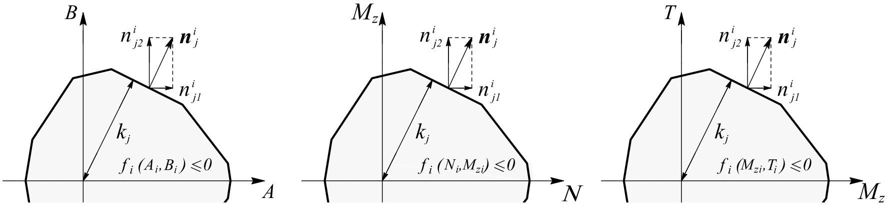

(a) General domain B-A. **(b)** Plastic domain M_z-N. **(c)** Plastic domain T-M_z.

Figure 5.4: Yielding criterion for each *i-th* plastic domain, specialized according to the active generalized stresses.

The dimension of these quantities depends on the quality of the stepwise linearization chosen. Matrix $\mathbf{N}_i$ and vector $\mathbf{k}_i$ have this expression:

$$\mathbf{N}_i = \begin{bmatrix} n^i_{11} & n^i_{12} \\ n^i_{21} & n^i_{22} \\ \cdots & \cdots \\ n^i_{j1} & n^i_{j2} \\ \cdots & \cdots \\ n^i_{q1} & n^i_{q2} \end{bmatrix} \qquad \mathbf{k}_i = \begin{bmatrix} k^i_1 \\ k^i_2 \\ \cdots \\ k^i_j \\ \cdots \\ k^i_q \end{bmatrix} \tag{5.11}$$

Therefore, the yielding criterion for each *i-th* critical cross-section can be rewritten in matrix form as:

$$\boldsymbol{\Phi}_i = \mathbf{N}_i \mathbf{r}_i - \mathbf{k}_i \leq 0 \tag{5.12}$$

where $\mathbf{r}_i$ is the vector whose components are the generalized stresses acting in the *i-th* section. By using the equilibrium equation, the internal forces $\mathbf{r}_i$ in a generic section of the element can be expressed in function of the basic forces $\bar{\mathbf{Q}}$. For each element the yield criterion becomes:

$$\boldsymbol{\Phi}_i = \mathbf{N}_i \bar{\mathbf{Q}}_i - \mathbf{k}_i \leq 0 \tag{5.13}$$

and assembling these conditions for the whole structure the *structural yielding criterion* results:

$$\boldsymbol{\Phi}_t = \sum_{j=1}^{ne} \mathscr{A}\left(\boldsymbol{\Phi}_j\right) = \mathbf{N}\mathbf{Q}_t - \mathbf{k} \leq 0 \tag{5.14}$$

The associated flow rule for the *i-th* critical cross-section is given by:

$$\mathbf{d}_i = \begin{cases} a_i & = \mu_i \dfrac{\partial f_i}{\partial A_i} \\ b_i & = \mu_i \dfrac{\partial f_i}{\partial B_i} \end{cases} \tag{5.15}$$

where $\mu_i > 0$ is the multiplier that allows plastic flows only for the points lying on the yielding curve, for which the normal is oriented outside the domain, that is $\mu_i f_i(A_i, B_i) = 0$. For the linearized case with q sides, by introducing the vector:

$$\boldsymbol{\mu}_i = \begin{bmatrix} \mu^i_1 & \mu^i_2 & \cdots & \mu^j_1 & \cdots & \mu^i_q \end{bmatrix}^T \tag{5.16}$$

and collecting the terms μ_i^j relative to each side of the linearized frontier, we finally have:

$$\mathbf{d}_i = \mathbf{N}_i^T \cdot \boldsymbol{\mu}_i \tag{5.17}$$

with

$$\begin{cases} \mu_j^i \cdot \phi_j^i = 0 \qquad j = 1, \cdots, q \\ \boldsymbol{\mu}_i \geq 0 \end{cases}$$

Thus, the flow rule can be written for the generic element by connecting the vector of plastic strain $\mathbf{d}_i$ with the vector of basic displacement $\bar{\mathbf{q}}_j$ by means of the compatibility equations:

$$\bar{\mathbf{q}} = \mathbf{N}_i^T \ \boldsymbol{\mu_i} \tag{5.18}$$

By assembling all the element contributions for the entire structure, the corresponding *structural flow rule* becomes:

$$\mathbf{q}_t = \sum_{j=1}^{ne} \mathscr{A}\left(\bar{\mathbf{q}}_j\right) = \mathbf{N}^T \cdot \boldsymbol{\mu} \tag{5.19}$$

with

$$\begin{cases} \mu_j^i \cdot \phi_j^i = 0 \qquad j = 1, \cdots, q \\ \boldsymbol{\mu} > 0 \end{cases}$$

5.2.4 THE STATIC AND THE KINEMATIC THEOREMS

With reference to a generic structure, let $\mathbf{P}_0$ be a vector of constant loads and $\mathbf{P}$ a vector of loads whose intensity varies proportionally to a unique multiplier $\lambda \geq 0$. For $\lambda = 0$, let equilibrium and compatibility be satisfied. We search for the multiplier λ_c associated to the collapse load. On the basis of the two fundamental theorems of plasticity, we can restate the Limit Analysis as a problem of linear mathematical programming. In mathematical terms, the *upper* (5.20) and *lower* (5.21) bound theorems are traduced in the following dual linear constrained optimization problems, solved here by means of the Simplex Method. The *lower bound theorem* states that λ_c is the maximum of the multipliers associated with stress fields that satisfy both the equilibrium conditions and the yielding criterion. In mathematical terms:

$$\lambda_c = max\left\{\lambda \quad | \quad \lambda\mathbf{P} - \mathbf{H}\ \mathbf{Q}_t = -\mathbf{P}_0, \quad \mathbf{N}\ \mathbf{Q}_t \leq \mathbf{k}, \quad \lambda \geq 0\right\} \tag{5.20}$$

The *upper bound theorem* states that λ_c is the minimum of the multipliers associated with plastic flows that satisfy both compatibility conditions and flow rule. In mathematical terms:

$$\lambda_c = min\left\{\mathbf{k}^T\boldsymbol{\mu} - \mathbf{P}_0^T\mathbf{s} \quad | \quad \mathbf{N}^T\boldsymbol{\mu} - \mathbf{H}^T\mathbf{s} = \mathbf{0}, \quad \mathbf{P}^T\mathbf{s} = 1, \quad \boldsymbol{\mu} \geq 0\right\} \tag{5.21}$$

In this way, (5.20) requires finding a maximum multiplier, while (5.21) a minimum one. It must be underlined that in the second case, the minimum condition is related to the work done by the proportional loads $\mathbf{P}$ for the displacements $\mathbf{s}$ associated with the collapse mechanism. Since this mechanism is correlated to an

THEOREM		INPUT		OUTPUT
Lower Bound	$\mathbf{H}$	equilibrium matrix	λ_c	collapse multiplier
	$\mathbf{N}$	yielding criterion matrix	$\mathbf{Q}$	basic forces
	$\mathbf{k}$	yielding distance vector		
Upper Bound	$\mathbf{H}^T$	Compatibility matrix	λ_c	collapse multiplier
	$\mathbf{N}$	yielding criterion matrix	$\mathbf{s}$	nodal displacement
	$\mathbf{k}$	yielding distance vector	$\boldsymbol{\mu}$	flow parameters vector

Table 5.1: Limit Analysis Theorems: Input & Output variables.

arbitrary multiplier, it results univocally identified by the condition $\mathbf{P}^T\mathbf{s} = 1$. The solution of the two linear programs gives the *complete solution* of the structural problem. However, as known, the uniqueness of λ_c does not necessarily mean the uniqueness of the collapse mechanism, or that of the stress field at collapse.

Finally, it must be pointed out that computationally speaking the two theorems are not equal. In fact, in the case of the upper bond theorem, the solution is search in a space defined by equilibrium, on which the yielding criterion acts like a constrain: the unknowns of the problem are λ_c and the basic forces $\mathbf{Q}_t$ in all the elements. Instead, in the case of the upper bond theorem, the solution is search in a space defined by compatibility, but the flow rule and, in particular, vector $\boldsymbol{\mu}$ enters in the definition of the space: the unknowns of the problem are λ_c, the displacement vector $\mathbf{s}$ and vector $\boldsymbol{\mu}$. Since the last has a dimension that depends on the number of stepwise linearization used for domains, it is clear that the lower bond theorem is more computational demand with respect the upper bond one.

5.3 Applicability of Limit Analysis on RC structures

As previously reported, Limit Analysis is based on the main assumption that the material can reasonably be consider as rigid-perfectly plastic. In many cases, the ultimate limit state can be adequately evaluated by assuming perfectly plastic behavior and neglecting second order effects, which make the general theory of Limit Analysis applicable to steel structures only. On the contrary, it seems very risky to use the assumptions of the theory of plasticity for calculating the carrying capacity of a structure made of a material like reinforced concrete. Since reinforced concrete is a composite material, made of concrete and reinforcing steel, the use of a plastic approach is acceptable in the cases where the strength is governed mainly by the reinforcement, e.g., flexure of beams and slabs. Also in this case, however, concrete properties can modify the ultimate structural behavior. If it is simple to assume that the tensile strength of concrete can be neglected, concerning the compression strength is much more difficult to propose reasonable assumptions, since concrete exhibits a significant strain softening. In addition, local mechanical properties can be influenced by cracks phenomena or interaction mechanisms between steel and concrete. As a consequence, convex and invariant properties and normality rule are not satisfied.

For these reasons, Limit Analysis seems not generally applicable to reinforced concrete structures. However, several experiences suggest that Limit Analysis can be successfully applicable to RC problems if (Biondini, 1999):

- concrete tensile strength is neglected;
- concrete compression strength is modify trough a coefficient ν_e called *effectiveness factor*:

$$f_c^* = \nu_e \; f_c \qquad \text{with } \nu_e \in [0;1] \tag{5.22}$$

By its nature, the effectiveness factor should be derived from experimental tests. In (Nielsen and Hoang, 1984), it is highlighted that many parameters are involved in its definition: a) structural and sectional geometry, b) support conditions, c) loading conditions and d) material texture. Of course, adequate values for ν_e are required and different formulations have been recommended.
(Exner, 1979) proposes the evaluation of the effectiveness factor by using the energy equivalence as reported in Fig. 5.5.

$$\nu_e = \frac{k}{\sqrt{f_c}} \qquad \text{with } k = k(\varepsilon_{cu}) \tag{5.23}$$

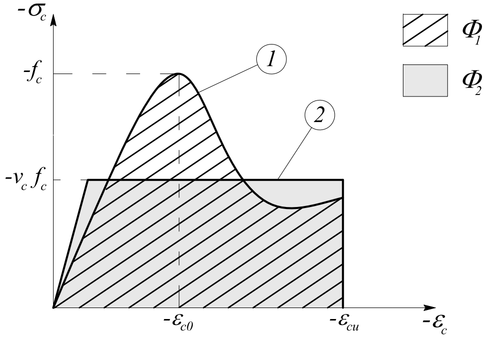

Figure 5.5: Energy equivalence for the definition of the effectiveness factor.

However, it must be pointed out that concrete properties alone cannot define such a coefficient, because several informations must be considered, e.g., properties and position of reinforcing steel, structural geometry and the dominant behaviors (flexural or shear type). For these reasons, prudential values has been proposed, such as $\nu_e = 0.60$ suggested in (Marti, 1985) and (Rogowsky and MacGregor, 1986).

An exhaustive treatment of the effectiveness factor can be found in (Biondini, 1999). For example, in the Italian Code (NTC, 2008) the design concrete compressive strength f_{cd} is derived as:

$$f_{cd} = \frac{\alpha_{cc}}{\gamma_c} f_c = \frac{0.85}{1.5} f_c = 0.56 \cdot f_c \tag{5.24}$$

where:

- α_{cc} is the coefficient to take account of long term effects on the compressive strengths;

- γ_c is the partial safety factor for concrete.

In this case, the effects due to the time-variant behaviour are implicitly included in ν_e. As a result, the concrete compressive strength falls by 56%.
Differently, Eurocode 2 defines the effectiveness factors, in case of coupling between normal and tangential stresses only, as:

$$\nu_e = 0.7 - \frac{f_c}{200} \qquad \text{with } f_c \text{ in MPa} \tag{5.25}$$

(Nielsen and Hoang, 1984) states that (5.25) is assumed generally valid. If $f_c = 30\,MPa$, the effectiveness factor results $\nu_e = 0.7 - 30/200 = 0.55$.

Finally, it must point out that the Limit Analysis results seem not not consistent because concrete is treated as material with infinite ductility. Thus, Limit Analysis can be applicable to RC structures only if a suitable effectiveness factors is considered. Difficulties arise in defining that factor, since it is based on theoretical, empirical and experimental observations. Due to the aleatory of the parameters involved in its evaluation, the main suggestion is to use prudential values. However, as demonstrated in the following applications, the effectiveness factor plays a crucial role only in defining the bearing capacity of highly compressed zones, while for the others the effects on the results are negligible.

5.4 INPUT FOR AN ARBITRARY RC SECTION

With reference to an arbitrary RC section, Limit Analysis requires as an input a reliable yielding criterion. The proposed formulation is here specialized in order to consider to two distinct situations:

1. only Axial and Bending Moment as the active generalized plastic forces;
2. only Bending Moment and Torsion as the active generalized plastic forces.

for which the definition of the corresponding resistant domain is presented.

5.4.1 AXIAL AND BENDING INTERACTION DOMAIN

Dealing with a generic RC section, the interaction domain is a volume which contains all the states $[N, M_z, M_y]$ acceptable within certain limits, stated according to given hypotheses. Its frontier is the locus of the points corresponding to an ultimate sectional state. In such a surface frontier lie the points having as coordinates the triplets of values $[N, M_z, M_y]$ which lead a fiber of concrete or a bar of steel to reach its ultimate strain. In this paragraph we deal with the problem to define such a surface. According to the *Element State Determination* presented in par. 7.11b, the problem may be solved both in the space of the deformations $\mathbf{e}_s(x)$ as well as in the space of the forces $\mathbf{f}_s$. In the first case we have to solve an ordinate succession of problems Type 1 (direct problems). The succession will explore all the deformative states corresponding to an ultimate value of the material strains. In the second case, working in the space of forces, we have to solve problems Type 2, involving repeated solutions of nonlinear equations. This second way is time consuming, but more effective from a practical point of view, because it works defining the 3D domain N, M_z, M_y as a succession of 2D domains $\overline{N}, M_z, M_y$, reckoned for a constant value of the axial force. According to (Bontempi, 1992), we work through the following steps:

1. we chose a value $\overline{N} = N \in [N^+; N^-]$;
2. in the plane $\overline{N}, M_z, M_y$ we have to find the points associated to an ultimate limit state. To this purpose:
    - we chose at first an angle $\varphi = 0 \div 2\pi$;
    - this angle gives a line on which we define a local variable λ so that:

$$\begin{aligned} M_z &= \lambda \cdot \cos\varphi \\ M_y &= \lambda \cdot \sin\varphi \end{aligned} \tag{5.26}$$

    - with the bisection method we find the value of λ to which correspond the forces producing an ultimate state;

By repeating this search for a discrete set of angles φ and axial forces $\overline{N}$ the surface frontier is built point wise. The same approach is applicable to the definition of 2D M-N domains, as explained also in (Briccola *et al.*, 2013). These domains represent the input for the Limit Analysis approach when only axial force and bending moment are assumed as active and interacting plastic stresses.

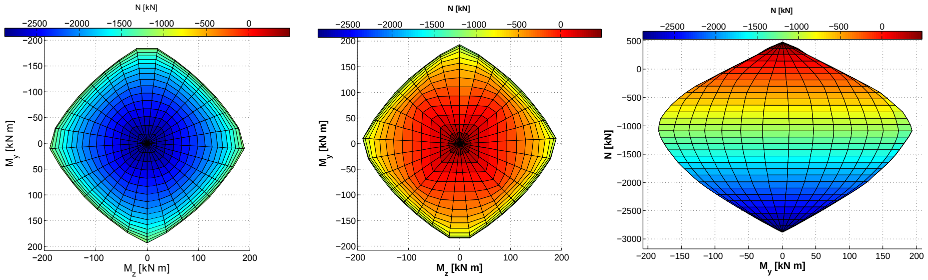

(a) Bottom view. **(b)** Top view. **(c)** Lateral view.

Figure 5.6: Interaction domain for a RC square section (Briccola *et al.*, 2013).

5.4.2 Bending and Torsion interaction Diagram

Considerable work has been carried out in the past to assess the strength of reinforced members subjected to combined bending and torsion (Rausch, 1929) (Collins *et al.*, 1967) (Lampert, 1970) (Hsu, 1984). The theories differ mainly in the formulation of failure mechanisms and the number of components of the resisting system being considered. Two different patterns of behavior have been observed for beams in combined torsion and bending. If torsion dominates, there is a truss-like behavior up to failure, as in pure torsion. If bending dominates, the behavior is similar to that in pure bending, except that the compression zone becomes inclined. As a result, two different approaches have been developed to explain that interaction behavior, the space truss theory (Lampert, 1970) and the skew bending theory (Collins, 1969).

In the present work, the space truss analogy is adopted. As shown in Fig. 5.7a through 5.7c, the space truss model consists of longitudinal bars considered to be concentrated into stringers at the corners, legs of the hoops, which act as posts, and the compression diagonals made by concrete between the inclined cracks. The full lines indicate tension chords and the strips between diagonal crack lines, inclined at an angle α_c, suggest compression struts. The angle is such that both the longitudinal and stirrup reinforcement reach their yield stresses before failure and the compressive strength of the concrete is not primarily decisive for the load carrying capacity (condition of under-reinforced members in torsion).

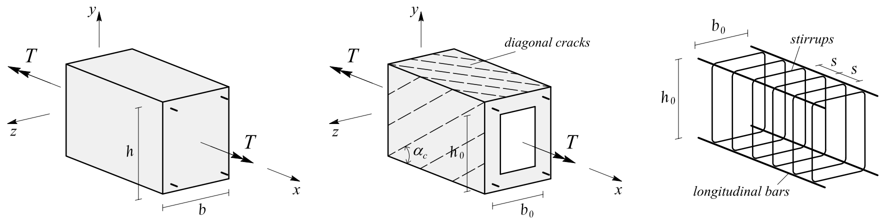
y
T
z
h
T
b
x
y
diagonal cracks
T
z
α_c
h_0
T
b_0
x
b_0
stirrups
s
s
h_0
longitudinal bars

(a) Uncracked R.C element. **(b)** Cracked RC element. **(c)** Detail of steel bars.

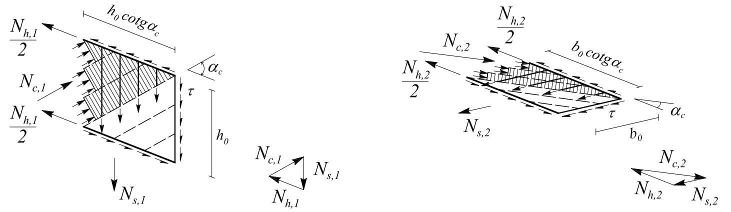
$h_0 \cot g\alpha_c$
$\frac{N_{h,1}}{2}$
$N_{c,1}$
$\frac{N_{h,1}}{2}$
α_c
τ
h_0
$N_{s,1}$
$N_{c,1}$
$N_{s,1}$
$N_{h,1}$
$\frac{N_{h,2}}{2}$
$N_{c,2}$
$b_0 \cot g\alpha_c$
$\frac{N_{h,2}}{2}$
$N_{s,2}$
τ
α_c
b_0
$N_{c,2}$
$N_{h,2}$
$N_{s,2}$

(d) Truss forces in transverse section. **(e)** Truss forces in horizontal section.

Figure 5.7: Torsional resistance by the space truss model.

5.4.2.1 STRENGTH IN PURE TORSION AND PURE BENDING

By studying the equilibrium of the truss model, the following expression for the *torsional resistance* of a reinforced cross-section is obtained:

$$T_p = 2A_0\sqrt{\frac{A_l f_{ly}}{p_0} \cdot \frac{A_t f_{ty}}{s}} \tag{5.27}$$

where A_0 is the area enclosed by the lines connecting the longitudinal corner bars (b_0,h_0) and p_0 the relative perimeter. The term $A_t f_{ty}$ represents the yield force of one hoop leg and $A_l f_{ly}$ represents the yield force of the weaker longitudinal steel bars of the section. In particular, A_l is two time the minimum area between the top (A'_s) and bottom (A_s) longitudinal bars. The torsional strength is thus a function of the yield force of both longitudinal bars and hoop steel, and the geometry of the reinforcing cage. Apart from providing the compression diagonals, the concrete not contributes to the torsional strength.

In the evaluation of the *flexural resistance*, the internal level arm h_0 corresponding to the dimension of the truss is assumed to be constant throughout the whole range. Since for the collapse under positive bending moment the bottom stingers yield ($A_s f_{sy}$), the ultimate flexural capacity for pure bending of this model is:

$$M_{z,p} = A_s f_{sy} h_0 \tag{5.28}$$

5.4.2.2 STRENGTH IN TORSION-BENDING

According to (Lampert and Thürlimann, 1972) (Lampert and Collins, 1972), in the truss analogy a parabolic interaction relationship between the pure bending capacity $M_{z,p}$, given by the conventional formula (5.28) and the pure torsional capacity T_p given by the space truss formula (5.27) has been found. For a reinforced rectangular cross-section, the intersection formulas are:

$$\left(\frac{T}{T_p}\right)^2 = r\left(1 - \frac{M_z}{M_{z,p}}\right) \tag{5.29}$$

when yielding of the bottom longitudinal steel occurs in the flexural tension zone and

$$\left(\frac{T}{T_p}\right)^2 = 1 + r\left(\frac{M_z}{M_{z,p}}\right) \tag{5.30}$$

when, on the other hand, the yielding of the longitudinal steel occurs in the flexural compression zone. In (5.29) and (5.30) M_z and T indicates respectively the applied ultimate bending moment and ultimate torsion and r is the ratio of yield forces of flexural tension and compression reinforcement:

$$r = \frac{A_s f_{sy}}{A'_s f_{s'y}} \tag{5.31}$$

So, for every value of r it exists a corresponding interaction diagram. The form of the two parabolic curves for the interaction between torsion and bending is plotted in Fig. 5.8 for varying ratios r. It is interesting to note that in a symmetrically reinforced beam (*r=1*) even a small moment decreases a torsional strength by causing earlier yield in the longitudinal steel. On the other hand, in the case of *r=3* (asymmetrically reinforced beam), a small amount of bending increases the torsional capacity because the yielding of the longitudinal bars in the flexural compression zone arises much later as a consequence of the tension generated by torsion.

Based on (5.29) and (5.30), the resistant domain (M_z-T) of an arbitrary RC cross-section can be evaluated and be used here as a reliable yielding criterion in the Limit Analysis problems.

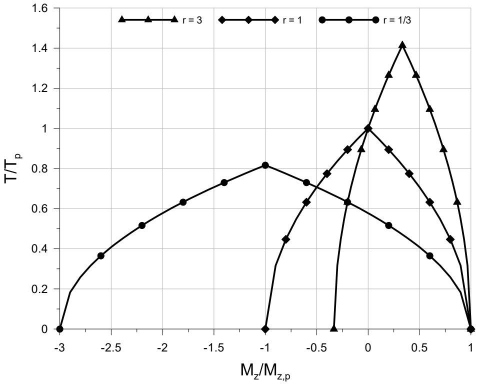

Figure 5.8: Interaction Torsion-Bending moment for a rectangular cross-section with different ratios r.

5.5 A benchmark. The Corace Bridge

A reinforced concrete slender arch bridge, crossing the Corace River (Gimigliano, Cosenza, Italy, 1955) is studied (Galli and Franciosi, 1955).

The bridge presents a span equal to $80\,m$ and a dept equal to 26.10. At platform level the total height is $27\,m$. The structural model in Fig. 5.9b, as well as the sections geometry, the reinforcements and the material chracteristics refers to the data presented in (Ronca and Cohn, 1979) and (Conti *et al.*, 2017b). The applied load is composed of a fixed contribution, corresponding to the dead loads of the girder ($g_0 = 102.90\,kN/m$) and of the arch ($g_1 = 85.00\,kN/m$), and of a variable part, corresponding to the live load ($p = 53.30\,kN/m$), to be increased until to the collapse.

With reference to this structure, different type of analysis not only with the aim of compare them, but mainly in order to understand the structural behavior have been carried out.

- Nonlinear Analysis:
    - with mechanical and geometric non linearities;
    - with mechanical non linearities only;
- Limit Analysis:
    - without considering geometric non linearities and without applying effectiveness factor.

It is recalled that with Limit Analysis only informations related to the collapse are obtained. In contrast, with Non Linear Analysis we can follow the real structural behavior for all the range of loadings and the definition of effectiveness factor is not required. Hence, interesting comments arise by comparing Limit with Nonlinear results.

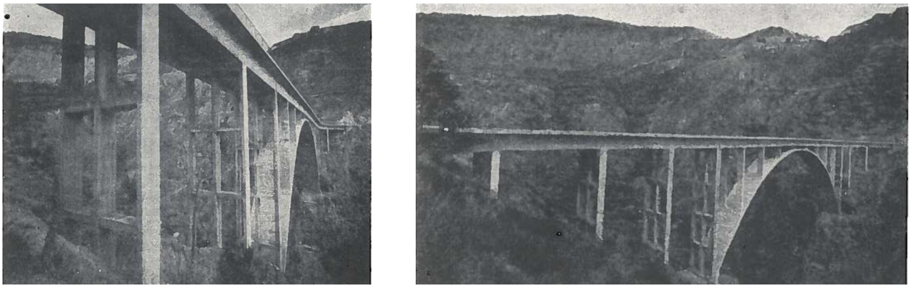

(a) View of the bridge.

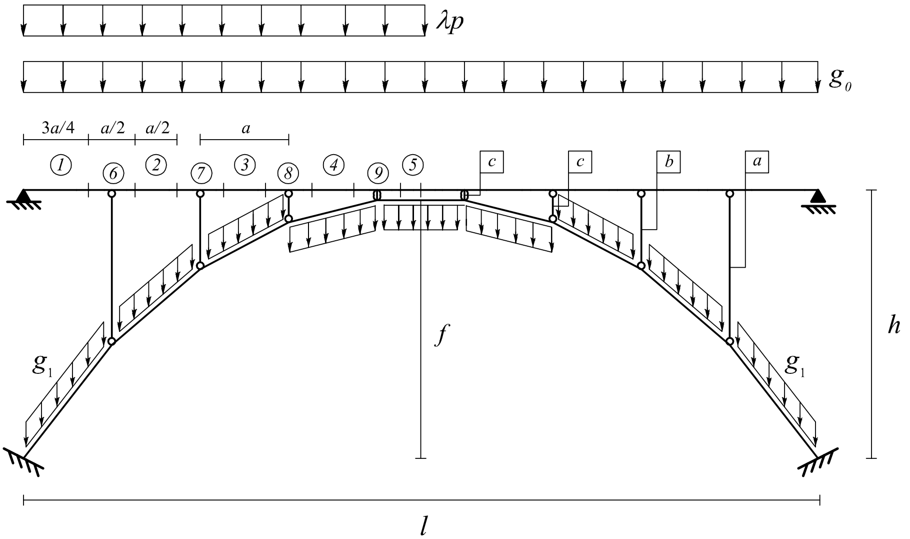

(b) Geometric characteristic and loading conditions.

Figure 5.9: Corace Bridge (Calabria, Italy).

5.5.1 Limit Analysis

Limit Analysis requires the definition of the interaction domains for all the sections of the bridge. Concerning the arch and the beam, the domain used in the analysis are derived through the procedure exposed in par. 5.4.1. Axial force and bending moment are the active generalized stresses assumed. Since the supporting walls are only compressed, they are assumed infinitely resisting. The results of the Limit Analysis are reported in Fig. 5.10. Figs. 5.11a and 5.12a show the axial force and bending moment distributions at incipient collapse. The lower bound theorem predicts the formation of the twelve plastic hinges, shown in Fig.6.6a on the scheme which presents the collapse mechanism of the structure. Figs. 5.10b, 5.10c and 5.10d show the points representing the ultimate values of the internal forces N and M on the linearized frontiers of the most relevant sections corresponding to plastic hinges in the arch and in the upper girder. The collapse load obtained by Limit

Analysis is equal to $p = 217\,kN/m$.

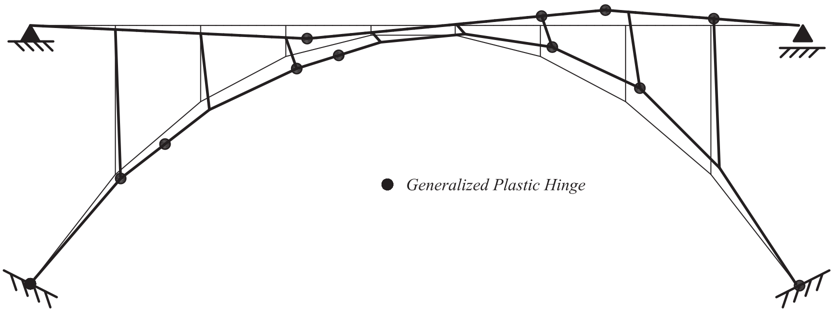

(a) Collapse Mechanism ($\lambda = 4.08$).

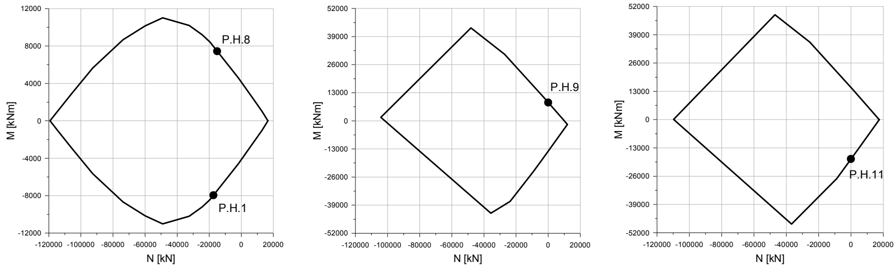

(b) Arch. **(c)** Girder - Segm. 4. **(d)** Girder - Segm. 3.

Figure 5.10: Limit Analysis. (a) Distribution of the plastic hinges which transform the structure into a mechanism. (b÷d) Points representing the ultimate values of the internal forces N and M on the linearized frontiers of the most relevant sections corresponding to plastic hinges in the arch and in the upper girder.

5.5.2 NONLINEAR ANALYSIS

Nonlinear Analysis results are reported in Fig. 5.13 for two different values of the load p acting on the deck. $p = 112\,kN/m$ is the collapse load obtained by considering both mechanical and geometrical non linearities. Instead, the collapse load due to mechanical non linearities only is equal to $p = 157\,kN/m$ (see Tab. 5.2). Fig. 5.13 shows the progressive evolution of the deformed shapes obtained from the step-by-step nonlinear analyses for the live loading levels equal to 0%, 10%, 50%, 90% of the collapse load. Finally, Figs. 5.11b and 5.12b show the axial force and bending moment distributions just before the collapse.

5.5.3 COMMENTS OF THE RESULTS AND COMPARISONS

A slender arch bridge has been studied by means of two approaches based on completely different assumptions: the LA highlights the mechanism of collapse and determines the ultimate value of the load multiplier; the NLA represents the

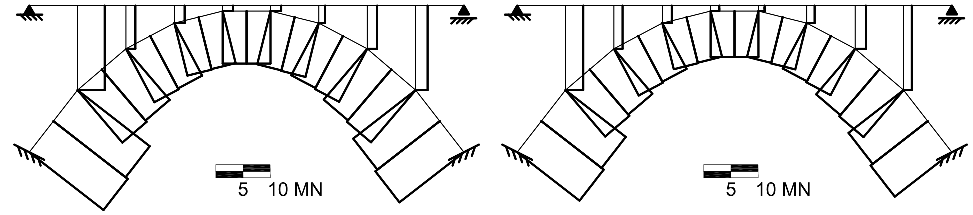

(a) Limit Analysis. **(b)** Nonlinear Analysis.

Figure 5.11: Axial force N diagram derived through both the analyses at incipient collapse.

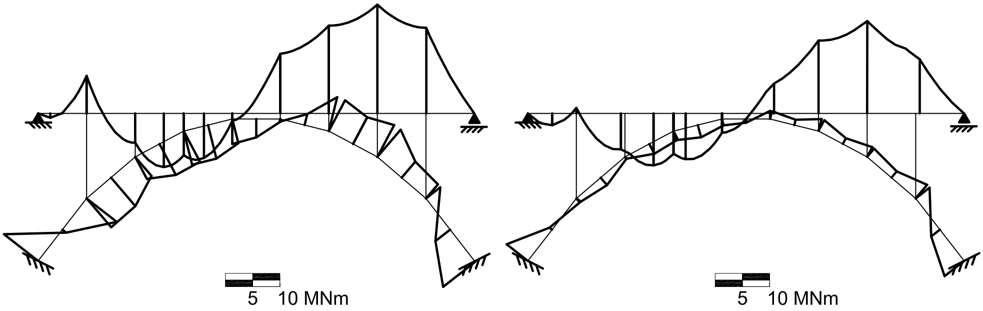

(a) Limit Analysis. **(b)** Nonlinear Analysis.

Figure 5.12: Bending moment M diagram derived through both the analyses at incipient collapse.

evolution of the structural behavior in terms both of displacements and internal forces, all along the load path until the collapse. A comparison is possible in terms of the global response of the structure: the deformed shape of the structure at the incipient collapse given by the NLA (Fig. 5.13) agrees with the shape of the collapse mechanism given by the LA (Fig. 6.6a) and the location of the main plastic hinges well corresponds to that of the most stressed sections according to NLA. The geometrical effects on the collapse load can be estimated with a percentage that is approximately equal to 40 %. There is also a good correspondence between the axial force and bending moment distributions at incipient collapse.

However, a direct comparison between the intensities of the collapse loads of numerical quantities is not possible. Such a difference, which lead to an ultimate load $p_{NLA} = 157\,kN/m$ versus $p_{LA} = 217\,kN/m$, can be explained by a set of comparative studies, which started from an initial response, very similar to that just exposed.

First of all, the Limit Analysis is based on the radical assumption that a material maintains its maximum stress level for strains of arbitrary magnitude (infinite ductility) and on the application of the normality criterion. It follows that these

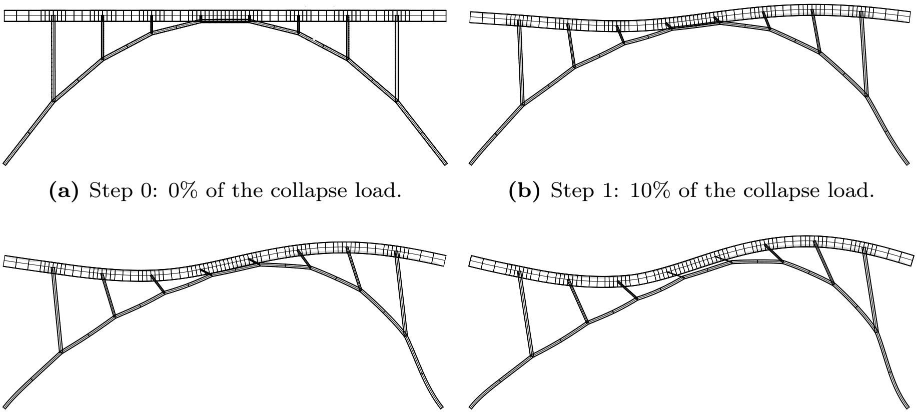

(a) Step 0: 0% of the collapse load. (b) Step 1: 10% of the collapse load.

(c) Step 2: 50% del carico di collasso. (d) Step 3: 90% of the collapse load.

Figure 5.13: Non Linear Analysis: deformed configuration until collapse.

Analysis	N.L.G.	N.L.M.	Collapse load	Load Factor
(1)	√	√	$112\,kN/m$	2.10
(2)	-	√	$157\,kN/m$	2.95

Table 5.2: Different analysis for the Corace Bridge. N.L.G. = Non Linear Geometry, N.L.M. = Non Linear Mechanics.

assumptions lead to overestimate the load carrying capacity. In order to take into account the fact that the assumptions of the LA are not always and fully satisfied when applied to reinforced concrete structures, many Authors (Exner, 1979), (Nielsen and Hoang, 1984) suggest the introduction of a corrective effectiveness factor $\nu_e \leq 1$, which factorizes the characteristic concrete strength before its use for the calculation of the carrying capacity of a structure. Design standards and literature (as explained in par. 5.3) suggest as conservative value $\nu_e = 0.85 - f_c/300$, which, for $f_c = 30\,N/mm^2$, results $\nu = 0.75$. By using such a reduction factor, the Limit Analysis gave as ultimate load $p = 210$kN/m equivalent to (-3.2%) with respect the initial one, as shown in Tab. 5.3. Such negligible difference is fully justified. The effectiveness factor plays a crucial role in defining the bearing capacity of highly compressed concrete zones, like the stress block in bending, the struts of the shear mechanisms or the struts of a strut and tie model. In the present case, all the sections have a low degree of reinforcement and the collapse is steered by the yielding the steel.

On the other side, in the evolutive Nonlinear Analysis the ultimate load is that for which the model reaches for the last time an equilibrium configuration, without violating the convergence conditions. This depends on the degree of refinement of the structural discretization and on the level of the loading increments at high level of the strains. The last iterations struggle to converge and usually lead to

Limit Analysis	N.L.G.	N.L.M.	ν_e	Collapse load	Load Factor
(1)	-	$\surd$	1	$217\,kN/m$	4.08
(2)	-	$\surd$	0.75	$210\,kN/m$	3.94

Table 5.3: Comparisons among different Different Limit Analysis for the Corace Bridge. N.L.G. = Non Linear Geometry, N.L.M. = Non Linear Mechanics.

Nonlinear Analysis	N.L.G.	N.L.M.	E_h/E_s	Collapse load	Load Factor
(1)	-	$\surd$	0	$157\,kN/m$	2.95
(2)	-	$\surd$	0.02	$214\,kN/m$	4.02

Table 5.4: Comparisons among different Nonlinear Analysis for the Corace Bridge. N.L.G. = Non Linear Geometry, N.L.M. = Non Linear Mechanics.

underestimate the ultimate load. In fact, if the steel strain hardens soon after the onset of yielding, the elastic perfectly plastic law leads to underestimate the steel stress at high strains (Park and Paulay, 1975). The introduction of a light hardening property in the steel constitutive law, in this case $E_h/E_s \approx 0.02$, contributes in stabilizing and in extending the solution (Tab. 5.4). As noted by (Kappos and Penelis, 2014), the steel strain hardening better describes the behavior of plastic hinge zones, since it allows the development of bending moments higher than those corresponding to first yielding at sections beyond the critical one, spreading of a plastic mechanism in larger parts of the member. Such a choice stabilizes the solution and, as shown, allows a better comparison between the two sets of results.

From the computational point of view, it would be appropriate to dedicate a future research to the study of the effects of light strain hardening of the steel on the structural response in the area immediately before the collapse.

5.6 CLOSING REMARKS

A systematic approach to the Limit Analysis of frame structures has been presented. The approach neglects shear failures and considers either axial force and bending moment or bending moment and torsion as active interacting generalized plastic stresses. After a recall of the main hypotheses and the matrix formulation, the Upper and Lower Bound Theorems have been here rewritten as dual linear constrained optimization problems. Since the Limit Analysis is based on the main assumption that the material can reasonably be consider as rigid-perfectly plastic, it seems at the beginning not generally applicable to reinforced concrete structures. In practice, the problem can be solved by introducing an effectiveness factor to reduce the concrete compressive strength, where the ultimate behaviors are not governed by the yielding of steel bars.

Since Limit Analysis requires as an input a reliable yielding criterion, the resistant domains of an arbitrary RC section here deal with respectively:

1. axial force-bending moment interaction. The resistant $M_z - N$ domain is

built;

2. bending moment-torsion interaction. The resistant $T - M_z$ domain is derived through space truss analogy.

Finally, to validate the proposed approach, the analysis of a RC Maillart type arch bridges has been carried out not only by means of Limit Analysis, but also by the Non Linear Approach presented in the previous chapter. From the parallel study between Limit and Non linear Analyses, the most important conclusion are:

- the complementarity of the information given by the two methods. Firstly, the shape of the collapse mechanism given by the LA agrees with the deformed shape of the structure at the incipient collapse given by the NLA. Then, the plastic hinges well correspond to the most stressed sections according to Non Linear Analysis;
- the intensity of the ultimate loads. In an ideal comparison, the ultimate load provided by the two different analyses is the only common and comparable result and, apart from truncation and rounding approximations, one expects this value to be unique. Actually, some differences exist. Within the limits of the two methodologies, such differences are principally due to the effects on the numerical solutions of the concrete effectiveness factor and of the steel strain hardening.
- Limit Analysis is the most immediate and synthetic tool in order to understand the structural behaviour.
- Non Linear Analysis presents an high level of generality and includes not only the mechanical non linearities but also the geometrical ones. However, sometimes the interpretation of the results is not a simple task and, as consequence, requires some additional consideration;
- The effectiveness factor plays a crucial role in defining the bearing capacity of highly compressed concrete zones, like the stress block in bending, the struts of the shear mechanisms or the struts of a strut and tie model. On the contrary, sections which have a low degree of reinforcement and the collapse is steered by the yielding the steel, a negligible difference in the use of this factor is evident. In general, working without an effectiveness factor produces results on the safe side.

The case study has proved that the procedure based on the plastic theorems can be considered effectively a suitable technique to face to the problems of structural safety and also to characterize the structural robustness, as discussed in the next chapter.

6 Assessment of a RC Existing Structure

This chapter deals with the assessment of an existing RC bridge. A virtual loading test is carried out, consisting in the exam of a structure at different damaged states and in the evaluation of the structural performance for a given additional traffic load distribution. In order to estimate the lifetime structural robustness, the structural analyses are carried out by a complete parallel study between Limit and Nonlinear Analysis.

6.1 INTRODUCTION

For existing bridges, a typical problem is to assess their residual bearing capacity in the actual damage state, reached after a certain amount of years from construction time. This problem is here solved through a unique approach (*a virtual loading test*) consisting of an analysis of the diffusion of the deterioration processes induced by aggressive agents, followed by the analysis of the structure at different damage states. The diffusion process is carried out through Cellular Automata technique (recalled in Appendix A) and allows to evaluate the effects of corrosion at the material level, by considering, for example, the reduction of steel bars areas and the reduction of steel ductility. Known the effects at the material level, the corresponding effects at the sectional level and then at the global structural level are deeply investigated by computational structural analysis techniques. The main aim of such an approach is to highlight the collapse mechanism and the redistribution capacity of the internal forces, in order to detect the weakest parts, to assess the influence of a certain type of damage and to explore the effectiveness of repair hypotheses. The search for these limit behaviors may be seen as a *lifetime structural robustness estimation*, tailored on the actual or supposed damaging characteristics of a given structure.

In this way, the time-variant capacity accounting for environmental hazards of a RC grillage deck is presented. Firstly, a series of Limit Analysis is carried out on the sound and damaged structure. Then, for the complementary of the results, Nonlinear Analyses are performed under increasing applied loads and for a specific damage state at a given time. Such an approach allows outlining the consequences due to different damage factors and the modes which lead to sudden collapses when neither weakness signals nor intermediate anomalous behaviors appear.

6.2 SOUND RC GRILLAGE DECK

An old 34.70 m long and 9.20 m wide RC grillage deck, composed of four longitudinal beams and five cross-beams, is studied (Fig. 6.1). This deck is part of 28-spans viaduct built in Italy in 1968 and it is half a century old.

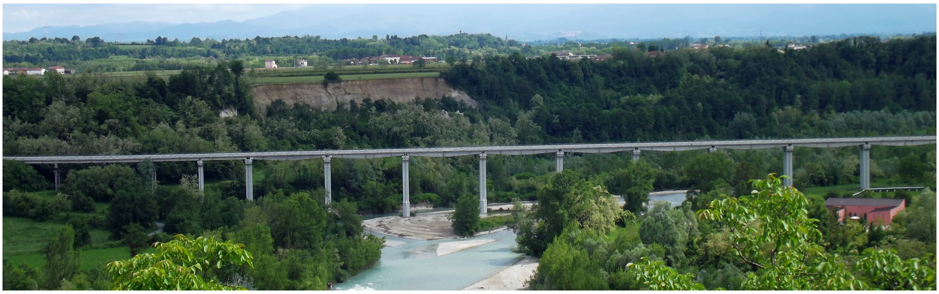

(a) View of the bridge.

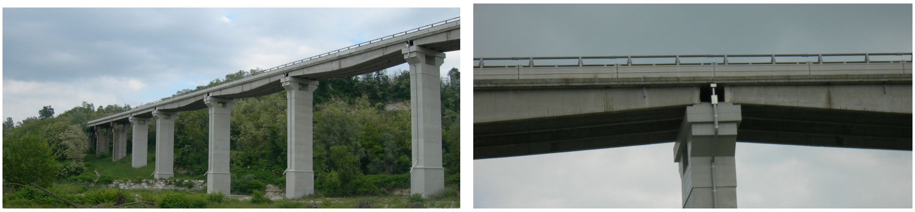

(b) Details of the structure.

Figure 6.1: An existing RC grillage deck in Italy.

The main dimensions of the grillage, as well as the geometry, dimensions and reinforcement layout of the main structural members are shown in Fig. 6.2.
In particular, the longitudinal beams present a variable section, with height and width respectively increasing and decreasing from the abutments to the mid-span of the viaduct. On the contrary, the cross-beams have constant main dimensions and are reinforced with (3+3) bars with a nominal diameter equal to 28 mm. Fig. 6.3 shows further details of the reinforcement layout of the longitudinal beams. Tab. 6.1 lists the type of stirrups in all the members.

With reference to the beam model shown in Fig. 6.4, the grillage deck is modeled by four simply supported longitudinal beams and five cross-beams, arranged according to a 2.63 (transversal) x 8.66 (longitudinal) m mesh. The deck is considered to be subjected to:

1. a fixed load, corresponding to the self-weight: $g = 30\,kN/m$;
2. a variable part, due to traffic loads. According to *Load Model 1* defined by (EN, 1991), the traffic load acting on the deck consists of concentrated loads $Q = 300\,kN$, represented by a tandem system with two axles, and of uniformly distributed loads $q = 13.5kN/m$, as shown in Fig. 6.4.

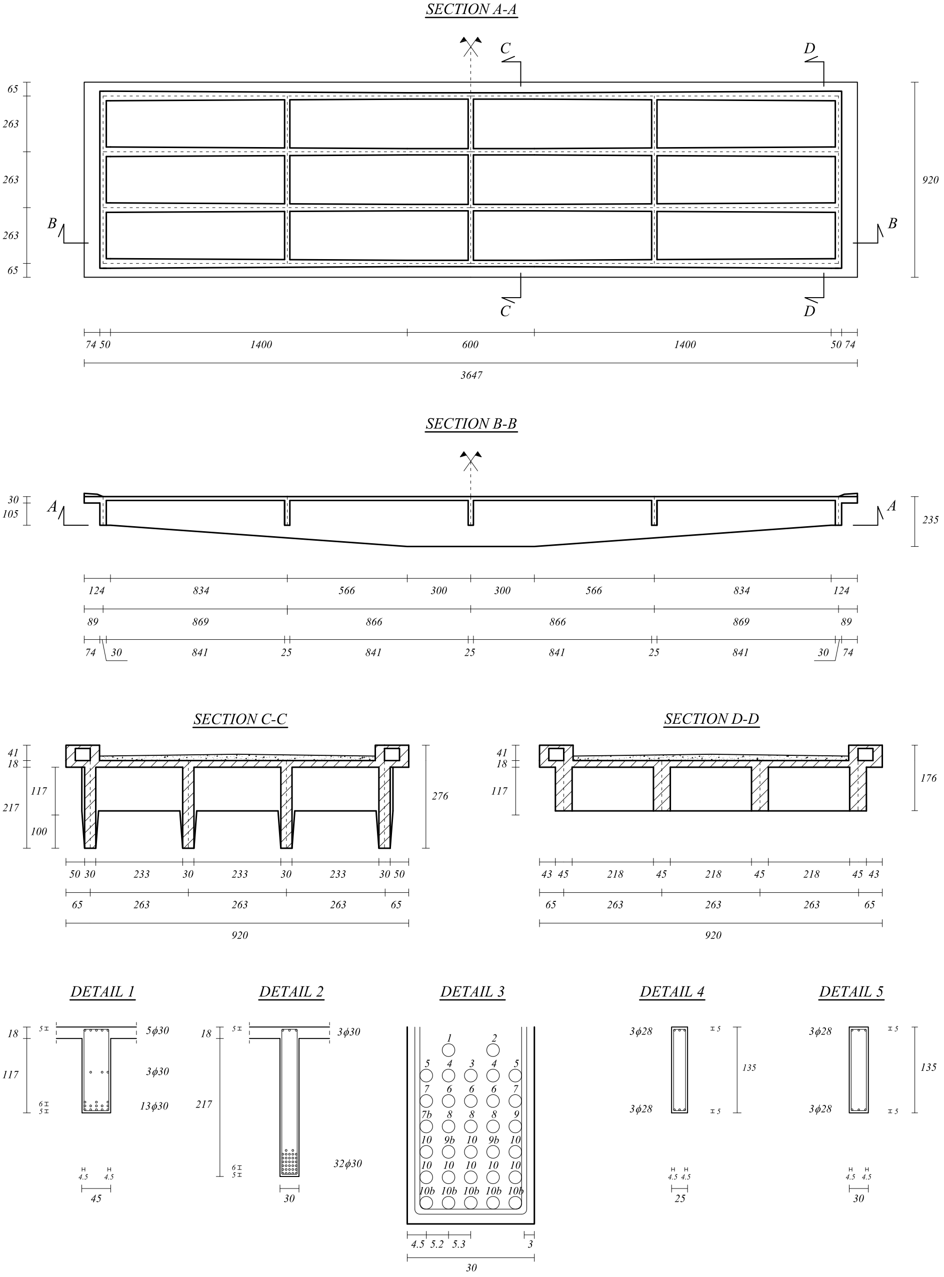
SECTION A-A
C
D
B
65
263
263
263
65
920
74 50
1400
600
1400
50 74
3647
SECTION B-B
A
30
105
235
124
834
566
300
300
566
834
124
89
869
866
866
869
89
74
30
841
25
841
25
841
25
841
30
74
SECTION C-C
41
18
117
217
100
276
50 30
233
30
233
30
233
30 50
65
263
263
263
65
920
SECTION D-D
41
18
117
176
43 45
218
45
218
45
218
45 43
65
263
263
263
65
920
DETAIL 1
18
117
5φ30
3φ30
13φ30
4.5
4.5
45
DETAIL 2
18
217
3φ30
32φ30
30
DETAIL 3
1
2
5 4 3 4 5
7 6 6 6 7
7b 8 8 8 9
10 9b 10 9b 10
10 10 10 10 10
10b 10b 10b 10b 10b
4.5 5.2 5.3
3
30
DETAIL 4
3φ28
3φ28
5
5
135
4.5 4.5
25
DETAIL 5
3φ28
3φ28
5
5
135
4.5 4.5
30

Figure 6.2: RC grillage deck. Geometry and reinforcement of the characteristic sections. Details 1, 2 and 3 refer to the longitudinal beams section. Details 4 and 5 identify the cross-beams section (units in cm).

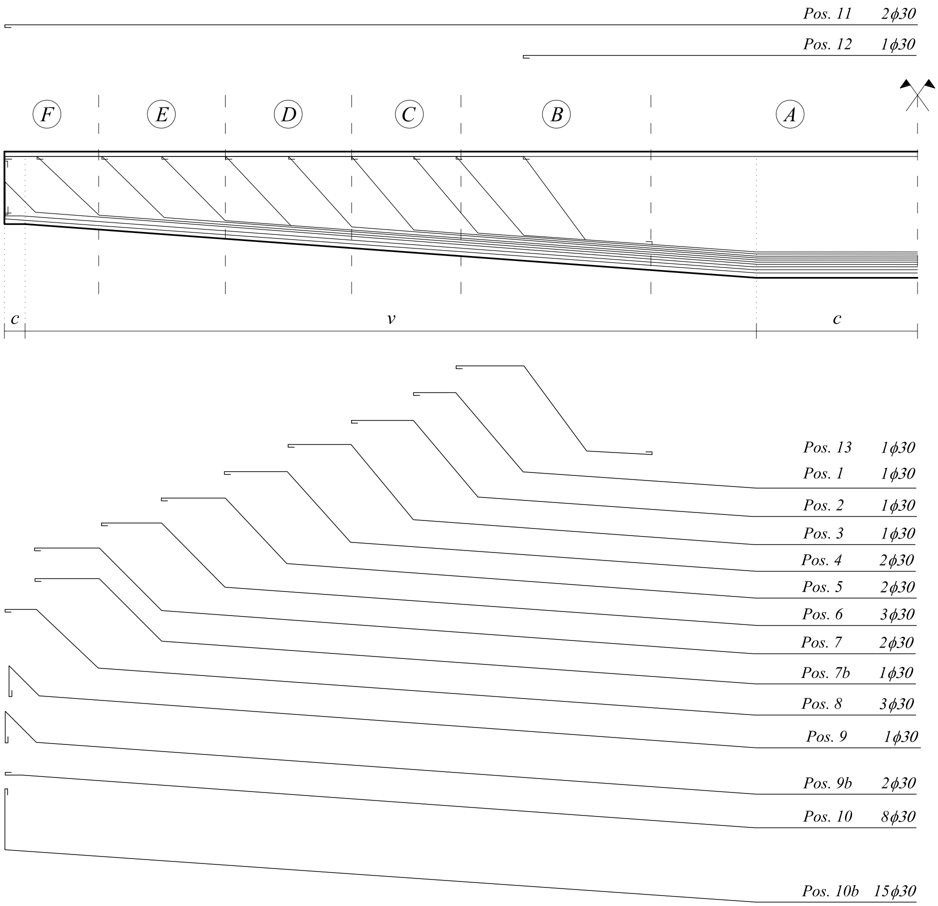
Pos. 11 2ϕ30
Pos. 12 1ϕ30
F
E
D
C
B
A
c
v
c
Pos. 13 1ϕ30
Pos. 1 1ϕ30
Pos. 2 1ϕ30
Pos. 3 1ϕ30
Pos. 4 2ϕ30
Pos. 5 2ϕ30
Pos. 6 3ϕ30
Pos. 7 2ϕ30
Pos. 7b 1ϕ30
Pos. 8 3ϕ30
Pos. 9 1ϕ30
Pos. 9b 2ϕ30
Pos. 10 8ϕ30
Pos. 10b 15ϕ30

Figure 6.3: Reinforcements chracteristic and layout for the longitudinal beams. The encircled letters identify the type of stirrups. The letters c and v identify respectively the constant and variable segments of the longitudinal beam's section.

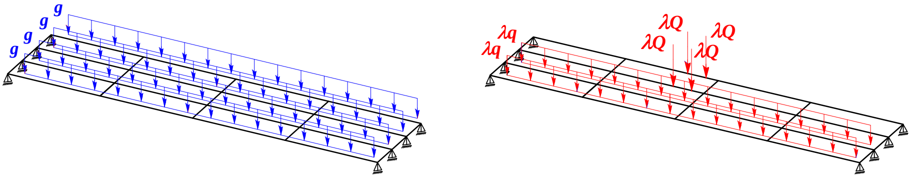
g
g
g
g
λq
λq
λQ
λQ
λQ
λQ

(a) Dead load g.

(b) Traffic load q and Q.

Figure 6.4: Structural model and loading conditions. The applied loads are composed of two parts: the fixed one, corresponding to dead loads and a variable part, distributed according to the traffic load arrangement.

The sound RC grillage deck is analyzed with different type of analysis, not only with the aim of compare them, but principally in order to understand the structural behavior:

- Nonlinear Analysis, with mechanical non linearities only;
- Limit Analysis, without considering geometric non linearities and without applying effectiveness factor.

As concerns the material characteristics reported in Tab. 6.2, in the Limit Analysis, only the concrete compression strength $f_c = -30\,MPa$ and the steel yielding stress $f_{sy} = 375\,MPa$ are involved. On the other hand, in Nonlinear Analysis concrete is modeled by a no-tension, uniaxial stress-strain law, according to the parabola-rectangle law. For steel, the stress-strain diagram is described by an elastic-perfectly plastic stress-strain diagram, symmetric both in tension and compression.

	A	*B*	*C*	*D*	*E*	*F*	*Cross-Beam*
ϕ [mm]	12	12	12	14	14	14	10
s [cm]	20	22	20	20	16	15	20

Table 6.1: Distribution of stirrups in the beams.

Calcestruzzo	fc	$= -30\,MPa$	E_c	$= 33000\,MPa$	ε_{cu}	$= -0.0035$
Acciaio	f_{sy}	$= 375\,MPa$	E_s	$= 206000\,MPa$	ε_{su}	$= 0.06$

Table 6.2: Material's characteristics

For the analyses, in order to model the layout and the areas of steel reinforcements, each longitudinal beam is subdivided into 30 finite beam-elements (Fig. 6.5), while each cross-beam is subdivided into 6 elements. Only for the Limit Analysis the distributed loads are replaced by statically equivalent concentrated loads.

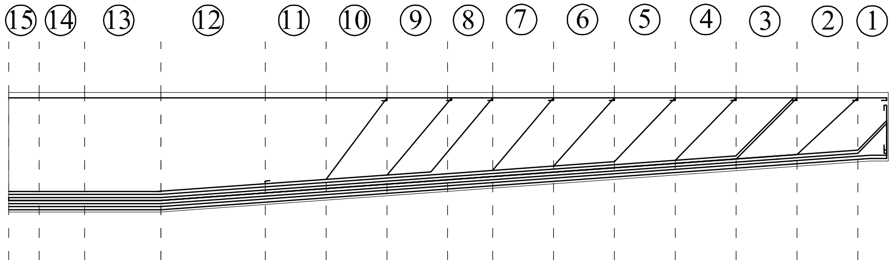

Figure 6.5: Subdivision of longitudinal beam.

6.2.1 LIMIT ANALYSIS

Limit Analysis requires the definition of the interaction domains T-M_z for all the sections of the bridge. The collapse load multiplier obtained by Limit Analysis is equal to $\lambda = 2.48$ and the relative mechanism is show in Fig. 6.6. Figs. 6.6b and 6.6c show the points representing the ultimate values of the internal forces M_z and T on the linearized frontiers of the most relevant sections corresponding to plastic hinges in the longitudinal and cross beams.

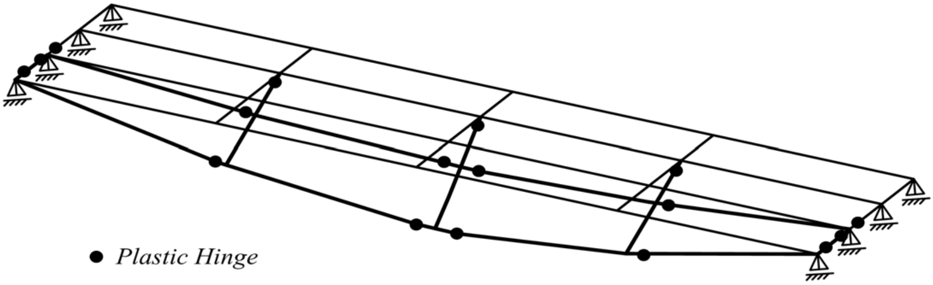

(a) Collapse Mechanism ($\lambda = 2.48$).

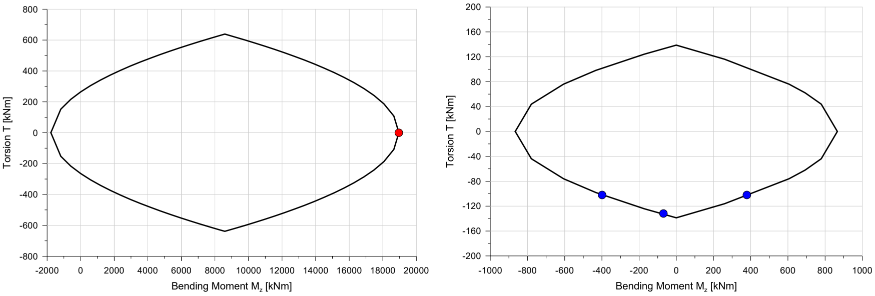

(b) Edge longitudinal beam. **(c)** End cross-beam.

Figure 6.6: Limit Analysis of the sound grillage deck. Distribution of the plastic hinges in the structure and on the linearized frontiers of the most relevant sections.

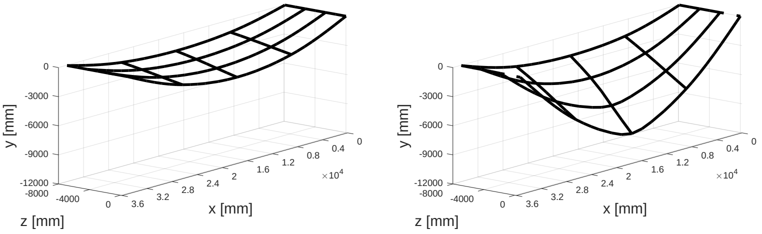

(a) Step 1: 40% of the collapse load. **(b)** Step 2: 90% of the collapse load.

Figure 6.7: Nonlinear Analysis of the sound grillage deck: progressive evolution of the whole deformed configuration until collapse (scale equal to 25).

6.2.2 Nonlinear Analysis

The overall deformed shapes of the deck in Fig. 6.7 is obtained from the step-by-step Nonlinear Analysis for the traffic loading levels equal to 30% and 90% of the collapse load. $\lambda = 2.698$ is the collapse load multiplier obtained by considering the mechanical non linearities only.

6.3 Damaged RC Grillage Deck

As previously exposed, the existing grillage deck is half a century old. Thus, visual inspections have been done in order to investigate the actual state of the system. From the survey, it was found that the deck exhibits a severe damage state, as shown in Fig. 6.8.

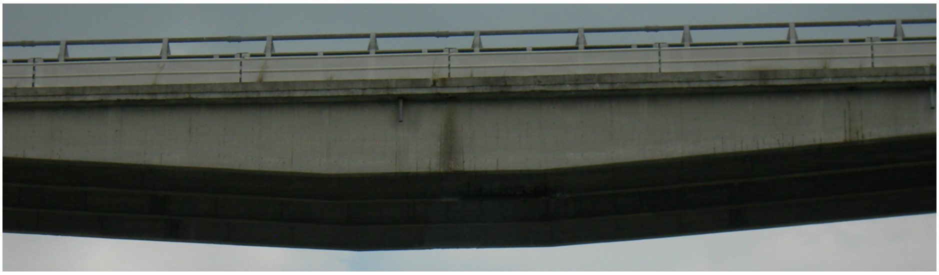

(a) View of the bridge.

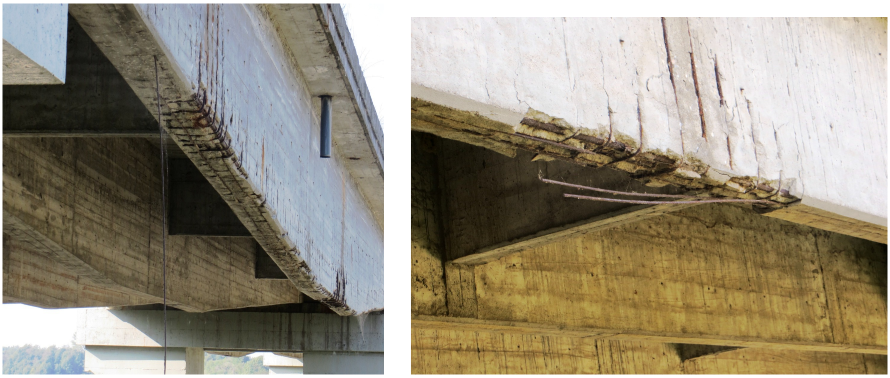

(b) Detail of the structure.

Figure 6.8: Severe damage state in correspondence of the edge longitudinal beam.

6.3.1 Corrosion scenario

Under the action of permanent loads, the intersection between the edge longitudinal beam and the cross-beam is usually affected by a negative bending moment which can lead to the cracking of the slab and cause some seepages on the edge beam. Since the water coming from the roadway platform is characterized by a high concentration of de-icing salts (chloride ions), a critical corrosion scenario may ensue causing premature losses of bearing and/or failure of the overall structure.

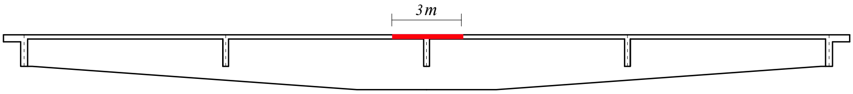

(a) Edge damaged longitudinal beam.

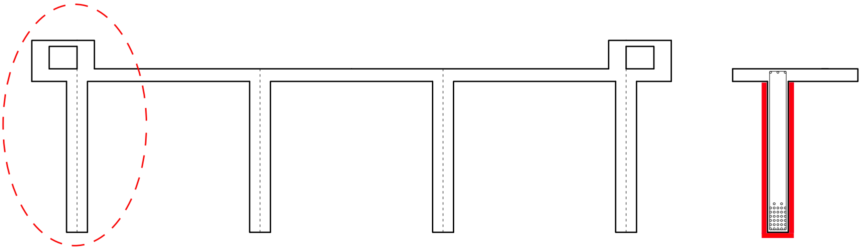

(b) Midspan cross-beam and cross-section of the damaged longitudinal beam.

Figure 6.9: Corrosion scenarios: longitudinal and sectional distribution of the aggressive agent.

However, degradation processes may affect the steel and concrete, and the main structural effects are the corrosion of reinforcement, leading to a reduction of a cross-sectional area of steel bars and the loss of concrete, which leads to a reduction of the cross-sectional area of concrete. Without detailed information, it is commonly accepted that the description of all of these phenomena needs to be investigated by numerical simulation (as described in Appendix A).
Concerning such a corrosion scenario (Fig. 6.8), the chlorides corrosion attacks is defined as follow:

(i) the longitudinal position of the corroded zone is located in a 3 m long segment, astride the central zone of one of the edge longitudinal beams (Fig. 6.9a);

(ii) the sectional distribution of corrosion is assumed to be located along the two laterals and at the bottom sides of the corresponding cross-sections, with a constant concentration $C(t) = C_0 = 3\%$, as Fig. 6.9b shows.

Once the corrosion scenario has been defined, the diffusion problem must be solved both in the sectional domain and in time. The *Cellular Automata technique* is applied, considering a nominal diffusivity coefficient $D = 10^{-11}\,m^2/s$, a grid dimension $\Delta x = 10\,mm$ and a time step $t = 0.16$ years. According to the (Fib, 2006) provisions, the damage rates are defined by the values $C_{cr} = 0.6\%$, $C_c = C_0$ and $\Delta t_s = 50$ years. Since in this case the deterioration process reproduces a severe damage of materials, as it may occur for heavily chloride-contaminated concrete and high relative humidity (Bertolini, 2008), the steel damage rate coefficient ρ is assumed as $0.02/C_0$.
The results of the diffusion process are highlighted in Fig. 6.10, where the concentration maps $C(x,t)/C_0$ of the aggressive agent at different time step t are shown for the midspan cross-section.

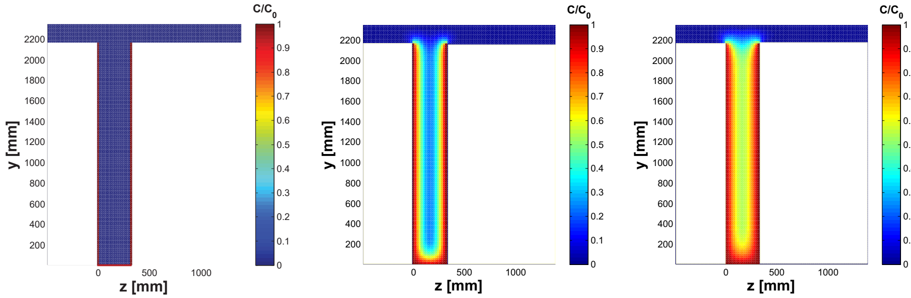

(a) *t=0 years.* **(b)** *t=10 years.* **(c)** *t=20 years.*

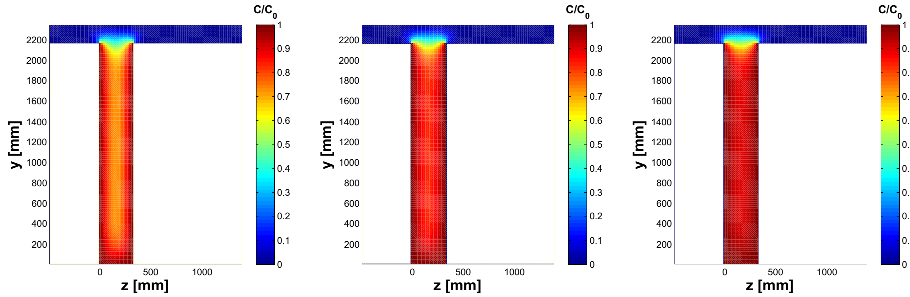

(d) *t=30 years.* **(e)** *t=40 years.* **(f)** *t=50 year.*

Figure 6.10: Maps of $C(x,t)/C_0$ concentration of the midspan section over time ($t = 0 \div 50$ years).

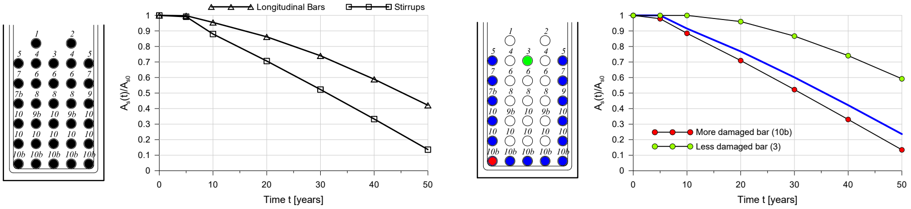

(a) Longitudinal bars. **(b)** External longitudinal bars only.

Figure 6.11: Reduction of the steel area over time for the midspan damaged cross-section.

The amount of mechanical damage induced by chloride diffusion and its evolution over time is plotted in Fig. 6.11. One can be observed that the corrosion propagation starts just after 2 years. As expected, stirrups begin to corrode earlier and have a more severe corrosion than the longitudinal steel bars. With reference to Fig. 6.11b, it is interesting to note how the reduction of the area significantly affects the longitudinal steel bars located near the sides exposed to corrosion.

In the following, aiming to describe the effects of damage at the structural level, two types of evaluations are presented:

1. the damage effects on the *ultimate* performance of the bridge, where Limit Analysis is then compared, in time, with Nonlinear Analysis;
2. the damage effects on the *service* performance of the bridge, where Nonlinear Analysis is used.

The aim is using the results to provide indication on the structural integrity limit state and to evaluate the robustness of the deck.

6.3.2 LIMIT ANALYSIS AT DIFFERENT TIME INSTANTS

A series of Limit Analysis over time accounting for chloride-induced corrosion was carried out to investigate the corresponding grillage deck performance at the Ultimate Limit States. As expected, Fig. 6.12 highlights a significant variation of the collapse load multiplier, which decreases from $\lambda_c = 2.48$ to $\lambda_c = 1.45$ as the damage increases over time.

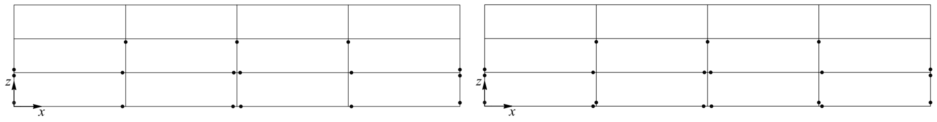

(a) *t=0 years* - $\lambda_c = 2.48$. **(b)** *t=10 years* - $\lambda_c = 2.41$.

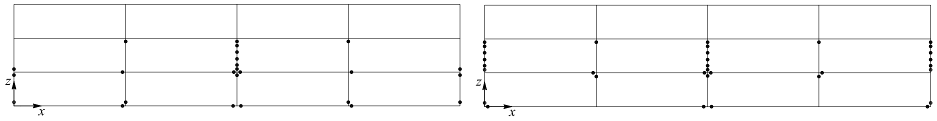

(c) *t=20 years* - $\lambda_c = 2.24$. **(d)** *t=30 years* - $\lambda_c = 2.01$.

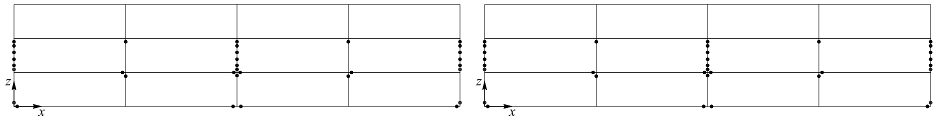

(e) *t=40 years* - $\lambda_c = 1.74$. **(f)** *t=50 years* - $\lambda_c = 1.45$.

Figure 6.12: Variation of the collapse multiplier and relative distribution of the plastic hinges on the deck at different time instants.

Interesting results are obtained also in terms of redistribution of the internal stress resultants and a consequent modification of the collapse mechanism. In fact, the effects of the localized corrosion scenarios involve not only the damaged longitudinal beam but also the undamaged cross-beams. Such a redistribution may be highlighted with reference to Fig. 6.12 through Fig. 6.15. Fig. 6.13 shows the bending moment and torsion diagram for the edge damaged longitudinal beam. The moment progressively reduces in time, gradually exhibiting a pronounced kink at the section in correspondence of the cross-beam at the quarter. On the contrary, as time increase, the torque moment increases in the portions at the quarter while in the central part remains null. The values of the limit stresses M_z and T are marked over time on the linearized frontier of the midspan cross-section corresponding to the plastic hinge in the edge damaged longitudinal beam, as reported in Fig. 6.16. The location of the generalized plastic hinges corresponding to the damage state from $t = 0$ to $t = 50$ years is shown in Fig. 6.12. As the reduction of the mechanical properties for the damaged longitudinal beam becomes evident (t=*20 years*), the Limit Analysis predicts the formation of new plastic hinges in the central cross-beam and its relative collapse may occur.

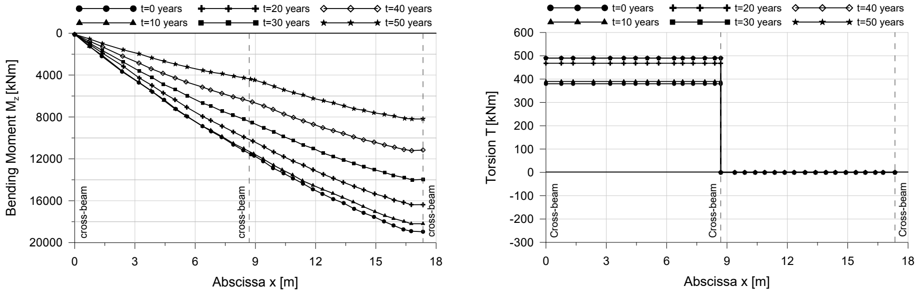

Figure 6.13: Bending and torque moments along the edge longitudinal beam at incipient collapse for different sampling times ($t = 0 \div 50$ years).

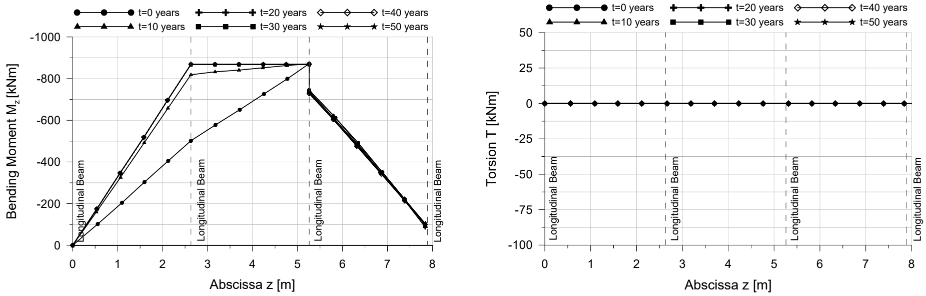

Figure 6.14: Bending and torque moments along the central cross-beam at incipient collapse for different sampling times ($t = 0 \div 50$ years).

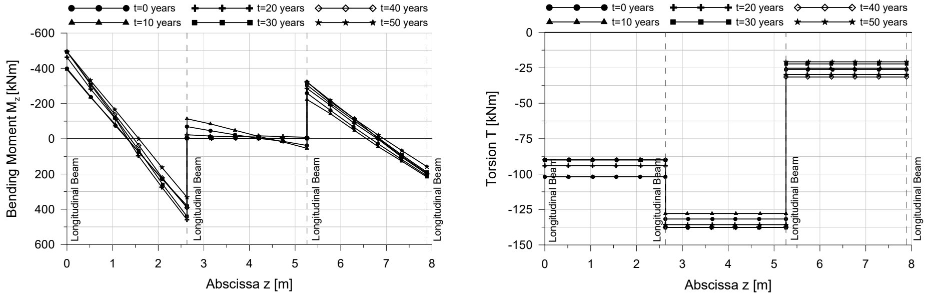

Figure 6.15: Bending and torque moments along the end cross-beam at incipient collapse for different sampling times ($t = 0 \div 50$ years).

These results are confirmed by the bending moment and torsion diagram at incipient collapse for the central cross-beam, as shown in Fig. 6.14. As time increases (*t=30 years*), additional hinges will form in the end cross-beams which collapse under the combined action of bending moment and torsion (Fig. 6.15). In the redistribution process, the collapse mechanism moves from the central to the end undamaged cross-beams, searching for, in the grillage deck, new load paths through the contribution of new collaborating parts. Typical, from this point of view, is the torsional contribution of the end cross-beams (Fig. 6.15), accentuated by the increasing of the relative rotations of the longitudinal beams at the supports.

These results have to be taken into account in the actual design of the deck repairing interventions. In fact, the design must be focused not only on substituting/repairing the elements which had undergone the most damage (the edge longitudinal beam), but also on verifying that the undamaged elements (the cross-beams) had sufficient bearing capacity to carry the increase of internal forces derived from the redistribution mechanism.

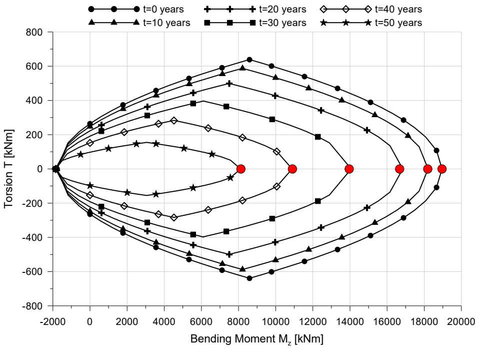

Figure 6.16: Position of the point representing the ultimate values of the internal forces M_z and T on the linearized frontier of the midspan damaged cross-section over time corresponding to the plastic hinge in the edge longitudinal beam.

6.3.3 NONLINEAR ANALYSIS AT DIFFERENT TIME INSTANTS

For a given environmental and loading conditions, at each sampling time, the nonlinear finite element analysis of the deck is carried out, so that it is possible to assess its structural response in the damage state under different loading combinations. The damage effects are sampled separately at $0 \div 50$ years with intervals of 10 years.

6.3.3.1 DEAD LOADS EFFECTS

A first analysis investigates the behavior of the grillage under the dead loads only, as shown in Fig. 6.4a. The results show the decay of the structure demonstrated by the modification of the deformed shape and the internal forces redistribution. At different sampling time, the localized damage involves both an increase of the deformability of the longitudinal and transversal beams and a redistribution of the internal forces, as shown in Figs. 6.18, 6.19 and 6.20. As the time increases, we notice that under symmetrical dead loads *(a)* the overall deformed shape and the transverse displacements lose their symmetry and *(b)* that the vertical displacements of the edge beams show a progressive increase of the curvature at midspan indicating a progressive formation a plastic hinge in that zone.

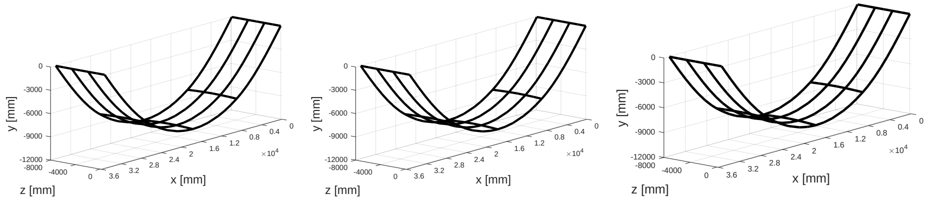

(a) *t=0 years.* **(b)** *t=10 years.* **(c)** *t=20 years.*

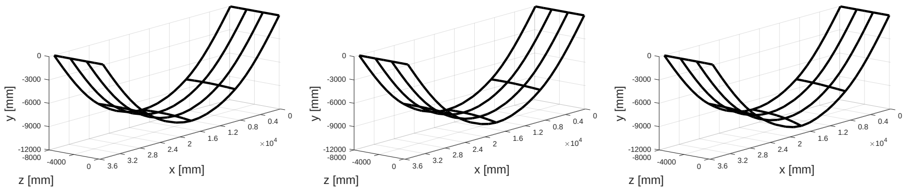

(d) *t=30 years.* **(e)** *t=40 years.* **(f)** *t=50 years.*

Figure 6.17: Deformed shapes of the deck at different time instant under dead load only (scale factor equal to 180).

Fig. 6.19 shows the changes of the longitudinal bending moments and the torsional moments along the edge beam. In this case, we can observe how the longitudinal beam, growing weaker with the progression of the deterioration process, calls for a supporting contribution from the central transverse. Such contribution causes a visible local kink at midspan in the longitudinal bending moment diagram and an increase of the torsional moment at midspan due to the concentrated transversal moment transmitted by the cross-beam. Such a behavior highlights the progression of this redistribution mechanism for $t = 0 \div 50$ years.

Fig. 6.20 shows the changes in the bending moment in the transverse direction along the cross-beam and, as a check, the constant zero value of the torsional moment along the cross-beam, because the symmetry with respect the middle transverse plan is maintained. The bending moment diagram shows how the unloading of the edge beam redistributes its supporting contribution to the other beams and how the moment intensity on the transverse in correspondence of the second longitudinal beams increases rapidly: this may lead to severe harm of the cross-beams, even if previously undamaged and without load increments.

The localized damage involves both an increase of the deformability of the longitudinal and transversal beams and a redistribution of the internal forces, as shown in Figures 6.18, 6.19 and 6.20. As time increases, the results of these analyses show that: *(a)* the overall deformed shape loses its symmetry (Figure 6.17); *(b)* the weakening of the longitudinal beam under constant loading due to the dete-

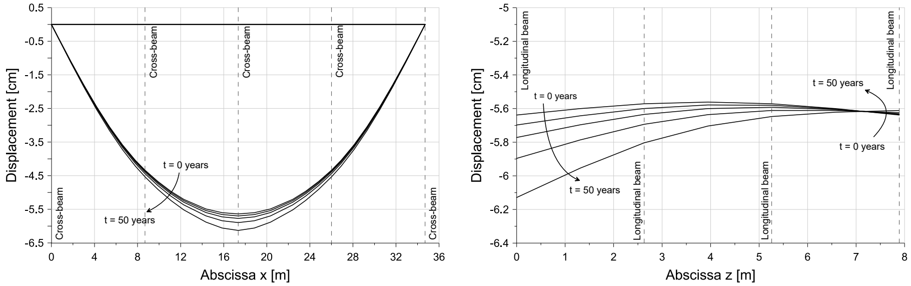

(a) Longitudinal damaged edge beam. **(b)** Central undamaged cross-beam.

Figure 6.18: Deformed shape under dead load only for different sampling times ($t = 0 \div 50$ years).

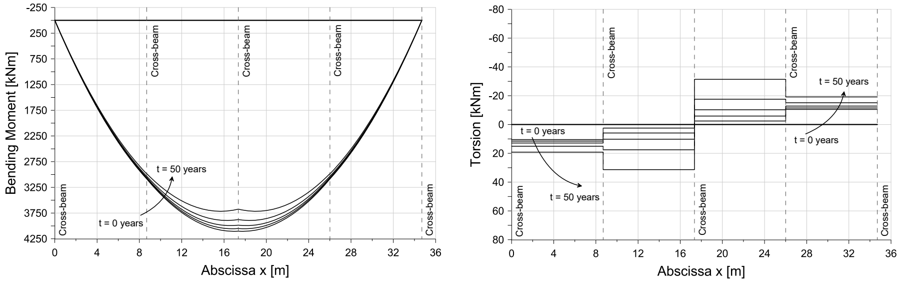

(a) Bending moment. **(b)** Torsion.

Figure 6.19: Bending and torque moments along the longitudinal edge beam under dead load only for different sampling times ($t = 0 \div 50$ years).

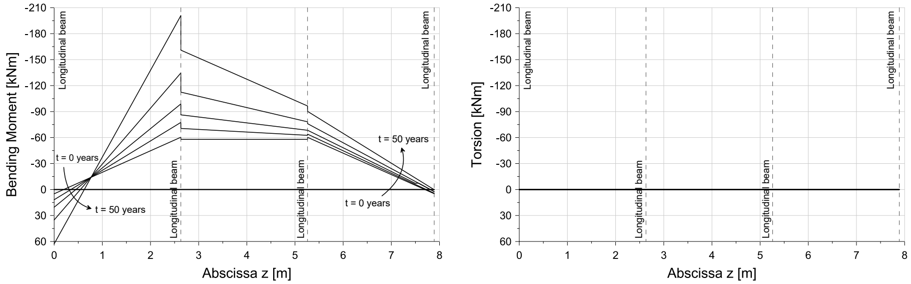

(a) Bending moment. **(b)** Torsion.

Figure 6.20: Bending and torque moments along the central cross-beam under dead load only for different sampling times ($t = 0 \div 50$ years).

rioration process calls for a supporting contribution from the central cross-beam increasing over time. The kinks at midspan in the bending moment diagrams of the longitudinal beams, shown in Figure 6.19a, highlight the progression of this redistribution mechanism for $t = 0 \div 50$ years; *(c)* the corresponding contribution of the central cross-beam, shown in Figure 6.20a, through the plot of its bending moments diagram, becomes clear just after 10 years and rapidly increases from $t = 10$ to $t = 50$ years, and this may lead to the failure of the cross-beams, even if undamaged.

6.3.3.2 COMBINED ACTION OF SELF-WEIGHT AND LIVE LOAD

Another series of assessments concerns the performance of the deck at the Ultimate Limit States (ULS) under the combined action of dead and traffic loads.

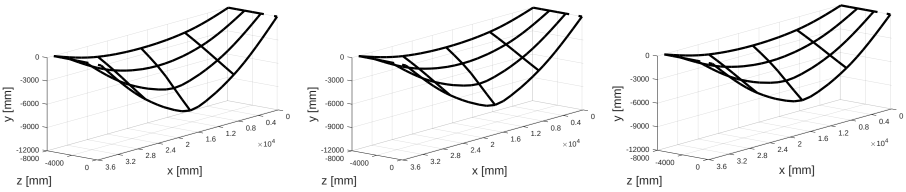
y [mm]
0
-3000
-6000
-9000
-12000
-8000
-4000
0
z [mm]
3.6
3.2
2.8
2.4
2
1.6
1.2
0.8
0.4
0
×10^4
x [mm]

(a) *t=0 years.* **(b)** *t=10 years.* **(c)** *t=20 years.*

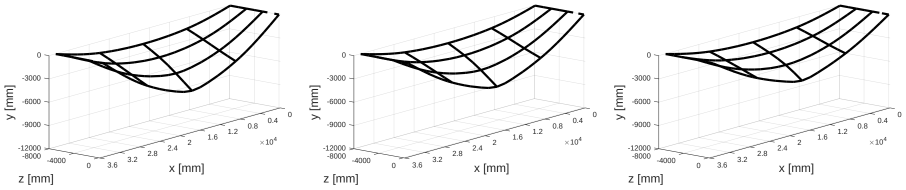
y [mm]
0
-3000
-6000
-9000
-12000
-8000
-4000
0
z [mm]
3.6
3.2
2.8
2.4
2
1.6
1.2
0.8
0.4
0
×10^4
x [mm]

(d) *t=30 years.* **(e)** *t=40 years.* **(f)** *t=50 years.*

Figure 6.21: Deformed shapes of the deck at different time instant under the combined action of dead and traffic loads (scale factor equal to 25).

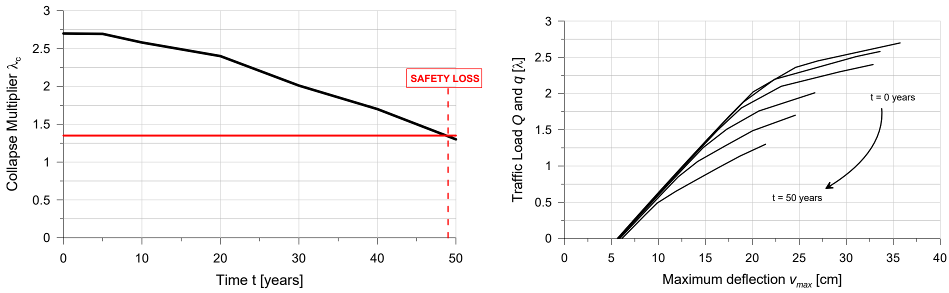

(a) Collapse multiplier. **(b)** Load versus maximum deflection.

Figure 6.22: The load-bearing capacity of the deck under the combined action of dead and traffic loads at different time instant.

The severe reduction of the cross-section of the steel bars, starting from 20 years from the end of construction (Fig. 6.11a), leads to a remarkable decrease of the ultimate load bearing capacity over time. Fig. 6.22a shows the progressive reduction of the load multiplier over time, whereas the red line represent its safety: safety limit is crossed at 48 years. Fig. 6.22b shows that the ductility of the deck decreases as corrosion propagates over time. Therefore, the steel area and ductility reductions involve not only a remarkable deterioration of load carrying capacity but also of the ductility of the overall structure. The deformed shape of the whole deck at different time instants under the combined action of dead and traffic loads is highlighted in Fig. 6.21. As damage propagates, the distribution of the vertical reaction at the supports is also shown in Figure 6.23. It is worth to notice that a significant reduction appears in correspondence of the damaged edge longitudinal beam while the reaction of the opposite edge beam shows a little increment over time due to the role played by the undamaged components.

While the analyses under dead loads only highlight the redistribution of the bearing functions in the deck due to the damage progression even without service loads, the ULS results give fundamental information as concerns the loss of bearing capacity for the worst combination of the traffic loads. Both these types of results provide a reliable reference to answer to the basic questions concerning the safety level of a bridge structure and the decisions in terms of proper maintenance actions and/or rehabilitation interventions.

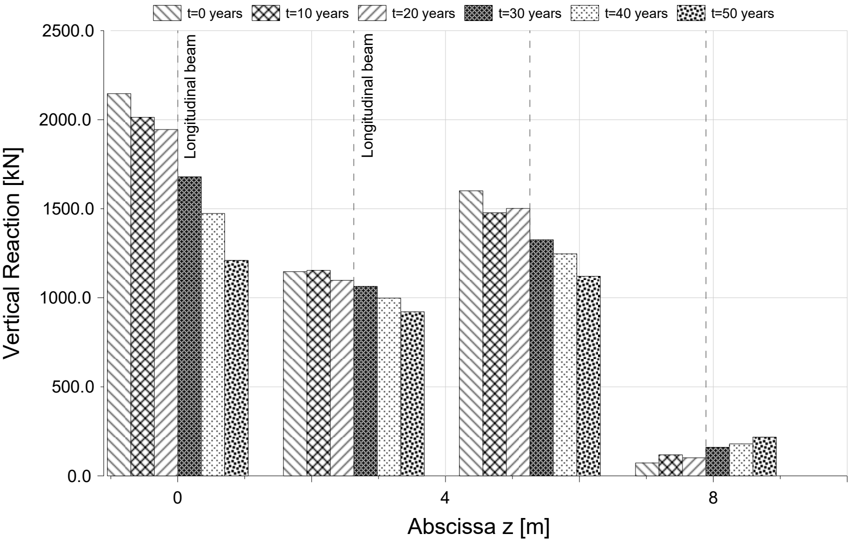

Figure 6.23: Distribution of the vertical reactions at the supports under the combined action of dead and traffic loads at different time instants.

6.3.4 Lifetime structural robustness estimation

Inspection and monitoring of existing bridge structures have highlighted the sensitivity of this kind of structures to the damaging effects associated with diffusive attacks from environmental aggressive agents. A series of Limit and Nonlinear Analysis at different time instants corresponding to certain damage state and under the most severe loading distribution has been performed. The obtained results are mainly useful to show to the significant variation of structural performance over time. In addition, the problem to estimate structural *bearing capacity* and *safety* after a certain amount of years from construction time can be seen as a *lifetime structural robustness estimation*, tailored on the actual or supposed damaging characteristics of a given structure.

At time $t = 0$ years, the comparison is possible only in terms of the global response of the structure: the shape of the collapse mechanism given by the Limit Analysis agrees with the deformed shape of the structure at the incipient collapse given by the Nonlinear Analysis and the location of the main plastic hinges well corresponds to that of the most stressed sections according to the nonlinear analysis.

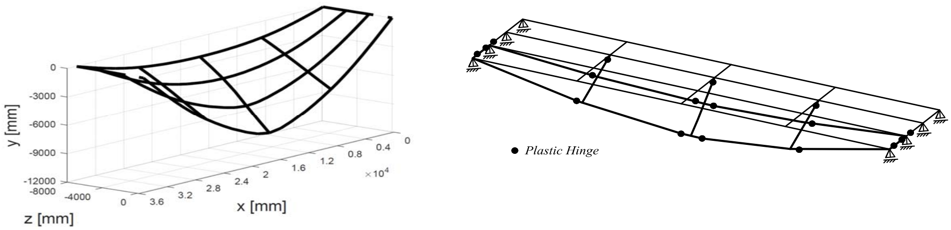

Figure 6.24: Comparison between collapse mechanism derived by LA and deformed shape obtained through NLA.

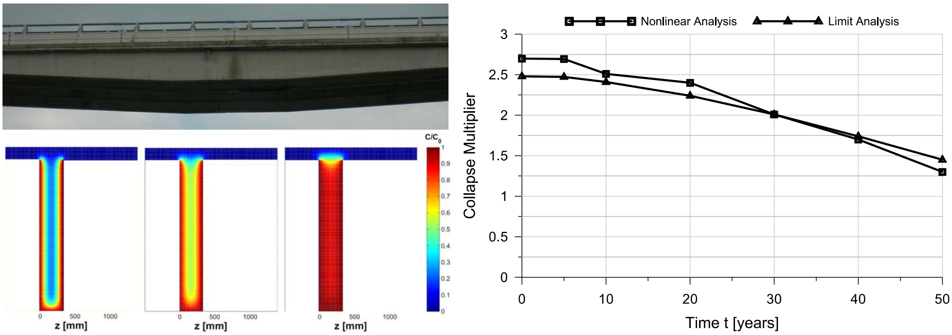

Figure 6.25: Collapse multiplier over time by means of Limit and Nonlinear Analysis at certain damage state.

As time increases, in order to detect the weakest parts of the structures, Limit Analysis highlight the collapse mechanism and the redistribution capacity of the internal forces as damage develops. At a first look, one expect that the weakness is represented by the edge damaged longitudinal beam only. This is confirmed by the collapse mechanism until time t=10 years, when the locus of plastic hinges is dominant in the edge longitudinal beam. However, as the reduction of the steel area in the beam become evident, formation of new plastic hinges appear in the undamaged central cross-beam. After 20 years, the corrosion scenario in the longitudinal beam produced a redistribution of internal forces that is moved from the damaged longitudinal beam to the undamaged cross one. This happens until a flexural collapse affects the cross beam. Starting from time t=30 years, searching for new load path through the collaboration of sound parts, a concentration of plastic hinges occurs in correspondence of the end cross-beam.

A general a measure of *lifetime structural robustness* of the damaged grillage deck is here done according to the procedure exposed in (Biondini, 2009). In this case, the methodology applied for the lifetime assessment of a structure, based on a local definition the dimensionless damage indices δ_s and δ_c, not seems handy for global evaluations of system robustness. A more synthetic global measure of damage may be derived from δ_s and δ_c by a weighted average over the volume of the materials. The global damage index $\Delta = \Delta(t)$ can be defined at the cross-sectional level as follows:

$$\begin{aligned}
\Delta(t) &= [1-\omega(t)]\Delta_c(t) + \omega(t)\Delta_s(t) \\
\Delta_c(t) &= \frac{\int_{A_c} w_c(\mathbf{x},t)\delta_c(\mathbf{x},t)d\mathbf{x}}{\int_{Ac} w_c(\mathbf{x},t)d\mathbf{x}} \\
\Delta_s(t) &= \frac{\sum_m w_{sm}(t)\delta_{sm}(t)A_{sm}}{\sum_m w_{sm}(t)A_{sm}}
\end{aligned} \tag{6.1}$$

where $\Delta_c(t)$ and $\Delta_s(t)$ are respectively the contribution of concrete and steel, $\omega = \omega(t)$ is the mechanical ratio of reinforcement, $w_c = w_c(\mathbf{x}, t)$, $w_{sm} = w_{sm}(t)$ are weight functions here assumed equal to 1, A_c is the area of the concrete matrix, and A_{sm} is the area of the *m-th* steel bar. Fig. 6.26a shows the corresponding time evolution of the global damage index Δ obtained for the grillage deck for the considered damage scenario (Fig. 6.8). However, the damage index Δ investigates only the severity of the damaged scenario. In order to provide meaningful information for robustness evaluations, the damage index Δ can be put in comparison with the variation of the collapse multiplier given by Limit Analysis at different sampling times. This goal can be achieved by relating a performance index $\rho = \rho(t)$ to the global damage $\Delta = \Delta(t)$. By setting the performance index as follows:

$$\rho(t) = \frac{\lambda_c(t)}{\lambda_{c0}} \tag{6.2}$$

the functional $\rho(\Delta)$ can be regarded as a robustness index. This index can be effectively used to compare the robustness associated to different systems and damage scenarios. Fig 6.26b shows the relationships $\rho(\Delta)$ obtained for the grillage deck.

In the end, the robustness index $\rho = \rho(\Delta)$ can also be used to formulate a robustness criterion to verify if a structural system is robust or weak. The following criterion is adopted (Biondini, 2009):

$$R(\rho, \Delta) = \rho(t)^{\alpha} + \Delta(t)^{\alpha} \geq 1 \tag{6.3}$$

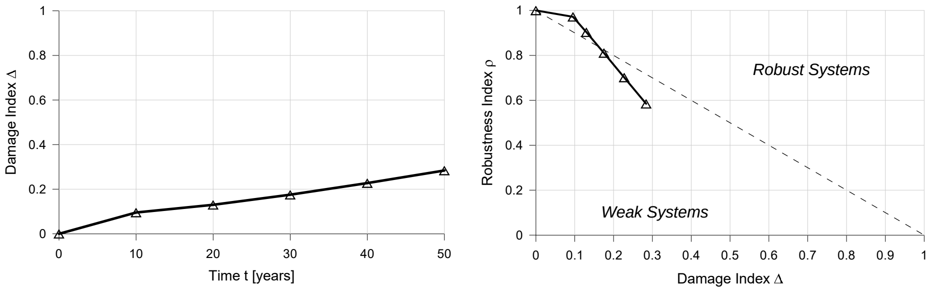

(a) Global damage index Δ over time. **(b)** Robustness index ρ vs global damage Δ .

Figure 6.26: Global measure of damage and robustness index at different sampling times.

where $R = R(\rho, \Delta)$ is a robustness factor, and α is a shape parameter of the boundary $R = R(\rho, \Delta) = 1$. The structural system is robust when the criterion is satisfied (R≥1), and weak otherwise (R≤1). The value of the parameter α can be properly selected according to the acceptable level of damage susceptibility for the structure under investigation. A value $\alpha = 1$, which indicates a proportionality between acceptable loss of performance and damage, is assumed. Fig. 6.27 shows the robustness factor $R = R(t)$ at different sampling times, as the corresponding linear boundary of the robustness criterion is represented by a dashed line. The diagram highlights that the bridge is robust until $t = 20$ years and weak otherwise.

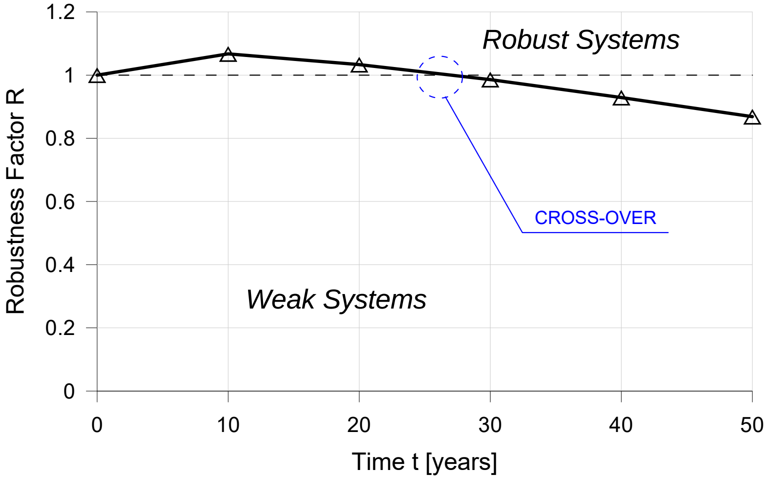

Figure 6.27: Robustness factor R estimation over time for the damaged grillage deck.

It must be pointed out that the diagram $R = R(t)$ is useful to assess the robustness at the global level but it does not provide an exhaustive description of the evolution of the collapse mechanisms over time in a given damage scenario.

This interesting interpretation comes out only from a systematic examination of the results of the analysis. The Limit Analysis results at the ultimate limit state are very important and fundamental for the robustness assessment.

The concentration of plastic hinges, but also the distribution of internal forces, can directly see which parts of the structures are not only the most damaged but also the weakest. In fact, the flow of the forces moves progressively toward the sound parts, which have to be properly verified. Since the structure varies its behavior in time (from damaged to undamaged elements), these results can be taken into account to plan robust repairing interventions.

6.4 CLOSING REMARKS

In this chapter, the assessment of an existing bridge has been presented. In particular, a procedure for *a virtual loading test* is proposed, consisting in the exam of a structure at different damaged states and in the evaluation of the multiplier at the collapse of the worst traffic load distribution has been adopted. Such an approach has outlined the consequences due to different damage factors and the modes which lead to sudden collapses when neither weakness signals nor intermediate anomalous behaviors appear.

By means a complementary and parallel study between Limit Analysis and Nonlinear, the most important conclusions arise:

- it is possible to identify the structural components that more significantly affect the system performance when damage develops;
- the damage reduces the local bearing capacity and progressive reduction of the load multiplier over time;
- there is a progressive redistribution of internal forces towards undamaged structural elements, called to collaborate with the damaged ones in new load paths configurations;
- lack of ductility of the overall structure.

The search for the limit behaviors of the structure has been seen as a *lifetime structural robustness estimation*, tailored on the actual or supposed damaging characteristics of a given structure. According to the results, the design must be focused not only on substituting/repairing the elements which had undergone the most damage, but also on verifying that the undamaged elements (the cross-beams) had sufficient bearing capacity to carry the increase of internal forces derived from the redistribution mechanism.

7 Limit Analysis of RC Structural Elements

This chapter proposes a coupling of Limit Analysis and Framework Modeling in studying RC membrane elements. Such a discretization technique, in addition to the determination of the load multiplier and the mechanism of collapse of the structural elements, allows also to provide useful indications on the position and orientation of the compressed and tensioned elements, with results comparable with those of conventional strut and tie models.

7.1 INTRODUCTION

As previously exposed in chapter 5, *Limit Analysis* is an effective and synthetic tool capable of assessing the load-bearing capacity and collapse mechanisms of reinforced concrete structures and also to identify the most critical parts, corresponding to the zones of formation of plastic hinges. In addition, by extending this type of analyses to structures damaged by wearing of time and rebar corrosion, it is possible to investigate how the consequences of mechanical deterioration may lead a sudden collapse, without weakness signals.

In this chapter, the attention moves from the global to the level of sub-systems, which represent in many cases the weaknesses of the whole system (as shown in par. 2.4). Typically the local behaviors are the object of separated local analyses, limited to those zones in which concentrated stress diffusion state appear. Thus, the basic idea is to use a framework of bars/trusses (1D model) to discretize the continuous systems. Using this approximation, the accuracy of the solution may decrease but, at the same time, the results are more immediate, due to the reduced computational costs and the simplified scheme adopted.

Then, an attempt consists in coupling the framework modeling with Limit Analysis in studying the RC structural elements. In this way, the discretization technique adopted, in addition to the determination of the load multiplier and the mechanism of collapse, should also provide useful indications on the position and orientation of the plasticization in the tensioned and compressed elements in function of their ultimate capacity. This approach could also useful in assessing and validating the bearing schemes assumed in the design practice.

7.2 RC STRUCTURAL ELEMENTS

The development of numerical methods for the study of RC structural elements during both the service conditions and at the ultimate limit state is still today under investigation. As already mentioned, in a structural system, the so-called D-regions cannot be treated according to the beam theory and sometimes are subjected to an incorrect modelization.

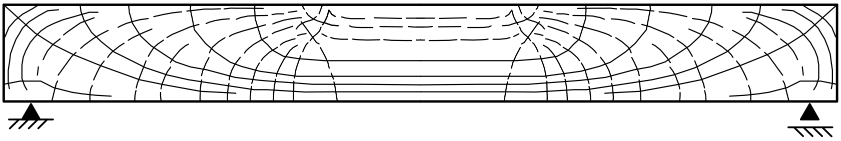

(a) Beam with no cracks. Principal stress directions.

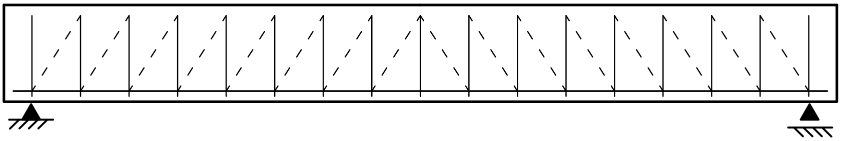

(b) Ritter's model.

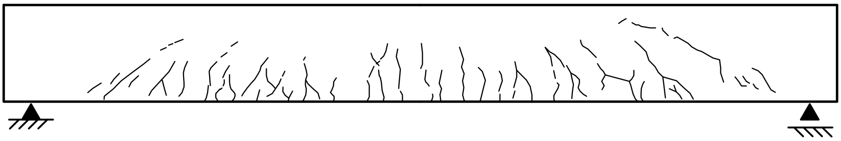

(c) Shear and flexure cracks before reaching the collapse load.

Figure 7.1: Historical development of structural techniques for RC structures.

In the usual (past) approaches, the study of RC structural elements is often based on linear elastic analysis, in particular, by computing the internal forces through with steel reinforcements and structural elements can be designed. These linear analyses are useful and valid in order to understand the global system mechanics (Fig. 7.1a). Since the theory of reinforced concrete works through generalized stresses and not with local stresses, the introduction of the Strut-and-Tie mechanism as in Fig. 7.1b allows a synthetic description of the global structural behavior. In the Literature, in 1899 Ritter proposed a simple model to simulate the nonlinear behavior of RC beams, while Morsch in 1912 proposed a practical and organic application. Finally, (Leonhardt and Walther, 1963) further amplified their field of applications. In the meantime, with the development of finite element methods, bidimensional and tridimensional models became very common. In these models, constitutive relationship based on smeared approaches in which the concrete is treated as a composite material were adopted. Thanks to experimental investigation on concrete panels, the aims were *(i)* to understand the crack pattern evolution (Fig. 7.1c) and *(ii)* to develop a robust theory suitable for practice engineering.

On the contrary, the strategy here proposed is completely different. It consists on adopting an equivalent framework of bars (Fig. 7.2), which is introduced only for

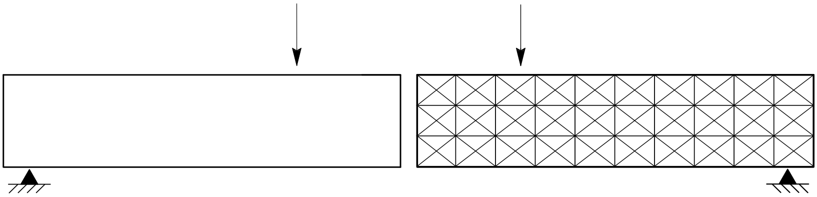

(a) Bidimensional element. **(b)** Trusswork modeling.

Figure 7.2: Discretization technique in studying RC structural elements.

meshing purposes, in order to fit the geometrical characteristics and the arrangement of all the reinforcements, followed by the Limit Analysis of the discretized structural element.

7.3 Framework Modeling

Considerable efforts have been devoted in the past to the structural analysis of two-dimensional continuous systems involving elastic materials. As well known, the difficulties which arise in treating analytically the general equations of elasticity, under given boundary conditions, are overcome according to different possibilities: *(i)* by introducing numerical solutions of the analytical equations, *(ii)* by physical modelization of the structure domain by means of finite elements or similar approaches, based on approximation theories.

A particular technique, introduced in the middle of the past century and proposed by (Hrennikoff, 1941) and (Absi, 1972), studies the elastic problems modeling the continuous systems through a finite number of *elementary "equivalent" frameworks* or trusses of bars. The aforementioned papers present a significant set of applications concerning membrane elements, plate systems, shells and also 3D structures. According to (Hrennikoff, 1941), the equivalence between the elementary framework model and the corresponding portion of the continuous structure is guaranteed by imposing equal average strains (kinematic principle). Similarly, (Absi, 1972) defines another equivalent criterion between the two models, which must present the same elastic potential energy (energy principle). Apart from small differences, the two approaches practically lead to the same results.

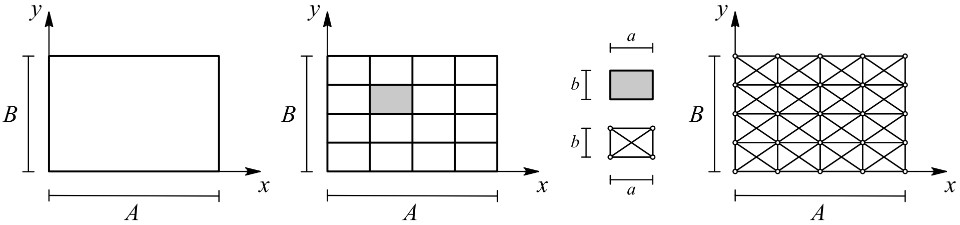

Figure 7.3: Pattern of the Framework modelization for continuous systems.

In this Thesis, we assume a type of discretization based on the *framework method* proposed by (Hrennikoff, 1941) and recalled by (Toniolo and Malerba, 1981). The continuous structure is here replaced by an equivalent mesh of truss elements with suitable and well defined sectional properties. Fig. 7.3 shows the meshing technique which consists of rectangular elements of sides a and b in the x and y directions respectively. The set of equations (7.1) defines the area of each element in the elementary framework (x=horizontal, y=vertical and d=diagonal), where t is the thickness of the structure and l is the length of the diagonal bars. The horizontal elements are spread across the depth while the vertical ones are spread along the span. Diagonal bars cross each other without a connection at the center.

$$A_x = \frac{3}{16} bt \left(3 - \alpha^2\right) \qquad A_y = \frac{3}{16} at \left(3 - \beta^2\right) \qquad A_d = \frac{3}{16} lt \left(\alpha + \beta\right) \tag{7.1}$$

with

$$\alpha = \frac{1}{\beta} = \frac{a}{b}$$

Both (Hrennikoff, 1941) and (Toniolo and Malerba, 1981) outline how this type of equivalence is rigorous for the elastic element having a Poisson's ratio $\nu = 1/3$.
It must be noted that in the present work aimed at the Limit Analysis of RC structural elements, the framework method is introduced only for meshing purposes and not to study an elastic problem. So, the analysis is carried out on the basis of the following assumptions:

- the whole framework model superimposes the properties of concrete and steel contributions;
- the cross-sectional areas of the bars simulating concrete are derived from (7.1);
- where the horizontal and vertical bars coincide with the actual position of bars of the reinforcement, the steel area is added to the area of the corresponding concrete truss elements;
- the bearing capacity of every single bar is given by the condition of the full plasticity of the corresponding cross-sectional area.

In the following, three benchmarks with increasing complexity are presented:

- Bresler & Scordelis A1 Beam;
- Deep Beam WT2;
- RC Corbel.

By performing a Limit Analysis, according to the formulation exposed in chapter 5, the results provide useful indications in terms of:

(a) the collapse multiplier and collapse mechanism;

(b) the role played by concrete and steel and the distribution ofload path.

7.4 BRESLER & SCORDELIS A1 BEAM

The first example deals with the RC beam, tested by (Bresler & Scordelis, 1963) and studied by (Bontempi *et al.*, 1995b). Specimen A1 is a simply supported beam with a span equal to 4.1 m and it is designed to obtain a shear-type collapse. The beam is subjected to a center-point force P, increased up to failure. The geometry of the structure and the adopted mesh ($a = 103.00\,mm$ and $b = 60\,mm$) are shown in Fig. 7.4. In Limit Analysis, only concrete strength and the steel yielding stress are involved, as detailed in Tab. 7.4.

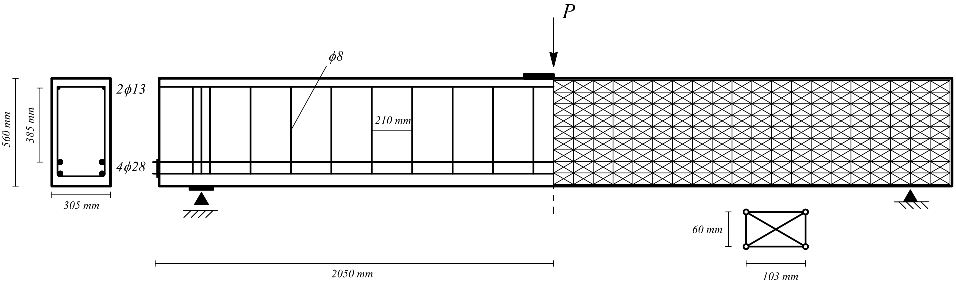

Figure 7.4: Bresler & Scordelis A1 Beam. Geometry and trusswork discretization.

ε_c'	$f_c'\,[MPa]$	$E_c\,[MPa]$	$f_{cr}\,[MPa]$	ε_{cr}
$-1.8\cdot10^{-3}$	-24.1	26778	1.62	$6.0\cdot10^{-5}$

(a) Concrete characteristics.

$\alpha\,[^o]$	$f_y\,[MPa]$	$E_s\,[MPa]$	$\phi\,[mm]$
90	325	190000	$\phi 8$

(b) Stirrups.

bars	$f_y\,[MPa]$	$E_s\,[MPa]$	$\phi\,[mm]$
sup.	345	201000	$2\phi 13.0$
inf.	555	218000	$4\phi 28.0$

(c) Reinforcing longitudinal steel.

Table 7.1: A1 Bresler & Scordelis Beam: materials characteristics.

According to the adopted discretization, the area of each element of the elementary trusswork results:

$$A_x = 182.05\,mm^2 \qquad A_y = 15672.15\,mm^2 \qquad A_d = 15672.15\,mm^2$$

These value are used to build the resistant domains, which represent the input for the Limit Analysis. In function of both the portion of concrete (c) assigned to each truss element and the position of steel reinforcement (s), in the simply supported

A1 beam nine types of domains are identified, as summarized in Tabs. 7.2 and 7.3. Fig. 7.6 compares the maximum and minimum axial resistance among the different domains.

Resistant Domain	N_r^-		N_r^+		*Type*	*Area*
$N-N_1$	-2.55	kN	0.38	kN	horizontal	A_x
$N-N_2$	-5.09	kN	0.77	kN	horizontal	A_x
$N-N_3$	-438.13	kN	65.82	kN	vertical	A_y
$N-N_4$	-219.08	kN	32.91	kN	diagonal	A_d

Table 7.2: Resistant domains in the equivalent trusses made by concrete only.

Resistant Domain	N_r^-		N_r^+		*Type*	*Area*
$N-N_5$	-695.82	kN	691.49	kN	horizontal	$A_x\ A_{s1}$
$N-N_6$	-102.99	kN	98.66	kN	horizontal	$A_x\ A_{s2}$
$N-N_7$	-231.78	kN	45.63	kN	vertical	$A_y\ A_{s3}$
$N-N_8$	-450.85	kN	78.54	kN	vertical	$A_y\ A_{s3}$
$N-N_9$	-444.49	kN	72.18	kN	diagonal	A_d

Table 7.3: Resistant domains in the equivalent trusses made by concrete and steel.

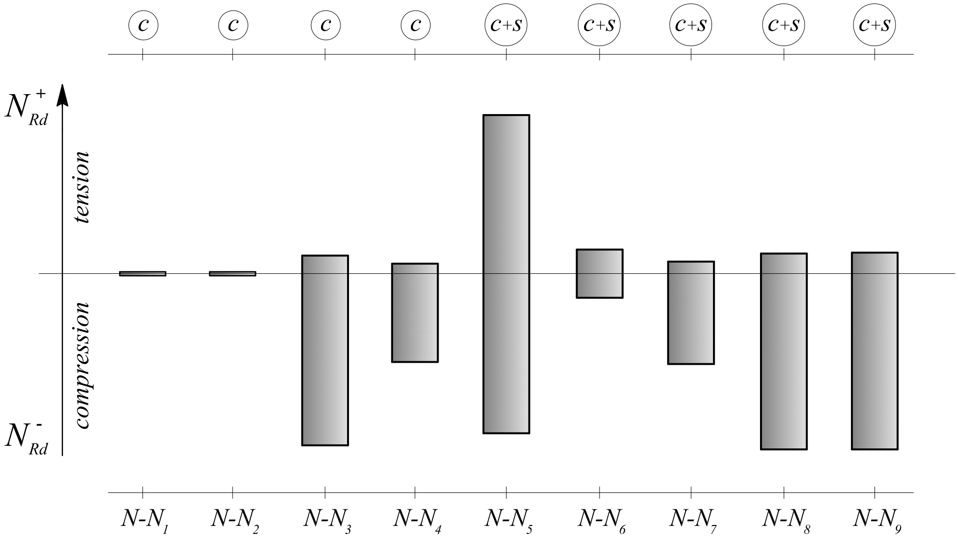

Figure 7.5: Comparison between ultimate values in the resistant domains.

Fig. 7.6a shows the plasticized elements in tension (red) and compression (blue) and corresponding collapse mechanism coming from the Limit Analysis. Fig. 7.6b highlights the location and direction of these elements, where the color intensity is proportional to their bearing capacity ($s[\%] = N/N_{Rd}$). On the bottom part of Fig. 7.6b, it is interesting to note that plasticity conditions both in tension and compression don't involve the whole length of rebars and the compressed strut follows a punching type mechanism directly from the point of application of the load. Such information may be useful in assessing and/or improving strut-and-tie solutions for a more refined reinforcement design. The collapse load resulting from the Upper and Lower Bound theorems is $P_u = 544.8\,kN$ while the experimental ultimate load is $P_{ex} = 460.0\,kN$. In the end, Fig. 7.7 shows a qualitative comparison with respect to results coming from other techniques.

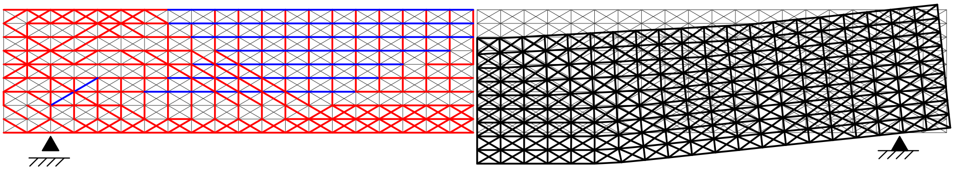

(a) Plasticized elements in tension (red) and compression (blue) and its collapse mechanism.

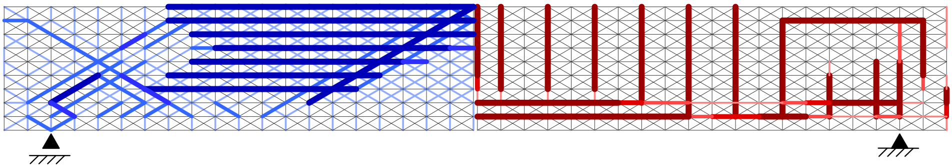

(b) Location and direction of the plasticized elements in function of their capacity.

Figure 7.6: Bresler & Scordelis A1 Beam. Limit Analysis results.

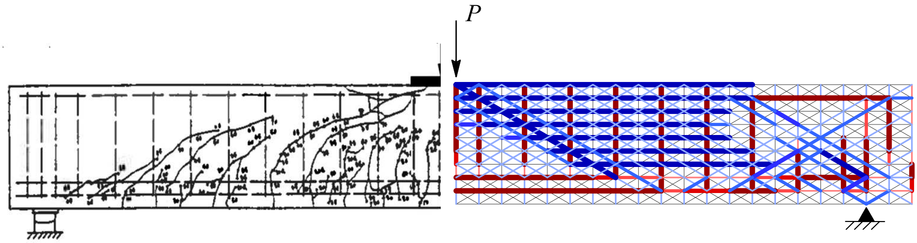

(a) Experimental results versus the distribution of plasticized elements.

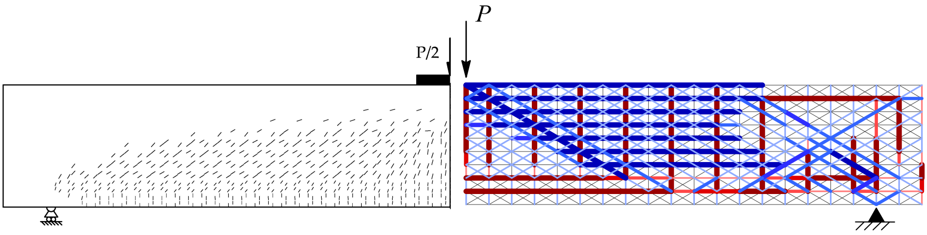

(b) MCFT results versus the distribution of plasticized elements.

Figure 7.7: Qualitative comparison for Bresler & Scordelis A1 Beam results.

7.5 DEEP BEAM WT2

(Leonhardt and Walther, 1963) conducted a well known and extensive series of tests on deep beams. Among these, the so-called WT2 beam illustrated in Fig. 7.8, is analyzed under a uniformly distributed load p, to be increased until collapse. The deep beam is here modeled through an equivalent mesh of truss elements of sides $a = b = 65\,mm$. The resistant domains for each element are determined by using material characteristic listed in Tab. 7.4.

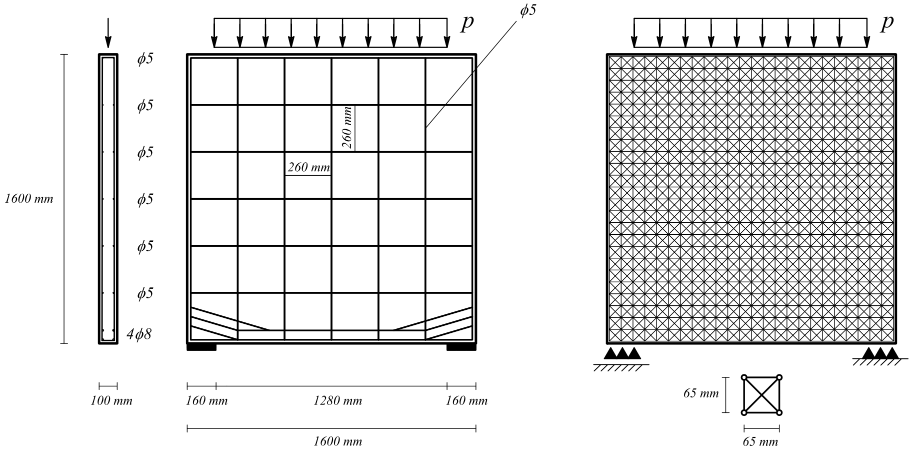

Figure 7.8: Deep Beam WT2. Geometry and trusswork discretization.

ε'_c	$f'_c\,[MPa]$	$E_c\,[MPa]$	$f_{cr}\,[MPa]$	ε_{cr}
$-1.8 \cdot 10^{-3}$	-29.6	31329	2.9	$6.0 \cdot 10^{-5}$

(a) Concrete characteristics.

$\alpha\,[^o]$	$f_y\,[MPa]$	$E_s\,[MPa]$	$\phi\,[mm]$
90	310	206100	$\phi 5.0$

(b) Stirrups.

bars	$f_y\,[MPa]$	$E_s\,[MPa]$	$\phi\,[mm]$
sup.	310	206100	$\phi 5.0$
inf.	428	206100	$4\phi 8.0$

(c) Reinforcing longitudinal steel.

Table 7.4: Deep Beam WT2: materials characteristics.

According to the adopted mesh, the area of each element of the elementary trusswork results:

$$A_x = 2437.50\,mm^2 \qquad A_y = 2437.50\,mm^2 \qquad A_d = 3447.15\,mm^2$$

Resistant Domain	N_r^-		N_r^+		*Type*	*Area*
$N - N_1$	-144.30	kN	14.14	kN	horizontal/vertical	A_x/A_y
$N - N_2$	-102.04	kN	10.00	kN	diagonal	A_d

Table 7.5: Resistant domains in the equivalent trusses made by concrete only.

Resistant Domain	N_r^-		N_r^+		*Type*	*Area*
$N - N_3$	-164.29	kN	99.21	kN	horizontal	$A_x\ A_{s1}$
$N - N_4$	-156.47	kN	26.31	kN	horizontal/vertical	$A_x/A_y\ A_{s2}/A_{s3}$
$N - N_5$	-121.26	kN	56.18	kN	horizontal	$A_x\ A_{s2}$
$N - N_6$	-84.32	kN	19.24	kN	vertical	$A_y\ A_{s3}$
$N - N_7$	-78.24	kN	13.16	kN	vertical	$A_y\ A_{s3}$

Table 7.6: Resistant domains in the equivalent trusses made by concrete and steel.

As before, in Tab. 7.5 and 7.6 the values of resistant axial forces are summarized and a comparison is shown in Fig. 7.9. Among the seven domains, the resistant domain number 3 is characterized by the higher tensile and compressive axial resistance.

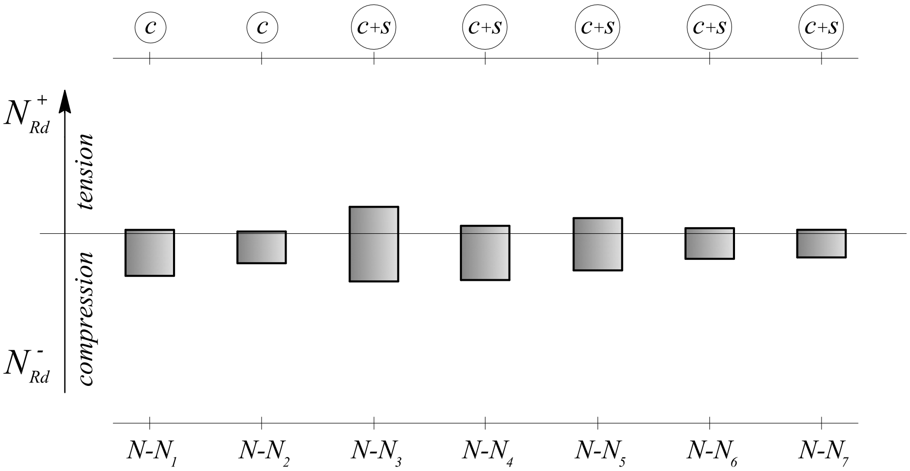

Figure 7.9: Comparison between ultimate values in the resistant domains.

Fig. 7.10a shows the collapse mechanism and Fig. 7.10a the pattern of axial forces at the collapse. As before, the color intensity is proportional to the rate of plasticization of tensioned (red) and compressed (blue) bars of elements $s[\%] = N/N_{Rd}$. Location and direction of the compressed members give an effective portrait of the load path from the upper edge to the lower supports. The tensioned elements highlight the role of the reinforcement as bottom chord tie and how the diffused reinforcement is involved by the shear action at the sides of the deep beam. Finally, the experimental failure load is $P_{ex} = 1195\,kN$ while the ultimate load given by Limit Analysis results $P_u = 1000.82\,kN$. Interesting comparison with the results coming from experimental investigation and bidimensional analysis are repoerted in Fig. 7.11.

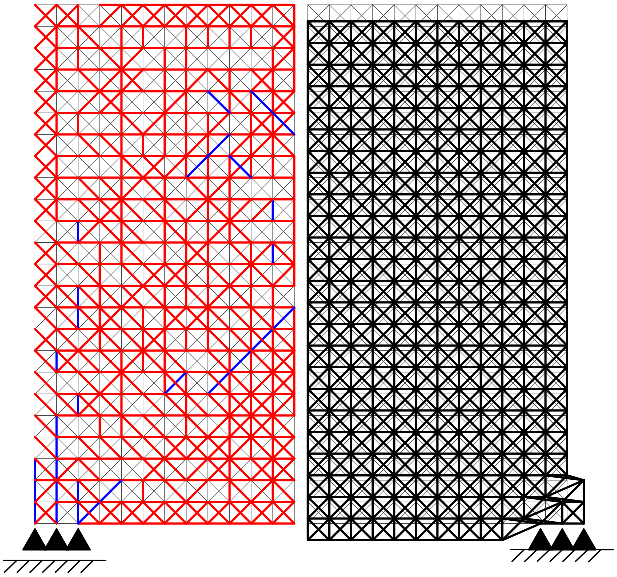

(a) Plasticized elements and relative collapse mechanism.

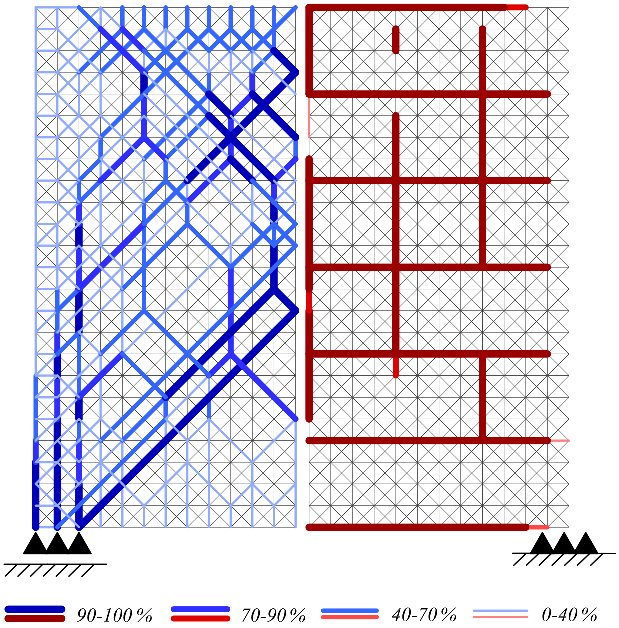

(b) Plasticized elements in function of their capacity.

Figure 7.10: Deep Beam WT2. Results coming from Limit Analysis.

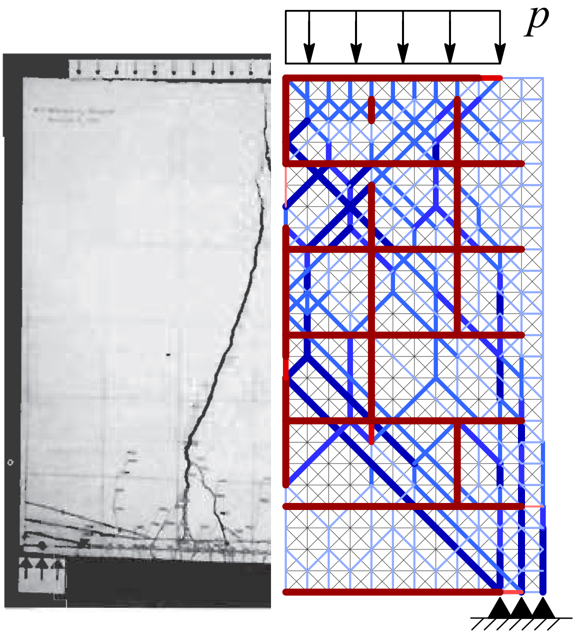

(a) Experimental results versus the distribution of plasticized elements.

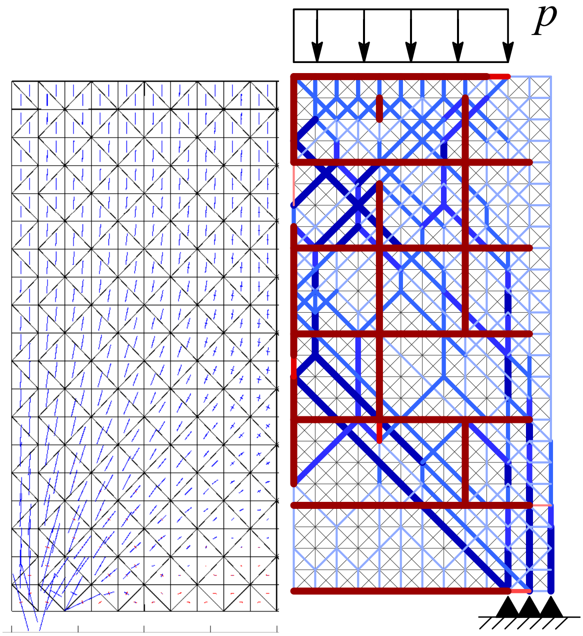

(b) MCFT results versus the distribution of plasticized elements.

Figure 7.11: Qualitative comparison for WT2 Deep Beam results.

7.6 RC CORBEL

Corbels are short-haunched cantilevers that project from the inner face of columns to support heavy concentrated loads or beam reactions. They are used extensively in precast concrete construction to support primary beams and girders. A corbel, illustrated in Fig. 7.12, is analyzed under a vertical concentrated load P, to be increased until the collapse. Details concerning the amount and arrangement of reinforcements are shown in Fig. 7.12. The resistant domains for each element are determined by using the material characteristics reported in Tab. 7.7. From the structural point of view, the corbel is modeled through an equivalent pattern of truss elements having $a = b = 50\,mm$.

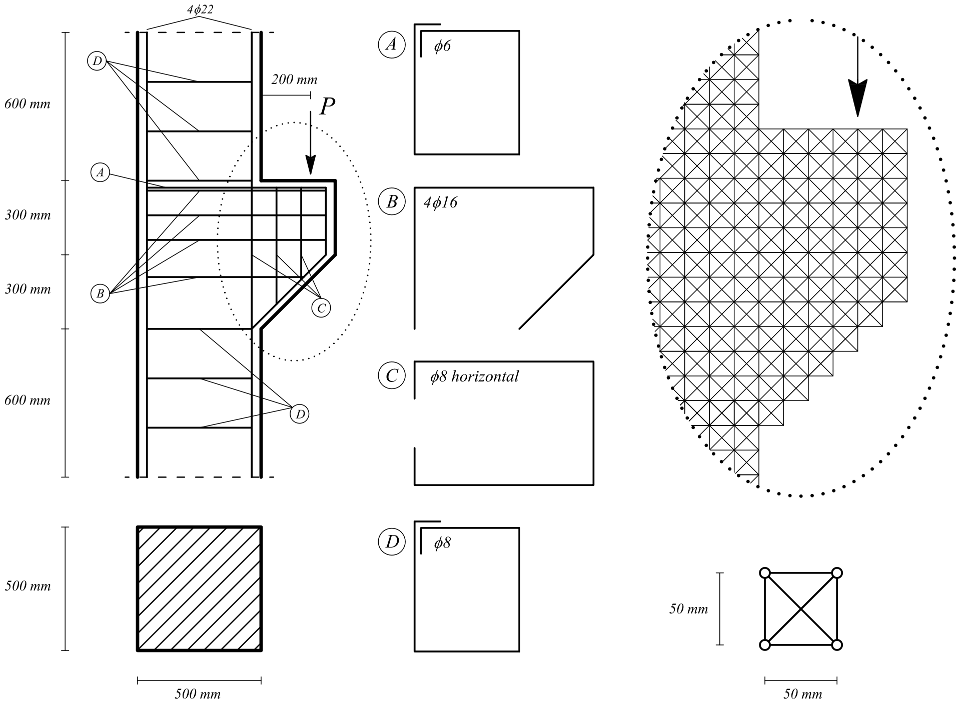

Figure 7.12: RC Corbel. Geometry and trusswork discretization.

According to the adopted mesh, the area of each element of the elementary trusswork results:

$$A_x = 9375.00\,mm^2 \qquad A_y = 9375.00\,mm^2 \qquad A_d = 13258.25\,mm^2$$

Tabs. 7.8 and 7.9 summarize the resultant axial forces for each domain. Fig. 7.13 compares the obtained resistant domains in order to emphasize the different contribution of steel (s) and concrete (c).

Fig. 7.15 shows the collapse mechanism and the distribution of axial forces at incipient collapse for both compressive and tensile elements. The color intensity is proportional to the rate of plasticization of tensioned (red) and compressed (blue)

ε'_c	$f'_c\,[MPa]$	$E_c\,[MPa]$	$f_{cr}\,[MPa]$	ε_{cr}
$-1.8 \cdot 10^{-3}$	-41.5	40299.0	3.6	$6.0 \cdot 10^{-5}$

(a) Concrete characteristics.

$\alpha\,[^o]$	$f_y\,[MPa]$	$E_s\,[MPa]$	$\phi\,[mm]$
90	440	210000	ϕ8.0

(b) Stirrups.

bars	$f_y\,[MPa]$	$E_s\,[MPa]$	$\phi\,[mm]$
A	440	210000	ϕ6.0
B	440	210000	4ϕ16.0
Column	440	210000	4ϕ22.0

(c) Reinforcing longitudinal steel.

Table 7.7: RC Corbel: materials characteristics.

Resistant Domain	N_r^-		N_r^+		*Type*	*Area*
$N - N_1$	-778.13	kN	67.50	kN	horizontal/vertical	A_x/A_y
$N - N_2$	-389.06	kN	33.75	kN	horizontal	A_x
$N - N_3$	-550.22	kN	47.73	kN	diagonal	A_d

Table 7.8: Resistant domains in the equivalent trusses made by concrete only.

Resistant Domain	N_r^-		N_r^+		*Type*	*Area*
$N - N_4$	-803.01	kN	92.38	kN	horizontal	$A_x\ A_{sD}$
$N - N_5$	-1058.10	kN	702.78	kN	vertical	$A_y\ A_{sPil}$
$N - N_6$	-1411.97	kN	1056.65	kN	vertical	$A_y\ A_{sPil}\ A_{sA}$
$N - N_7$	-1176.23	kN	465.60	kN	horizontal	$A_x\ A_{sA}\ A_{sB}$
$N - N_8$	-822.36	kN	111.73	kN	horizontal	$A_x\ A_{sB}$
$N - N_9$	-822.36	kN	111.73	kN	vertical	$A_y\ A_{sC}$
$N - N_10$	-1491.39	kN	780.77	kN	vertical	$A_y\ A_{sPil}\ A_{sC}$
$N - N_11$	-742.93	kN	387.62	kN	vertical	$A_y\ A_{sA}$
$N - N_12$	-904.09	kN	401.60	kN	diagonal	$A'\ \ A_{sA}$

Table 7.9: Resistant domains in the equivalent trusses made by concrete and steel.

bars of elements, $s[\%] = N/N_{Rd}$. Location and direction of the compressed members give an effective portrait of the load path from the point of application of the load to the restrains. In particular, it is interesting to note that the diagonal compressive strut is called to support the vertical tie due to the reinforcement. The tensioned elements are concentrated in correspondence to the cantilever part. Both Upper and Lower Bound Theorems provide a collapse load $P_c = 1250\,kN$. The obtained results are compared with stress pattern coming from 2D analysis in

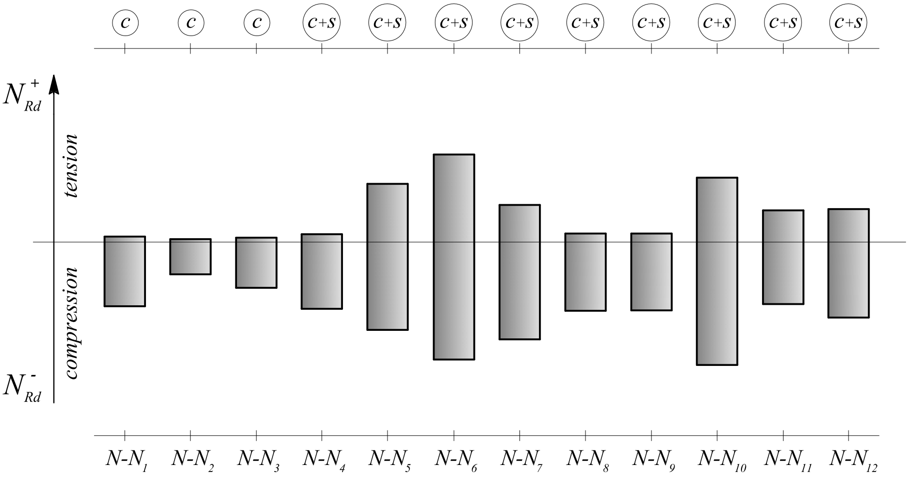

Figure 7.13: Comparison between ultimate values in the resistant domains.

which the collapse is reached for $P_{MCFT} = 1000\,kN$ (Fig. 7.14).

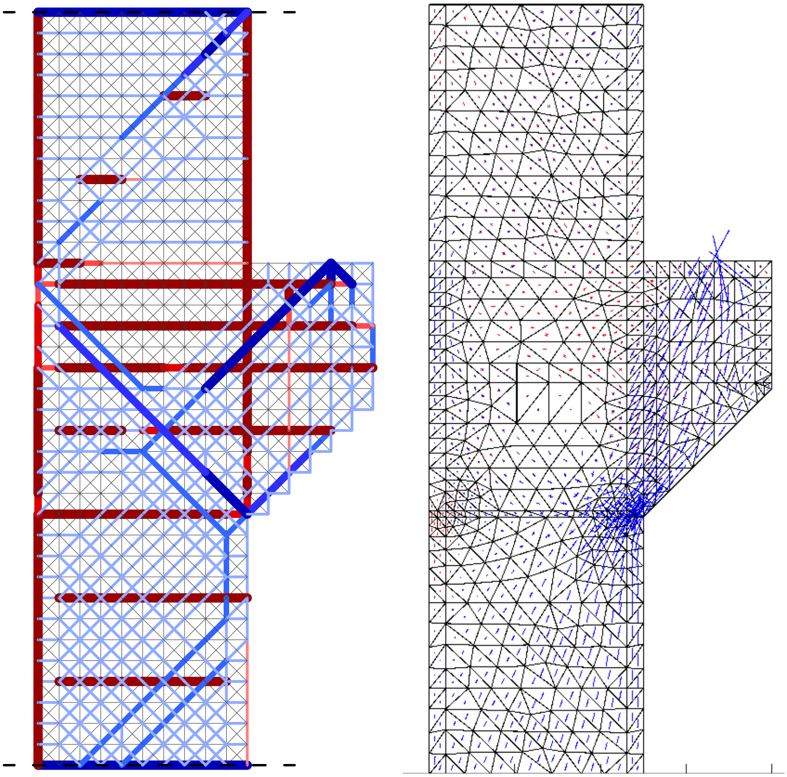

Figure 7.14: Qualitative comparison for the results of RC Corbel.

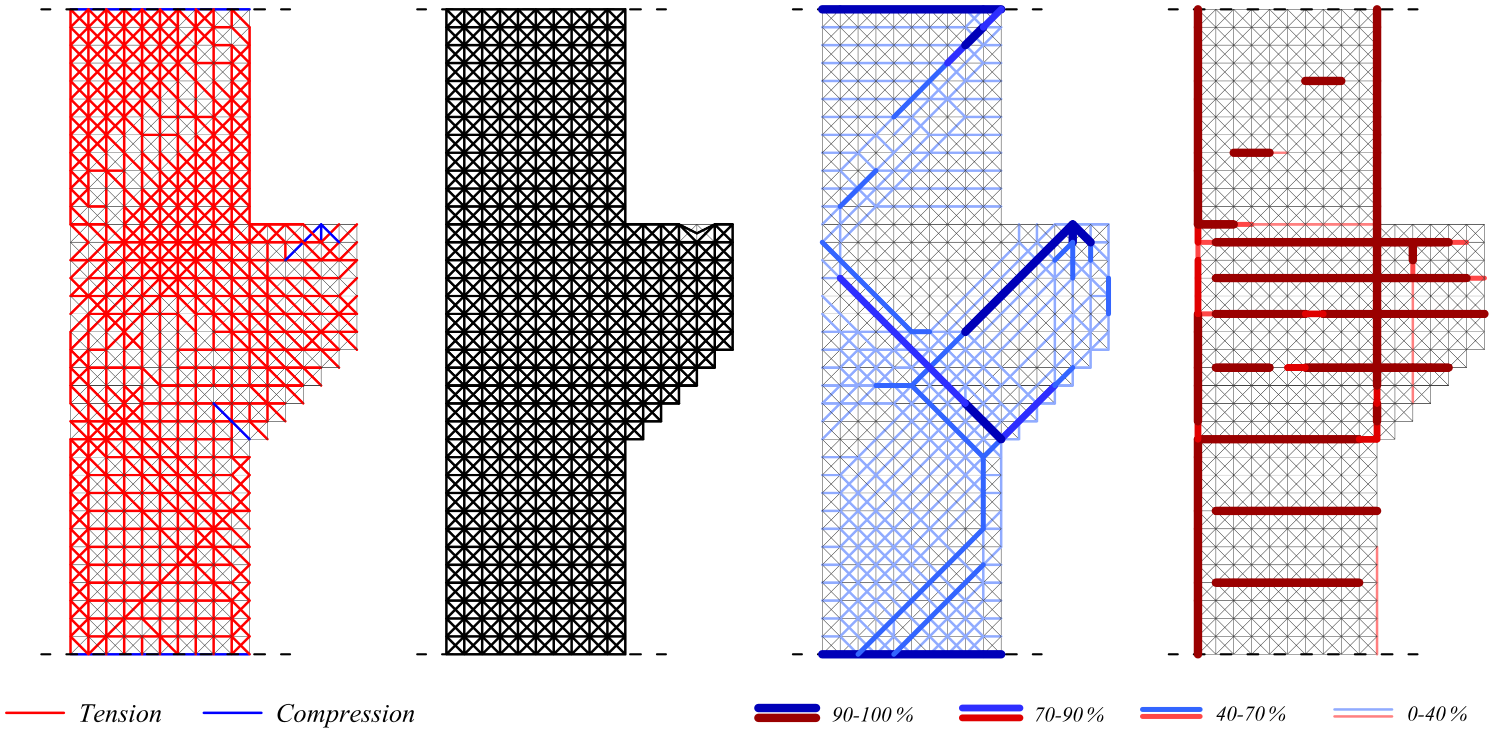
Tension
Compression
90-100 %
70-90 %
40-70 %
0-40 %

Figure 7.15: RC Corbel. Plasticized elements in tension (red) and compression (blue) and corresponding collapse mechanism (left). The sketch in the right side highlights location and direction of these elements, where the color intensity is proportional to their bearing capacity.

7.7 COMMENTS ON THE RESULTS

As known, Limit Analysis is an effective and synthetic tool to assess load bearing capacity and collapse mechanisms of steel and reinforced concrete structures. The type of applications here studied represent *an attempt* to coupling Limit Analysis and Framework Modeling in studying RC membrane elements. Such a discretization technique, in addition to the determination of the load multiplier and the mechanism of collapse, provides useful indications on the position and orientation of the compressed struts and on the distribution of the plasticization in the tensioned elements. After some numerical tests, the adopted equivalent meshes have shown a good accuracy of the predicted results with respect to the actual position of steel reinforcement, the diffusive mechanisms into the concrete and the combined system concrete and steel. The global results are compared and are in agreement with those of other studies. In particular, the mentioned experimental studies took place on a single specimen and cannot be treated into a statistic context that allows identifying systematic and accidental errors. In this sense, the difference observed between the experimental and obtained collapse loads result acceptable. The layout of the load paths recalls that of the conventional strut-and-tie models reported in the literature, but with this approach, it is possible to appreciate the actual length of the plasticized zones among in the stirrup and main reinforcement alignments. Both the layout of the load path and the plasticization distribution may be useful in assessing and validating the bearing schemes assumed in the design practice.

7.8 CLOSING REMARKS

In this chapter, the analysis of RC structural elements has been performed. After short recalls of the essentials of Framework Modeling for continuous systems, the equivalent pattern of bars/trusses has been introduced only for meshing purposes and not to study the elastic problem. In this way, the Limit Analysis presented in chapter 5 is coupled with the adopted discretization in order to investigate the structural performance of the sub-systems. Original results concern not only the complete solution of the problem at incipient collapse, but also the pattern of plasticization elements both in tension and in compression. This information could be very important in verifying and possibly increasing the bearing capacity of the components in light of the additional role that may be called to play, especially during designing repairing interventions. Further studies will be devoted to improving the Framework Modellization and to refine the post-processing graphics of the results, in order to make the bearing mechanisms more explicit.

A Damage modeling in RC structures exposed to corrosion

To predict the structural lifetime performance of RC structures, the damage, measured at a particular time after construction, is supposed to be induced by chlorides diffusion. In this chapter, the diffusion process over time is analyzed through a Cellular Automata algorithm. The corresponding mechanical damage is included by including the reduction of cross-sectional areas of corroded bars and the reduction of ductility of reinforcing steel, the deterioration of concrete strength and the spalling of the concrete cover.

A.1 INTRODUCTION

Concrete structures exposed to aggressive environments are subjected to lifetime degradation induced by the kinetic process of diffusion of chemical components, such as sulphates and chlorides, driven by concentration gradients inside the material volume (Glicksman, 2000). In the application studied in chapter 6, the attention is focused on chloride induced corrosion. In fact, when chlorides, which are critical in a marine environment or come from the application of deicing salts on bridge decks, increase beyond a threshold value in carbonated concrete, they may lead to the deterioration of the concrete and the corrosion of the reinforcement. Moreover, damage induced by mechanical loading interacts with the environmental factors and accelerates the deterioration process (C.E.B., 1992).

In order to estimate the residual bearing capacity of damaged structures, the evaluation of the current state of the structure, on the basis of the results of the *inspections* (visual surveys, physical-chemical analyses, experimental measurements), is firstly required. In many cases, information about damage is deduced from visual surface inspections and, at the most, some local samples. Although limited, such information may be assumed as the basis for better assessing the internal state of the structural members, by modeling the damage diffusion process through suitable *numerical techniques.* At a given time from the end of construction and for given environmental conditions such a simulation allows a better estimate of the amount of corrosion in the steel bars, their actual resistant area and ductility, and the deterioration of concrete strength and spalling of the cover.

The obtained results are then incorporated in the Limit and Nonlinear Analysis of the damaged structure.

A.1.1 MODELING OF THE DIFFUSION PROCESS

The simplest model to describe the kinetic process of chemical components diffusion in solids is represented by Fick's first law, which assumes a linear relationship between the mass flow and the concentration gradient by introducing an effective diffusion coefficient D_e. The combination of the Fick's model with the mass concentration principle leads to Fick's second law. Assuming an isotropic media, the problem is described by the following second-order partial differential equation:

$$-\nabla \cdot (-D_e \nabla C) = \frac{\partial C}{\partial t} \tag{A.1}$$

where $C = C(\mathbf{x}, t)$ is the mass concentration of the aggressive agent at point $\mathbf{x} = (x, y, z)$ at the t time, and $\nabla C = \mathbf{grad} C$. Even though D_e in reinforced concrete structures depends on relative humidity, on temperature and on the internal stress field, for the sake of simplicity a diffusion coefficient $D_e = D$, constant in time, is assumed.

From the numerical point of view, the analytical solution of the linear partial differential equation (A.1) exists only for a limited number of problems. In general, numerical procedures are necessary to deal with arbitrary domains, different position of steel bars and complex boundary conditions. In order to model the diffusion process, the evolutionary algorithm called *Cellular Automata* is adopted (Wolfram, 1994). This computational technique, presented in the works of (Biondini *et al.*, 2004b) and (Titi and Biondini, 2016), consists of a regular uniform grid of sites or *cells*, theoretically having an infinite extension, with a discrete variable in each cell that can take on a finite number of states. During time, cellular automata evolves in discrete time steps according to a parallel state transition determined by a set of local rules: the variables $s_i^{k+1} = s_i(t_{k+1})$ at each side i at time t_{k+1} are updated synchronously based on the values of the variables s_n^k in their "neighborhood" n at the preceding time instant t_k. The neighborhood n of a cell i is typically taken to be the cell itself and a set of adjacent cells within a given radius r, or $i - r \leq n \leq i + r$. Thus, the dynamics of a cellular automaton can be formally represented as:

$$s_i^{k+1} = \phi(s_i^k; s_n^k) \qquad i - r \leq n \leq i + r \tag{A.2}$$

where function ϕ is the *evolutionary rule* of the automaton. In particular, Fick's laws in two dimensions can be accurately reproduced by the following evolutionary rule:

$$C_i^{k+1} = \phi_0 C_i^k + \frac{1 - \phi_0}{4} \sum_{j=1}^{2} \left(C_{i-1,j}^k + C_{i+1,j}^k \right) \tag{A.3}$$

where the discrete variable $C_i^k = s_i^k = C(\mathbf{x}_i, t_k)$ represents the concentration of the aggressive agent at time t_k in the cell i of the automaton located at point $\mathbf{x}_i = (y_i, z_i)$ of the cross-section, $C_{i\pm1,j}^k$ is the concentration in the adjacent cells $i \pm 1$ in the direction $j = 1, 2$ and ϕ_0 is a suitable evolutionary coefficient related to the rate of mass diffusion. Fig. A.1 presents the typical pattern of cells involved in the evolutionary rule for 2D cellular automata with $r = 1$, but patterns of higher complexity can also be proposed. Additionally, the diffusion process can be regulated according to a given value of the diffusion coefficient D by relating the grid dimension Δx and the time step Δt through the relationship:

$$D = \frac{1-\phi_0}{4} \frac{\Delta x^2}{\Delta t} \tag{A.4}$$

To ensure a good accuracy of the automaton, a suitable value of the central evolutionary coefficient in case of constant diffusivity is $\phi_0 = 1/2$ (Titi and Biondini, 2016).

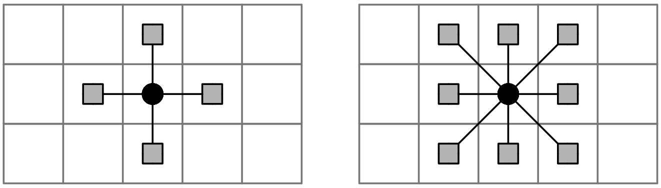

(a) Von Neumann. **(b)** Moore.

Figure A.1: Neighbourhoods for 2D Cellular Automata with radius $r = 1$.

A.1.2 MODELING OF THE MECHANICAL DAMAGE

The structural damage can be viewed as a degradation of the mechanical properties which make the structural system less able to withstand the applied loads. The main effect of corrosion in concrete structures is the reduction in the bar mass. Depending on the source of corrosion, different models can be applied in order to simulate it, Fig. A.2. Once the diffusion process is solved, such a damage can be evaluated by introducing a suitable degradation law for the steel area $A_s = A_s(t)$:

$$A_s(t) = [1 - \delta_s(t)]\, A_{s0} \tag{A.5}$$

where $A_{s0} = \pi\, D_0^2/4$ is the area of the undamaged bar at the initial time $t = t_0$ and $\delta_s = \delta_s(t)$ is the dimensionless damage index which gives a direct measure of the deterioration within the range [0;1].

In carbonated concrete, without a significant presence of chlorides, corrosion tends to develop in a uniform way around steel bars, Fig. A.2a. In this case the penetration depth is $p = 2x$, and the damage function δ_s has the following expression:

$$\delta_s = \delta\,(2 - \delta) \tag{A.6}$$

Exploiting (A.5), the uniform reduction of area is:

$$A_s(t) = \pi \left[\frac{D_0}{2} - x(t_p)\right]^2 \tag{A.7}$$

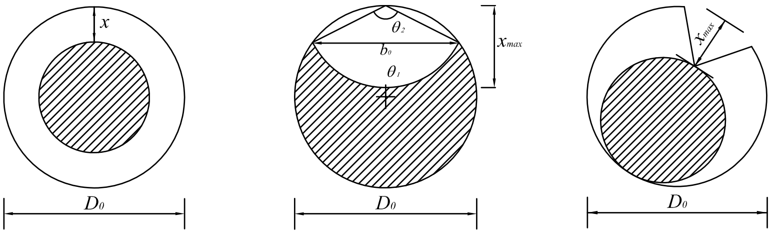

(a) Uniform corrosion. **(b)** Pitting corrosion. **(c)** Mixed corrosion.

Figure A.2: Modeling of cross section reduction of a steel bar, adapted from (Titi, 2012).

where t_p is the time in which corrosion begins.

If concrete is contaminated by chlorides, reduction of steel area is not uniform but tend to localize (pit), Fig. A.2b; the model presented above is therefore not suitable. From measures of current intensity it is possible to obtain a mean value of penetration depth; however, due to the localization of the damage, the maximum depth x_{max} in correspondence of the pit is significant higher. One solution is to define the pitting factor R, defined as:

$$R = \frac{x(t)_{max}}{x(t)_{mean}} \tag{A.8}$$

Indicative values for the pitting factor R can be found in (Gonzalez *et al.*, 1995).

The corrosion process causes not only a reduction in the steel area, but also a loss of ductility of the material that can lead to brittle failures of concrete members (Coronelli and Gambarova, 2004) and (Stewart, 2009). Tensile tests on corroded bars show that the steel behaviour may become brittle even for a quite limited (about 13%) mass loss (Almusallam, 2001). According to the experimental tests performed by (Apostolopoulos and Papadakis, 2008), the ductility reduction can be expressed as a function of mass loss. Based on these results, the steel ultimate strain ϵ_{su} is related to the damage index $\delta_s = \delta_s(t)$ as follow (Biondini and Vergani, 2012):

$$\varepsilon_{su}(t) = \begin{cases} \varepsilon_{su0} & 0 \leq \delta_s \leq 0.016 \\ 0.1521 \cdot \delta_s^{-0.4583} \varepsilon_{su0} & 0.016 < \delta_s \leq 1 \end{cases} \tag{A.9}$$

where ε_{su0} is the steel ultimate strain of the undamaged bar.

The effects of corrosion are not limited to damage of reinforcing steel bars. In fact, particularly in case of uniform corrosion, the formation of corrosion products may lead to the development of longitudinal cracks in the concrete surrounding the corroded bars and, consequently, to delamination and spalling of the concrete cover (Pantazopoulou and Papoulia, 2001). Concrete degradation can be taken into account by modeling the reduction of concrete compression strength f_c due to cover cracking:

$$f_c = [1 - \delta_c(\delta)]\, f_{c0} \tag{A.10}$$

where f_{c0} is the strength of undamaged concrete. The reduced concrete strength

f_c can be evaluated as follows (Coronelli and Gambarova, 2004):

$$f_c(t) = \frac{f_{c0}}{1 + \kappa \frac{\varepsilon_\perp(t)}{\varepsilon_{c0}}} \tag{A.11}$$

where κ is a coefficient related to bar diameter and roughness ($\kappa = 0.1$ for medium-diameter ribber bars), ε_{c0} is the strain at peak stress in compression, and $\varepsilon_\perp$ is an average (smeared) value of the tensile strain in cracked concrete at right angles to the direction of the applied stress. The transversal strain $\varepsilon_\perp$ is evaluated by means of the following relationship:

$$\varepsilon_\perp(t) = \frac{b_f(t) - b_i}{b_i} = \frac{\Delta b(t)}{b_i} \tag{A.12}$$

where b_i is the width of the undamaged concrete cross-section and b_f is the width after corrosion cracking. The increase Δb of the beam width is estimated as follows:

$$b_f - b_i = w_{tot}(t) \tag{A.13}$$

and hence:

$$\varepsilon_\perp(t) = \frac{w_{tot}(t)}{b_i} \tag{A.14}$$

where $w_{tot}(t) = \sum w_i(t)$ is the sum of the mean opening cracks of all the bars. Several relationships are proposed in literature to evaluate the crack opening w. The following empirical model is assumed in (Vidal *et al.*, 2004):

$$w = \kappa_w(\delta_s(t) - \delta_{s0})A_{s0} \tag{A.15}$$

where $\kappa_w = 0,0575\ mm^{-1}$ and δ_{s0} is the amount of steel damage necessary for cracking initiation. This damage threshold is evaluated as follow:

$$\delta_{s0} = 1 - \left[1 - \frac{R}{D_0}\left(7,53 + 9,32\frac{c}{D_0}\right) \times 10^{-3}\right]^2 \tag{A.16}$$

where c is the concrete cover. The crack opening increases with the expansion of corrosion products up to a critical width, conventionally sets to 1 mm. The *spalling of concrete cover* is assumed to occur when this threshold is reached.

According to (Biondini and Vergani, 2012), the reduction of concrete strength is not applied to the entire concrete cover, but it is limited to the zones adjacent to reinforcing bars. Fig. A.3 shows a model where the reduction of concrete strength is applied to a portion of concrete cover surrounding the corroded bars within a radius equal to the cover thickness. Through such an approach, both the mechanisms of *spalling* of the concrete cover and *delamination* phenomena can be dealt with.

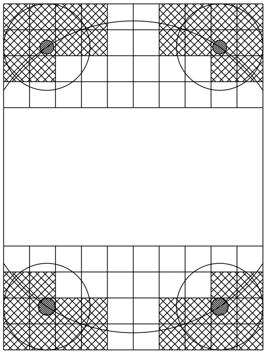

Figure A.3: Model.

When the deterioration is induced by aggressive agents such as chlorides, the corrosion damage depends, among other factors, on the level of concentration of the substance which diffuses inside the structure (Bertolini, 2008). Several formulations have been presented in order to correlate the rate of damage and the concentration of the aggressive agent (Camnasio, 2013). A critical comparison of the evolution in time of δ_s is discussed in (Quagliaroli, 2014). Despite the complexity of damage processes in concrete structures exposed to corrosion, the damage index $\delta_s = \delta_s(\mathbf{x}, t)$ at a point $\mathbf{x} = (y_i, z_i)$ of the generic cross-section is here correlated to the diffusion process by assuming a linear relationship between the rate of damage and the concentration $C = C(\mathbf{x}, t)$ of the aggressive agent (Biondini *et al.*, 2004b):

$$\frac{\partial \delta_s(\mathbf{x}, t)}{\partial t} = \frac{C(\mathbf{x}, t)}{C_s \Delta t_s} = \rho C(\mathbf{x}, t) \tag{A.17}$$

In this equation C_s represents the value of constant concentration $C(\mathbf{x}, t)$ in a certain position and at a specified time instant, which lead to a complete corrosion of the steel bar after the time period Δt_s. In addition, the initial conditions $\delta_s(\mathbf{x}, t_{cr}) = 0$ with $t_{cr} = max\,\{t\,|\,C(\mathbf{x}, t) \leq C_{cr}\}$ is assumed, where C_{cr} is a critical threshold of concentration. Finally, the damage rate coefficient $\rho = (C_s \Delta t_s)^{-1}$ is related to the materials properties and it must be set according to the actual rate of the damaging process (Bertolini *et al.*, 2013) and the the nature of the applications investigated. Some values are determined on the basis of particular experimental data, others come from numerical models and reasonable assumptions. For this reason, it would be of interest to study the 2D diffusion model in probabilistic terms, as in (Biondini and Garavaglia, 2005) and (Titi and Biondini, 2016).

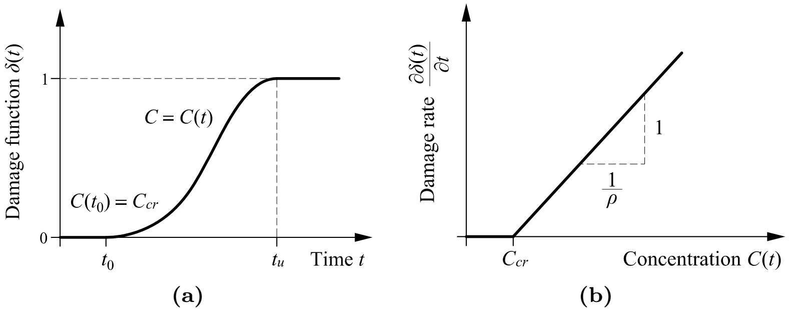

Figure A.4: Modeling of mechanical damage: (a) time evolution of the damage index during diffusion process; (b) linear relationship between rate of damage and concentration of the aggressive agent.

A.1.3 LIMIT ANALYSIS AT DIFFERENT TIME INSTANTS

In the previous Limit Analysis (chapter 5), the cross-sectional performance is quantified by using fixed values of the quantities **N** and **k**, which define the yielding criterion and the flow rule. However, due to the reinforcement and concrete deterioration corresponding to the damage state at certain time, such quantities, as well as the corresponding collapse multiplier λ_c, vary over time. In order to account for such a variability, a specific analysis of the deteriorating cross-sections is firstly required to build the modified frontiers $f(A, B) = 0$ and the functions $\mathbf{N} = \mathbf{N}(t)$ and $\mathbf{k} = \mathbf{k}(t)$. In this way, the two foundamental theorems of plasticity leading to the *complete solution* (collapse multiplier, collapse mechanism and internal stress distribution at the incipient collapse) of the problem are performed by solving the previous linear programs at different time instants.

A.1.4 NONLINEAR ANALYSIS AT DIFFERENT TIME INSTANTS

The damage effects associated to prescribed values of the corrosion penetration index δ_s are included in the formulation of the beam element by assuming $A_{sm} = A_{sm}(\delta_s)$ and $\varepsilon_{sum} = \varepsilon_{sum}(\delta_s)$ for the *m-th* steel bar located at $\mathbf{x}_m = (y_m, z_m)$ whereas no damage for concrete is assumed. As a consequence, at certain time instant t the corresponding deteriorating stiffness matrices $\mathbf{k}_s = \mathbf{k}_s(x, t)$ and $\mathbf{k} = \mathbf{k}(x, t)$ are computed (Biondini and Vergani, 2012). It is worth noting that corrosion can selectively be applied to damaged structural elements with a different level of penetration in each reinforcing bar. In this way, a set of Nonlinear Analysis leading to the evolution of the structural behavior over time is performed by solving the previous nonlinear problem at different sampling times.

Conclusions

OUTLINE & GENERAL CONCLUSIONS

A methodology for the robustness assessment of reinforced concrete existing structures has been presented. Structural analyses of the whole structure or selected parts of it subjected to a certain damage state have been carried out by means of Limit Analysis. The aim of the analysis is to highlight the collapse mechanism and the redistribution capacity of the internal forces, in order to detect the weakest parts, to assess the influence of a certain type of damage and to explore the effectiveness of repair hypotheses.

The thesis is organized as follow.

Chapter 1 frames the argument of the thesis, outlines the research significance and presents its aims.

Chapter 2 presents the general aspects and the main requirements related to the problem of assessing the structural safety of existing structures. In particular, the identification of the most common weaknesses during the lifetime of the structure may have an influence on both the local and global integrity. Thus, a review of the factors which have an influence on the durability of a structure and a collection of the most frequent lacks depending on the weakening of structural details is outlined.

In Chapter 3, the structural robustness is outlined with reference to recent tragic events that have shown catastrophic collapses. The measures for assessing the robustness can be classified according to three categories with increasing complexity: deterministic, probabilistic and risk-based measures. Since it is not always possible to refer the structural robustness to an ad hoc index, a *virtual loading test* is proposed to assess the safety of existing structure. In this way, the search for the limit behaviors of the structure may be seen as a lifetime structural robustness estimation.

Chapter 4 distinguishes the different and nested levels of analysis (structure, element, section, fiber). The basic characteristics of nonlinear beam elements are derived by using both a displacement-based and a force-based approach (dual formulation). At the sectional level, the main difficulties regard the treatment of normal and tangential stresses. For the Navier-Bernoulli beam only normal strains and normal stresses are involved, hence a mono-dimensional stress-strain relationship (at the fiber level) is sufficient. On the contrary, in a general sense, the nonlinear beam element should involve a richer kinematic field in which a coupling between normal and tangential stresses takes place. This last point is out of the scope of this Thesis but still today an object of many types of research.

Chapter 5 contains the matrix formulation of Limit Analysis, developed for the specific purpose of this Thesis. In dealing with RC structures, a force-based finite element for the Limit Analysis of 3D frame structures is presented. Since Limit Analysis requires as an input a reliable yielding criterion, the resistant domains of an arbitrary RC section deal with respectively:

1. axial force-bending moment interaction. In this case, the formulation assumes as active and interacting plastic stresses only N and M_z;
2. bending moment-torsion relationship. The Limit Analysis assumes only the bending and torque moments as active plastic stresses. The resistant domains $T - M_z$ are derived through space truss analogy.

Thus, the Upper and Lower Bound Theorems are rewritten as dual linear constrained optimization problems and the complete solution of the problem (i.e. the collapse loads, a stress distribution at the incipient collapse and a collapse mechanism) is obtained. Due to the necessity of validating the proposed approach, in this Chapter, a RC slender arch bridge is studied. For complementary reasons, the results coming from Limit Analysis are compared with the Nonlinear ones. Due to the different nature of the two approaches (force versus displacement-based method), the complementary of the information is outlined and the sources of differences are discussed and motivated.

The assessment of an existing RC grillage deck subjected to a severely damaged state is shown in Chapter 6. The aim of the analyses is to highlight the collapse mechanism and the redistribution capacity of the internal forces, in order to detect the weakest parts, to assess the influence of a certain type of damage, and to explore the effectiveness of repair hypotheses. The search for these limit behaviors is seen as a lifetime structural robustness estimation, aimed to outline the consequences due to different damage factors and the modes which lead to sudden collapses, when neither weakness signals nor intermediate anomalous behaviors appear.

In Chapter 7, a coupling of Limit Analysis and Framework Modeling in studying RC membrane elements is proposed. The continuous structure is replaced by an equivalent mesh of truss elements with suitable and well-defined sectional properties. Such a discretization technique, in addition to the determination of the load multiplier and the mechanism of collapse of the structural elements, allows also to provide useful indications on the position and orientation of the most compressed and tensioned elements. Both the layout of the load path and the plasticization distribution is useful in assessing and validating the bearing schemes assumed in the design practice.

Finally, in Appendix A, the damage diffusion process and its modeling through the diffusivity equation is presented. The diffusion problem is solved through the Cellular Automata algorithm. The effects of the damage are specialized to reinforced concrete elements.

ORIGINAL CONTRIBUTIONS

In developing the theoretical formulations and in setting up the numerical algorithms, several original contributions have been carried out.

In dealing with the assessment criteria for existing structures, a procedure for a virtual loading test is proposed, consisting in the exam of a structure at different damage states and in the evaluation of the multiplier at the collapse of the worst traffic load distribution. The search for the limit behaviors is seen as a lifetime structural robustness estimation, tailored on the actual or supposed damaging characteristics of a given structure. Such an approach allows outlining the consequences due to different damage factors and the modes which lead to sudden collapses when neither weakness signals nor intermediate anomalous behaviors appear.

Concerning the structural model, the main contribution is the Limit Analysis of 3D framed structures, developed and coded in a finite element-based program. According to the given structure, the formulation is specialized for two distinct situations: (1) only axial force-bending moment as active and interactive plastic stresses, (2) only bending-torque moments as active and interactive plastic stresses. It has been shown that such a computational technique can be successfully applied in dealing with the limit behavior of RC structures for all range off loadings. The results have been proved the great ability of Limit Analysis to synthesize the information. Clearly, since the monodimensional modeling offers a good balance between accuracy and computational efficiency, such a choice has permitted to couple the Limit Analysis and Framework Modeling in studying RC membrane elements. Original results concern not only the complete solution of the problem at incipient collapse but also the pattern of plasticization elements both in tension and in compression. This is the second original aspect of the present work.

Concerning the damage model, a general computational approach based on the Cellular Automata algorithm has been formulated in dealing with damage processes affecting RC structures. Through such an approach, it is possible to deal with: (a) the reduction of steel bars areas, (b) the reduction of steel ductility, (c) the reduction of concrete strength until (d) the spalling of concrete cover occurs.

Due to its generality, the so-obtained damage model can be linked with any kind of structural model. Hence, a general methodology aiming both to assess the structural performance at different time instants and to detect the weakest parts of a generic RC framed structures has been obtained. This is the most important and practical contribution to this work.

In developing the applications, a complete parallel study between Limit and Nonlinear Analysis has been carried out. Through such parallelism, the complementary of the information given by the two methods (the load history versus the collapse mode) and the intensity of the ultimate loads are highlighted particularly when the structure is progressively affected by damage.

FINAL CONCLUSIONS

The main aim of this work is to propose a synthetic and effective procedure for the robustness assessment of RC existing structures. Structural analyses of the whole structure or selected parts of it subjected to a certain damage state are carried out by means of Limit Analysis. At a given time and according to different loading scenarios, a virtual loading test under the worst traffic load distribution is proposed. The analyses allow detecting the onset of the reduction of local bearing capacities, the internal force redistribution from damaged towards undamaged structural elements, and the evolution of the collapse mechanisms towards the ultimate state. These results provide a reliable reference to estimate qualitatively a lifetime structural robustness, tailored on the actual or supposed damaging characteristics of a given structure.

In developing applications concerning existing structures, the results provides a reliable reference to answer to the basic questions concerning the bridge maintenance, that are estimating their bearing capacity after a certain amount of years, assessing their residual bearing capacity in the damaged state, assessing their residual life-cycle and the possibility of a sustainable service life extension.

In dealing with RC structural elements, both the layout of the load path and the plasticization distributions are useful in assessing and validating the bearing schemes assumed in the design practice.

In this work, through a virtual loading test, the structural behavior at different damage states and the evaluation of the multiplier at the collapse of a given additional traffic load distribution is obtained. The analysis of the sequence of the damage evolution and the loading capacity allows the computation of a robustness index over time. In addition, the data resulting from the Limit Analysis is useful to highlight the essential details of such an evolution, showing how the internal forces redistribute from damaged to undamaged structural parts.

Such a contribution may be suitable for solving the aforementioned problems and in assessing the effectiveness of repairing and strengthening interventions.

FURTHER DEVELOPMENTS

Based on the achieved results, several future developments of this work are possible:

- concerning Limit Analysis:
  it has been shown that limit analysis is the most synthetic approach. If small displacement hypothesis is assumed, the complete solution of the problem (i.e. the collapse load, a stress distribution at the incipient collapse and a collapse mechanism) is obtained by linear programming. In the formulation exposed in the thesis, the second order effects due to the configuration changing are not accounted for. A possible development could be the formulation of limit analysis by removing the hypothesis of small displacement. In addition, plane interaction domains are only considered. In the space, however, three are the six interacting generalized stresses: the axial force N, the shear forces V, the bending moments M and torsion T. If an adequate resistance criterion, that

considers, for example, a general interaction between the generalized active stresses, is proposed, then limit analysis can be extended also in the study of shear collapse mechanisms.

- dealing with continuous elements:
  an attempt to couple limit analysis and Framework Modeling has been proposed. Further studies will be devoted to improving the Trusswork Modellization and to refine the post-processing graphics of the results, in order to make the bearing mechanisms more explicit.

- extension to the non-deterministic field:
  it has been shown that the phenomena involved in damage processes are not so clear and, in addition, not so certain due to dependability on aleatory quantities such as the chlorides content and the position of the corrosion scenarios. A natural development of this work is to extend the proposed procedure in the non-deterministic field, in order to deal with the intrinsic uncertainties affecting the considered phenomena.

References

Absi, E. (1972), «La théorie des équivalences et son application á l'étude des ouvrages d'art», in «Annales de ITBTP», 295.

Agarwal, J., Blockley, D. and Woodman, N. (2003), «Vulnerability of structural systems», *Structural Safety*, vol. 25 (3), p. 263–286.

Almusallam, A. A. (2001), «Effect of degree of corrosion on the properties of reinforcing steel bars», *Construction and Building Materials*, vol. 15 (8), p. 361–368.

Apostolopoulos, C. and Papadakis, V. (2008), «Consequences of steel corrosion on the ductility properties of reinforcement bar», *Construction and Building Materials*, vol. 22 (12), p. 2316–2324.

Arangio, S. and Bontempi, F. (2010), «Soft computing based multilevel strategy for bridge integrity monitoring», *Computer-Aided Civil and Infrastructure Engineering*, vol. 25 (5), p. 348–362.

Ardito, R. (2004), *Diagnostic and Limit State Analyses of Concrete Dams by Optimization Methods*, PhD Thesis, Politecnico di Milano, Milan, Italy, Supervisor: Prof. G. Maier.

Ardito, R., Cocchetti, G. and Maier, G. (2008), «On structural safety assessment by load factor maximization in piecewise linear plasticity», *European Journal of Mechanics-A/Solids*, vol. 27 (5), p. 859–881.

Ardito, R., Cocchetti, G. and Maier, G. (2010), «Generalized limit analysis in poroplasticity by mathematical programming», *Archive of Applied Mechanics*, vol. 80 (1), p. 57.

Bäcklund, J. (1976), «Large deflection analysis of elasto-plastic beams and frames», *International journal of mechanical sciences*, vol. 18 (6), p. 269–277.

Bairan, J. and Mari, A. (2007), «Multiaxial-coupled analysis of RC cross-sections subjected to combined forces», *Engineering structures*, vol. 29 (8), p. 1722–1738.

Bairán García, J. M. (2005), *A non-linear coupled model for the analysis of reinforced concrete sections under bending, shear, torsion and axial forces*, PhD

Thesis, Technical University of Catalonia, Barcelona, Spain, Supervisor: Prof. A.R. Marí.

Baker, J. W., Schubert, M. and Faber, M. H. (2008), «On the assessment of robustness», *Structural Safety*, vol. 30 (3), p. 253–267.

Baron, F. (1961), «Matrix analysis of structures curved in space», *Journal of the Structural Division*, vol. 87 (3), p. 17–40.

Bentz, E. C. (2000), *Sectional analysis of reinforced concrete members*, PhD Thesis, University of Toronto, Canada, Supervisor: Prof. M.P. Collins.

Bertolini, L. (2008), «Steel corrosion and service life of reinforced concrete structures», *Structure and Infrastructure Engineering*, vol. 4 (2), p. 123–137.

Bertolini, L., Elsener, B., Pedeferri, P., Redaelli, E. and Polder, R. B. (2013), *Corrosion of steel in concrete: prevention, diagnosis, repair*, John Wiley & Sons.

Bertolini, L., Carsana, M., Gastaldi, M., Lollini, F., Redaelli, E. *et al.* (2016), «Corrosion of steel in concrete and its prevention in aggressive chloride-bearing environments», in «5th International Conference on the Durability of Concrete Structures», p. 13–25, Purdue University Press.

Biondini, F. (1999), «Il Fattore di Efficienza della Modellazione Strut-and-Tie di Elementi in Cemento Armato», *Aicap 1999 – Lo sviluppo del cemento armato e del precompresso in Italia e la lezione di questo secolo*, vol. 1, p. 129–138.

Biondini, F. (2009), «A Measure of Lifetime Structural Robustness», in «ASCE/SEI Structures Congress 2009», p. 1749–1757, American Society of Civil Engineers, ASCE.

Biondini, F., Bontempi, F. and Malerba, P. (2004a), «Fuzzy reliability analysis of concrete structures», *Computers & structures*, vol. 82 (13), p. 1033–1052.

Biondini, F. and Frangopol, D. M. (2008), «Probabilistic limit analysis and lifetime prediction of concrete structures», *Structure and Infrastructure Engineering*, vol. 4 (5), p. 399–412.

Biondini, F., Frangopol, D. M. and Restelli, S. (2008), «On structural robustness, redundancy, and static indeterminacy», in «ASCE/SEI Structures Congress 2008», p. 1–10, American Society of Civil Engineers, ASCE.

Biondini, F. and Garavaglia, E. (2005), «Probabilistic service life prediction and maintenance planning of deteriorating structures», in «International Conference on Structural Safety and Reliability (ICOSSAR 2005), Rome, Italy», p. 19–22.

Biondini, F. and Vergani, M. (2012), «Damage modeling and nonlinear analysis of concrete bridges under corrosion», in «Proceedings of the Sixth International Conference on Bridge Maintenance, Safety and Management (IABMAS 2012), Stresa, Italy, July», p. 8–12.

BIONDINI, F., BONTEMPI, F., FRANGOPOL, D. M. and MALERBA, P. G. (2004b), «Cellular automata approach to durability analysis of concrete structures in aggressive environments», *Journal of Structural Engineering*, vol. 130 (11), p. 1724–1737.

BONTEMPI, F. (1992), «Sulla costruzione dei domini di rottura di sezioni in C.A. e C.A.P. soggette a pressoflessione deviata.», *Studi e Ricerche - Politecnico di Milano. Scuola di Specializzazione in Costruzioni in cemento armato.*, vol. 13 (1), p. 261–277.

BONTEMPI, F. (2006), «Basis of design and expected performances for the Messina Strait Bridge», in «Proceedings of the International Conference on Bridge Engineering–Challenges in the 21st Century, Hong Kong», p. 1–3.

BONTEMPI, F., GIULIANI, L. and GKOUMAS, K. (2007), «Handling the exceptions: dependability of systems and structural robustness», in «Proc., 3rd International Conference on Structural Engineering, Mechanics and Computation (SEMC)», p. 10–12.

BONTEMPI, F. and MALERBA, P. (1998), «Metodi generali per l'analisi di strutture intelaiate in CA/CAP», *CISM*, p. 241–287.

BONTEMPI, F., MALERBA, P. and ROMANO, L. (1995a), «Formulazione diretta secante dell'analisi non lineare di telai in CA/CAP», *Studi e ricerche - Politecnico di Milano. Scuola di specializzazione in costruzioni in cemento armato*, vol. 16, p. 351–386.

BONTEMPI, F., MALERBA, P. and ROMANO, L. (1995b), «Il modello MFCT (Modified Compression Field Theory) nell'analisi per elementi finiti di strutture piane in CA», *Studi e ricerche - Politecnico di Milano. Scuola di specializzazione in costruzioni in cemento armato*, vol. 16, p. 173–207.

BRICCOLA, D., CONTI, E., MALERBA, P. G. and QUAGLIAROLI, M. (2013), «Multiaxial Interaction Domains of RC sections derived through a parametric subdomains discretization», *ASEM*, vol. 13, p. 925–942.

BS (2007), «EN ISO 19902:2007 - Petroleum and natural gas industries. Fixed steel offshore structures», *English version EN ISO*, vol. 19902, p. 182–202.

BUCKLE, I. and JACKSON, A. (1981), «A filamented beam element for the nonlinear analysis of reinforced concrete shells with edge beams», *University of Auckland, New Zealand.*

CALLAWAY, D. S., NEWMAN, M. E., STROGATZ, S. H. and WATTS, D. J. (2000), «Network robustness and fragility: Percolation on random graphs», *Physical review letters*, vol. 85 (25), p. 5468.

CAMNASIO, E. (2013), *Lifetime performance and seismic resilience of concrete structures exposed to corrosion*, PhD Thesis, Politecnico di Milano, Italy, Supervisor: Prof. F. Biondini.

Canisius, T., Sorensen, J. and Baker, J. (2007), «Robustness of structural systems–a new focus for the joint committee on structural safety (JCSS)», in «Proc., 10th Int. Conf. on Application of Statistic and Probability in Civil Engineering (ICASP10)», p. 179–180.

Capdevielle, S., Grange, S., Dufour, F. and Desprez, C. (2014), «Introduction of warping in a nonlinear multifiber beam model in torsion for reinforced concrete structures», in «EURO-C-Computational Modeling of Concrete and Concrete Structures», p. 7p.

Carol, I. and Murcia, J. (1989), «Nonlinear time-dependent analysis of planar frames using an 'exact' formulation. Theory», *Computers & structures*, vol. 33 (1), p. 79–87.

Casciati, F., Augusti, G. and Baratta, A. (2014), *Probabilistic methods in structural engineering*, CRC Press.

Cavaco, E. S. (2013), *Robustness of corroded reinforced concrete structures*, PhD Thesis, Universidade Nova de Lisboa, Portugal, Supervisors: Prof. L.A.C. Neves, Prof. J.R. Casas.

Cavaco, E. S., Casas, J. R., Neves, L. A. and Huespe, A. H. (2010), «A framework for robustness assessment in the context of corroded RC structures», in «Bridge Maintenance, Safety, Management and Life-Cycle Optimization: Proceedings of the Fifth International IABMAS Conference, Philadelphia, USA, 11-15 July 2010», p. 421, CRC Press.

Cavaco, E. S., Casas, J. R., Neves, L. A. and Huespe, A. E. (2013b), «Robustness of corroded reinforced concrete structures–a structural performance approach», *Structure and Infrastructure Engineering*, vol. 9 (1), p. 42–58.

C.E.B. (1992), *Durable Concrete Structures: Design Guide*, 183, Thomas Telford.

Ceresa, P., Petrini, L. and Pinho, R. (2007), «Flexure-shear fiber beam-column elements for modeling frame structures under seismic loading - State of the art», *Journal of Earthquake Engineering*, vol. 11 (S1), p. 46–88.

Chan, E. C. (1982), «Nonlinear geometric, material and time dependent analysis of reinforced concrete shells with edge beams», *Report UCB-SESM 82/8, Univ. of Calif., Berkeley.*

Chen, W.-F. and Saleeb, A. F. (2013), *Constitutive equations for engineering materials: Elasticity and modeling*, vol. 37, Elsevier.

Cocchetti, G. and Maier, G. (2003), «Elastic–plastic and limit-state analyses of frames with softening plastic-hinge models by mathematical programming», *International Journal of solids and structures*, vol. 40 (25), p. 7219–7244.

Collins, M. (1969), «The normal moment yield criterion applied to beams in flexure-torsion», *Proc. lnt. Conj on Shear, Torsion and Bond in Reinforced and Prestressed Concrete, Coimbatore, India.*

Collins, M. P., Walsh, P., Archer, F. and Hall, A. (1967), «Reinforced concrete in torsion», *UNICIV Report No. R-31*, p. 328.

Conti, E., Malerba, P. G. and Quagliaroli, M. (2017b), «Limit and Nonlinear Analysis of a slender arch bridge. A comparative study.», in «M2D2017-7th International Conference on Mechanics and Materials in Design», p. 937–952, JF Silva Gomes and SA Meguid.

Coronelli, D. and Gambarova, P. (2004), «Structural assessment of corroded reinforced concrete beams: Modeling guidelines», *Journal of Structural Engineering*, vol. 130 (8), p. 1214–1224.

Cruz, P., Mari, A. and Roca, P. (1998), «Nonlinear time-dependent analysis of segmentally constructed structures», *Journal of Structural Engineering*, vol. 124 (3), p. 278–287.

De, R. S., Karamchandani, A. and Cornell, C. A. (1989), «Study of redundancy in near-ideal parallel structural systems», in «Structural safety and reliability», p. 975–982, ASCE.

De Donato, O. and Maier, G. (1972), «Mathematical programming methods for the inelastic analysis of reinforced concrete frames allowing for limited rotation capacity», *International Journal for Numerical Methods in Engineering*, vol. 4 (3), p. 307–329.

De Sitter, W. (1984), «Costs of service life optimization "The Law of Fives"», in «CEB-RILEM Workshop on Durability of Concrete Structures (Copenhagen, Denmark, May 18-20, 1983)», Comité Euro-International du Béton.

Dorn, W. and Greenberg, H. (1957), «Linear programming and plastic limit analysis of structures», *Quarterly of Applied Mathematics*, vol. 15 (2), p. 155–167.

Drucker, D. C. and Prager, W. (1952), «Soil mechanics and plastic analysis or limit design», *Quarterly of applied mathematics*, vol. 10 (2), p. 157–165.

Ellingwood, B. R. and Dusenberry, D. O. (2005), «Building design for abnormal loads and progressive collapse», *Computer-Aided Civil and Infrastructure Engineering*, vol. 20 (3), p. 194–205.

EN (1991), «Eurocode 1: Actions on structures - Part 2: Traffic loads on bridges», *Brussels: European Standard EN*, vol. 2, p. 2003.

Ersdal, G. (2005), *Assessment of existing offshore structures for life extension*, PhD Thesis, University of Stavanger, Norway.

Exner, H. (1979), «On the Effectiveness Factor in Plastic Analysis of Concrete», *Plasticity in Reinforced Concrete, IABSE Colloqium*, vol. 29, p. 35–42.

Faber, M. (2006), «Robustness of structures: an introduction», *Structural Engineering International*, vol. 16 (2), p. 101–101.

FERREIRA, D. (2013), *A model for the nonlinear, time-dependent and strengthening analysis of shear critical frame concrete structures*, PhD Thesis, Technical University of Catalonia, Barcelona, Spain, Supervisors: Prof. A.R. Marí, Prof. J.M.Bairán, Prof. R.M. Marques.

FIB (2006), «Model code for service life design», *International federation for structural concrete (FIB). Switzerland*, p. 110.

FRANGOPOL, D. M. and CURLEY, J. P. (1987), «Effects of damage and redundancy on structural reliability», *Journal of structural engineering*, vol. 113 (7), p. 1533–1549.

GALLI, A. and FRANCIOSI, V. (1955), «Il calcolo a rottura dei ponti a volta sottile ed impalcato irrigidente», *Giornale del Genio Civile*, vol. 11, p. 686–700.

GHOSN, M. and MOSES, F. (1998), *Redundancy in highway bridge superstructures*, vol. 406, Transportation Research Board.

GIULIANI, L. (2009), *Structural integrity: robustness assessment and progressive collapse susceptibility*, PhD Thesis, University of Rome 'La Sapienza', Italy, Supervisors: Prof. F. Bontempi, Prof. U. Starossek.

GLICKSMAN, M. E. (2000), *Diffusion in solids: field theory, solid-state principles and applications*, Wiley.

GONZALEZ, J., ANDRADE, C., ALONSO, C. and FELIU, S. (1995), «Comparison of rates of general corrosion and maximum pitting penetration on concrete embedded steel reinforcement», *Cement and Concrete Research*, vol. 25 (2), p. 257–264.

GREGORI, J. N., SOSA, P. M., PRADA, M. F. and FILIPPOU, F. C. (2007), «A 3D numerical model for reinforced and prestressed concrete elements subjected to combined axial, bending, shear and torsion loading», *Engineering Structures*, vol. 29 (12), p. 3404–3419.

GUNER, S. (2008), *Performance assessment of shear-critical reinforced concrete plane frames*, vol. 71.

GVOZDEV, A. (1938), «Opredelenie velichiny razrushayushchei nagruzki dlya staticheski neopredelimykh sistem, preterpevayushchikh plasticheskie deformatsii», *Akademia Nauk SSSR, Moscow/Leningrad*, vol. 19, p. 38.

HABERLAND, M. (2007), *Progressiver Kollaps und Robustheit (Progressive collapse and robustness)*, PhD Thesis, Hamburg University of Technology, Germany.

HADDON, W. (1980), «The basic strategies for reducing damage from hazards of all kinds», *Hazard prevention*, vol. 16 (1), p. 8–12.

HRENNIKOFF, A. (1941), «Solution of problems of elasticity by the framework method», *J. appl. Mech.*

Hsu, T. T. (1998), «Stresses and crack angles in concrete membrane elements», *Journal of Structural Engineering*, vol. 124 (12), p. 1476–1484.

Hsu, T. T. C. (1984), *Torsion of reinforced concrete.*

Hubbard, F., Shkurti, T. and Price, K. (2004), «Marquette interchange reconstruction: HPS twin box girder ramps», *Structure magazine.*

Huber, P. J. (1996), *Robust statistical procedures*, vol. 68, Siam.

Kang, Y.-J. and Scordelis, A. C. (1980), «Nonlinear analysis of prestressed concrete frames», *Journal of the structural division*, vol. 106 (ASCE 15191).

Kappos, A. and Penelis, G. (2014), *Earthquake resistant concrete structures*, CRC Press.

Ketchum, M. A. (1988), «Redistribution of stresses in segmentally erected prestressed concrete bridges», *Report UCB/SESM-86/07.*

Kristek, V., Bazant, Z. P., Zich, M. and Kohoutkova, A. (2006), «Box girder bridge deflections», *Concrete international*, vol. 28 (01), p. 55–63.

Lampert, P. (1970), *Ultimate strength of Reinforced Concrete Beams in Torsion (Bruchwiderstand von Stahlbetonbalken unter Torsion und Biegung)*, PhD Thesis, Swiss Federal Institute of Technology, Zurich, Switzerland.

Lampert, P. and Collins, M. P. (1972), «Torsion, bending, and confusion-An attempt to establish the facts», in «Journal Proceedings», vol. 69, p. 500–504.

Lampert, P. and Thürlimann, B. (1972), «Ultimate strength and design of reinforced concrete beams in torsion and bending», in «Ultimate Strength and Design of Reinforced Concrete Beams in Torsion and Bending/Résistance et dimensionnement des poutres en béton armé soumises à la torsion et à la flexion/Bruchwiderstand und Bemessung von Stahlbetonbalken unter Torsion und Biegung», p. 107–131, Springer.

Le Corvec, V. (2012), *Nonlinear 3d frame element with multi-axial coupling under consideration of local effects*, PhD Thesis, University of California, Berkeley, USA, Supervisor: Prof. F.C. Filippou.

Lemaitre, J. and Chaboche, J.-L. (1994), *Mechanics of solid materials*, Cambridge university press.

Leonhardt, F. and Walther, R. (1963), *Schubversuche an Plattenbalkan mit unterschiedlicher Schubbewehrung*, Vertrieb durch Verlag von W. Ernst.

Lind, N. C. (1995), «A measure of vulnerability and damage tolerance», *Reliability Engineering & System Safety*, vol. 48 (1), p. 1–6.

Liu, W., Neuenhoffer, A., Ghosn, M. and Moses, F. (2001), «NCHRP report 458: redundancy in highway bridge substructures», *Transportation Research Board–National Research Council, National Academy Press, Washington. DC.*

Maier, G. (1973), «A shakedown matrix theory allowing for workhardening and second-order geometric effects», in «International Symposium on Foundations of Plasticity, Warsaw, Poland», p. 417–433.

Malerba, P. and Bontempi, F. (1989), «Analisi di telai in c.a. in presenza di non linearitá meccaniche e geometriche.», *Studi e Ricerche - Politecnico di Milano. Scuola di Specializzazione in Costruzioni in cemento armato.*, vol. 11 (1), p. 209–224.

Malerba, P. G. (2014), «Inspecting and repairing old bridges: experiences and lessons», *Structure and Infrastructure Engineering*, vol. 10 (4), p. 443–470.

Mari, A. and Scordelis, A. (1984), «Nonlinear geometric, material and time dependent analysis of three dimensional reinforced concrete and prestressed frames», *UC SESM Report*, vol. 84, p. 12.

Marti, P. (1985), «Basic tools of reinforced concrete beam design», in «Journal Proceedings», vol. 82, p. 46–56.

Massonnet, C. E. and Save, M. A. (1965), *Plastic analysis and design: beams and frames*, vol. 1, Blaisdell Publishing Company.

Meyer, B. (1988), *Object-oriented software construction*, vol. 2, Prentice hall New York.

Mohr, S. (2012), *Nonlinear static and dynamic model for the analysis of reinforced concrete frames under high shear forces*, PhD Thesis, Technical University of Catalonia, Barcelona, Spain, Supervisor: Prof. A.R. Marí.

Mohr, S., Bairán, J. M. and Marí, A. R. (2010), «A frame element model for the analysis of reinforced concrete structures under shear and bending», *Engineering structures*, vol. 32 (12), p. 3936–3954.

Neuenhofer, A. and Filippou, F. C. (1997), «Evaluation of nonlinear frame finite-element models», *Journal of Structural Engineering*, vol. 123 (7), p. 958–966.

Nielsen, M. P. and Hoang, L. C. (1984), *Limit analysis and concrete plasticity*, CRC press.

Onsongo, W. M. (1978), *Diagonal compression field theory for reinforced concrete beams subjected to combined torsion, flexure and axial load*, PhD Thesis, University of Toronto, Canada, Supervisor: Prof. M.P. Collins.

Pang, X.-B. D. and Hsu, T. T. (1995), «Behavior of reinforced concrete membrane elements in shear», *Structural Journal*, vol. 92 (6), p. 665–679.

Pantazopoulou, S. and Papoulia, K. (2001), «Modeling cover-cracking due to reinforcement corrosion in RC structures», *Journal of Engineering mechanics*, vol. 127 (4), p. 342–351.

Park, R. and Paulay, T. (1975), *Reinforced concrete structures*, John Wiley & Sons.

Petrangeli, M. and Ciampi, V. (1997a), «Equilibrium based iterative solutions for the non-linear beam problem», *International Journal for Numerical Methods in Engineering*, vol. 40 (3), p. 423–437.

Prager, W. (1955a), «The general theory of limit design», in «Proc. 8th Int. Congress Theoretical and Applied Mechanics, Istambul 1952», p. 65–72.

Prager, W. (1955b), «The theory of plasticity: a survey of recent achievements», *Proceedings of the Institution of Mechanical Engineers*, vol. 169 (1), p. 41–57.

Quagliaroli, M. (2014), *From bidimensional towards monodimensional modeling of sound and damaged reinforced concrete structures*, PhD Thesis, Politecnico di Milano, Supervisor: Prof. P.G. Malerba.

Quagliaroli, M., Malerba, P. and Sgambi, L. (2015), «A parametric subdomain discretization for the analysis of the multiaxial response of reinforced concrete sections», *Advances in Engineering Software*, vol. 82, p. 87–104.

Rahal, K. and Collins, M. P. (1995), «Analysis of sections subjected to combined shear and torsion-a theoretical model», *ACI Structural Journal*, vol. 92, p. 459–459.

Ranzo, G. (2000), *Experimental and numerical studies on the seismic performance of beam-column RC structural members subjected to high shear*, PhD Thesis, University of Rome 'La Sapienza', Rome, Italy.

Ranzo, G. and Petrangeli, M. (1998), «A fibre finite beam element with section shear modelling for seismic analysis of RC structures», *Journal of earthquake engineering*, vol. 2 (03), p. 443–473.

Rausch, E. (1929), «Design of reinforced concrete in torsion (Berechnung des eisenbetons gegen verdrehung)», *Technische Hochschule, Berlin, Germany (in German).*

Recupero, A., D'Aveni, A. and Ghersi, A. (2005), «Bending moment–shear force interaction domains for prestressed concrete beams», *Journal of Structural Engineering*, vol. 131 (9), p. 1413–1421.

Restelli, S. (2007), «Measure of structural robustness of deteriorating systems», *Degree Thesis, Politecnico di Milano, Milan, Italy (In Italian).*

Rogowsky, D. and MacGregor, J. (1986), «Design of reinforced concrete deep beams», *Concrete International*, vol. 8 (8), p. 49–58.

Ronca, P. and Cohn, M. (1979), «Matrix-MP method for the analysis of inelastic arch structures», *International Journal for Numerical Methods in Engineering*, vol. 14 (5), p. 703–725.

SARITAS, A. (2006), *Mixed formulation frame element for shear critical steel and reinforced concrete members*, PhD Thesis, University of California, Berkeley, USA, Supervisor: Prof. F.C. Filippou.

SCHLAICH, J. and SCHAFER, K. (1991), «Design and detailing of structural concrete using strut-and-tie models», *Structural Engineer*, vol. 69 (6), p. 113–125.

SLOTINE, J.-J. E., LI, W. *et al.* (1991), *Applied nonlinear control*, vol. 199, Prentice hall Englewood Cliffs, NJ.

SORENSEN, J. D. and CHRISTENSEN, H. H. (2006), «Danish requirements for robustness of structures: Background and implementation», *Structural Engineering International*, vol. 16 (2), p. 172–177.

SPACONE, E., CIAMPI, V. and FILIPPOU, F. (1996), «Mixed formulation of nonlinear beam finite element», *Computers & Structures*, vol. 58 (1), p. 71–83.

SPACONE, E., CIAMPI, V. and FILIPPOU, F. C. (1995), *A beam element for seismic damage analysis*, Earthquake Engineering Research Center, University of California.

STAROSSEK, U. (2006), «Progressive collapse of structures: Nomenclature and procedures», *Structural engineering international*, vol. 16 (2), p. 113–117.

STAROSSEK, U. (2007a), «Progressiver Kollaps von Bauwerken», *Beton-und Stahlbetonbau*, vol. 100 (4), p. 305–317.

STAROSSEK, U. (2007b), «Typology of progressive collapse», *Engineering Structures*, vol. 29 (9), p. 2302–2307.

STAROSSEK, U. (2008), «Collapse resistance and robustness of bridges», in «The 4th International Conference on Bridge Maintenance, Safety, Management», p. 13–17, Citeseer.

STAROSSEK, U. (2009), *Progressive collapse of structures.*

STAROSSEK, U. and HABERLAND, M. (2008), «Measures of structural robustness - Requirements and applications», in «Structures Congress 2008: Crossing Borders», p. 1–10.

STAROSSEK, U. and HABERLAND, M. (2009), «Evaluating measures of structural robustness», in «Structures Congress 2009: Don't Mess with Structural Engineers: Expanding Our Role», p. 1–8.

STEWART, M. G. (2009), «Mechanical behaviour of pitting corrosion of flexural and shear reinforcement and its effect on structural reliability of corroding RC beams», *Structural safety*, vol. 31 (1), p. 19–30.

TAYLOR, R., FILIPPOU, F., SARITAS, A. and AURICCHIO, F. (2003), «A mixed finite element method for beam and frame problems», *Computational Mechanics*, vol. 31 (1-2), p. 192–203.

TITI, A. (2012), *Lifetime Probabilistic Seismic Assessment of Multistory Precast Buildings*, PhD Thesis, Politecnico di Milano, Supervisor: Prof. F. Biondini.

TITI, A. and BIONDINI, F. (2016), «On the accuracy of diffusion models for life-cycle assessment of concrete structures», *Structure and Infrastructure Engineering*, vol. 12 (9), p. 1202–1215.

TONIOLO, G. and MALERBA, P. (1981), *Metodi di discretizzazione dell'analisi strutturale*, Masson Italia.

ULM, F.-J., CLÉMENT, J.-L. and GUGGENBERGER, J. (1994), «Recent advances in 3D non-linear FE-analysis of RC and PC Beam Structures», in «Structures Congress XII», p. 1427–1432, ASCE.

VECCHIO, F. (2000), «Disturbed stress field model for reinforced concrete: formulation», *Journal of structural engineering*, vol. 126 (9), p. 1070–1077.

VECCHIO, F. J. and COLLINS, M. P. (1988), «Predicting the response of reinforced concrete beams subjected to shear using modified compression field theory», *ACI Structural Journal*, vol. 85 (3), p. 258–268.

VECCHIO, F. J. and COLLINS, M. P. (1993), «Compression response of cracked reinforced concrete», *Journal of structural engineering*, vol. 119 (12), p. 3590–3610.

VIDAL, T., CASTEL, A. and FRANCOIS, R. (2004), «Analyzing crack width to predict corrosion in reinforced concrete», *Cement and Concrete Research*, vol. 34 (1), p. 165–174.

VROUWENVELDER, A. (1996), «Evaluation of existing structures, item codification», in «IABSE Congress, Copenhagen», .

WISNIEWSKI, D., CASAS, J. R. and GHOSN, M. (2006), «Load capacity evaluation of existing railway bridges based on robustness quantification», *Structural Engineering International*, vol. 16 (2), p. 161–166.

WITTFOHT, H. (1983), «Ursachen für den Teil-Einsturz des" Viadotto Cannavino" bei Agro di Celico.», *Beton-und Stahlbetonbau*, vol. 78 (2), p. 29–36.

WOLFRAM, S. (1994), *Cellular automata: collected papers*, Addison-Wesley, New York, USA.

ZWICKY, D. (2010), «SIA 269/2 The New Swiss Code for existing concrete structures», in «Proceedings of the Joint IABSE-fib Conference on Codes in Structural Engineering», vol. 1.